An Analysis of Hypercube Space for Solving the Snake-In-The-Box Problem

by

Ananta Palani

(Under the direction of Walter D. Potter)

Abstract

Finding the longest snakes and coils in a hypercube is a difficult and computationally complicated problem to solve. As higher dimension hypercubes are explored, the problem quickly grows beyond the capabilities of exhaustive search techniques. Previous research has attempted to maximize the length of snakes and coils (open and closed paths, respectively) with Artificial Intelligence (AI) techniques, especially the Genetic Algorithm (GA). Using the GA, researchers have generally represented the individual solutions (i.e., paths) as sequences of nodes visited in the hypercube, or as transitions. However, it appears that current methods are approaching their limits. Therefore, this thesis explores characteristics of n-dimensional hypercubes and properties of longest maximal snakes as they pass through hypercubes in order to facilitate discovery of new search methods through a better understanding of hypercube space. This thesis also introduces a new search scheme that separates the hypercube nodes into various levels based on Pascal's triangle.

Index words: Snake-In-The-Box, Evolutionary Computing, Evolutionary Algorithm, Genetic Algorithm, Pascal's Triangle, Hypercube, Polygon Projection, Graph Theory, Heuristic Search, Constraint Satisfaction

An Analysis of Hypercube Space for Solving the Snake-In-The-Box Problem

by

Ananta Palani

B.S., University of Nevada, 2008

A Thesis Submitted to the Graduate Faculty
of The University of Georgia in Partial Fulfillment
of the
Requirements for the Degree

Master of Science

Athens, Georgia

2010

An Analysis of Hypercube Space for Solving the Snake-In-The-Box Problem

by

Ananta Palani

Approved:

Major Professor:	Walter D. Potter
Committee:	Khaled Rasheed Ronald W. McClendon

Electronic Version Approved:

Maureen Grasso
Dean of the Graduate School
The University of Georgia
May 2010

Dedication

To my wonderful wife Katie.

The universe is an infinite sphere whose center is everywhere and whose circumference is nowhere.

— Bernard Jaffe, *I Heart Huckabees*

Acknowledgments

I would like to thank my wife for her patience and understanding over the past few years while I worked to complete my studies and for always journeying with me on this and every adventure. I would also like to thank my family for their constant support and understanding. I would like to thank Dr. Potter for simultaneously pressuring me to continue, yet providing me ample room to explore many ideas while I worked to complete this thesis. I would like to thank Dr. Rasheed and Dr. McClendon for their assistance on my thesis and for their insight as members of my committee. I would like to thank Thomas Drapela for his insight on the B_2 3-face type. I would like to thank Dr. Covington for his expert knowledge of LaTeX, without which this thesis would not look nearly so consistent. I would also like to thank Dr. Covington for his helpful writing advice during the last few years.

Table of Contents

Page

Appendix

List of Figures

List of Tables

Chapter 1

The Snake-In-The-Box Problem

1.1 Introduction

This thesis examines the *snake-in-the-box* (SIB) problem in order to improve the design of search techniques for the SIB problem and similar graph theory problems. The SIB problem is concerned with finding the longest path possible through a hypercube, where a hypercube is a multidimensional shape made up of nodes that are spaced a fixed distance from all of their neighbors. In the lower dimensions, these hypercubes are familiar shapes. For instance, a dimension-1 hypercube is simply two nodes connected together by a line, or edge. Likewise, a dimension-2 hypercube is a square with four nodes and four edges, while a dimension-3 hypercube is a cube with eight nodes and twelve edges. As the snake travels through the hypercube, its path must always remain a certain distance from itself (i.e. it cannot overlap or cross) in order to be considered a valid snake path. As the dimensionality of the hypercubes increase, the problem complexity increases exponentially. This complexity makes the SIB problem extremely difficult to solve in dimensions above seven [19, 20].

There is no thorough analysis of the relationship between hypercubes and the longest possible snakes, which makes it difficult to determine how to properly search for snake paths. Current search techniques use only a basic understanding of the relationship between snake path and hypercube structure, which may account for the slow progress in the last decade. The content of this thesis examines the properties and characteristics of the longest possible snakes in hypercube dimensions 1–7 and provides recommendations for using this analysis in the design of heuristic search techniques so that better solutions may be found in higher dimensions.

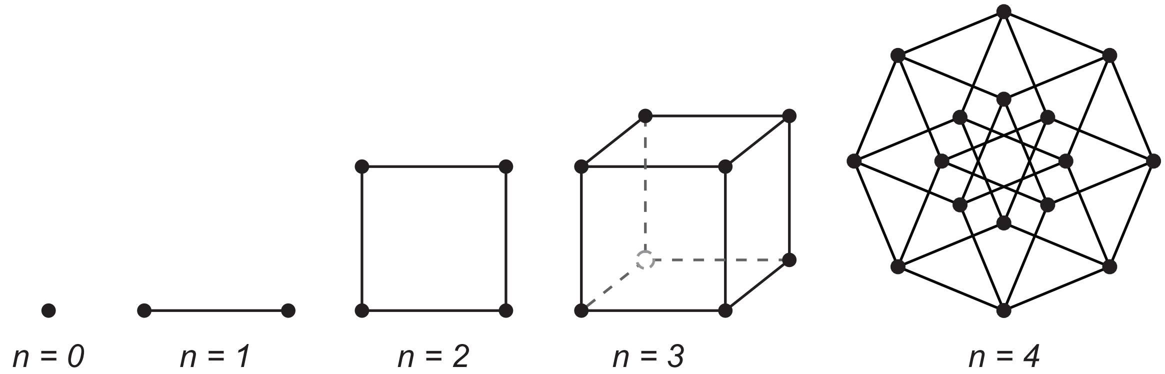

Figure 1.1: Projections of Hypercube Dimension 0–4 (n indicates dimensionality)

1.2 Background

A *hypercube* is a complicated network of vertices that are connected together by edges (they have an edge in common) where the distance between each vertex (node) is equal. All nodes connected to a given node are called *adjacent nodes*, where the number of adjacent nodes (and by proxy the number of edges) connected to the given node is equal to the dimensionality of the hypercube. For a 2-dimensional hypercube, every node has two adjacent nodes where each node is connected by an edge to the given node (i.e two edges connect to the given node). Additionally, every edge connected to a given node in the hypercube has a right angle between them. This is easy to visualize in the first three dimensions, but is much harder from dimension four and higher. Figure 1.1 shows projections of the first four hypercube dimensions.

The SIB problem is concerned with finding the longest path possible through an n-dimensional hypercube, with a few restrictions. Because the hypercube is a symmetrical shape, the snake path may begin from any node in the hypercube. This beginning node will be referred to as the *head* of the snake path, while the last node on the snake path will be referred to as the *tail* node. The path is a series of nodes connected by edges where the length of the path is the number of edges. *Adjacency constraints* require that all nodes on the path can only be connected (adjacent) to at most two other nodes on the path. A *coil* (also called a closed path or cycle) is a path where each node is connected to exactly two other nodes on the path (i.e. the head and tail connect, closing the path). A *snake* (also called an open path) is a path where all nodes are connected to exactly two other nodes except for the head and tail node which are connected to only one node. In a coil the number of nodes on the path is the same as the length of the path, while in a snake the number of nodes is one greater than the length of the path.

The SIB problem was initially proposed by Kautz in 1958 for use as error correction codes [16]. It is an NP-Hard problem that suffers from combinatorial explosion as the dimensionality increases [20]. Today there are many proposed uses for SIB codes including error correction, electronic combination locks, analog to digital conversion and signal processing, pattern recognition and classification, simplification of DNF in boolean algebra, electrical engineering, and network topologies [3, 4, 13, 16, 17, 18, 21].

Conventionally, the nodes in an n-dimensional hypercube are numbered beginning with zero and ending with $(2^n - 1)$. Nodes are adjacent if the binary value for their numbers only differ by a single bit. For instance, in a 2-dimensional hypercube the nodes one and three are adjacent because the binary value for one, $\{0,1\}$, and the binary value for three, $\{1,1\}$, differ only by the second bit (where the sequence is indexed right-to-left).

There are three main techniques for describing a path through the hypercube. The *node sequence* representation records the path as an ordered vector of nodes, where the first value in the vector is the head node and the last value is the tail node. The node sequence vector's length is equal to one greater than the path length. The *transition sequence* representation consists of an ordered vector of numbers called *transitions* that represent the bit that is changed in the previous node to arrive at the current node. The transition can also be thought of as the dimension or direction the path takes from the previous node to arrive at the current node. The transition sequence vector's length is equal to the length of the

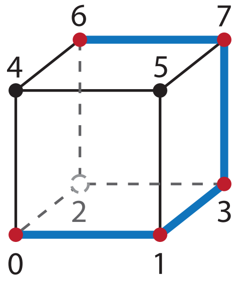

Figure 1.2: 3-Dimensional Hypercube with Snake Path

snake path. Note that a transition sequence is less constrained than a node sequence because it can represent 2^n snake paths depending on what the head node is, whereas the node sequence can only represent one path. However, both representations conventionally start from node zero. Additionally, any node sequence can be “moved” to start at any node in the hypercube by converting the node sequence to a transition sequence and then back to a node sequence with the head at the desired node. The conversion between a node sequence and a transition sequence representation is straight forward and simply involves determining the bit that is different between two consecutive nodes. The third representation is the *bit sequence* representation which consists of a vector containing positions for all 2^n nodes in the hypercube, where a “1” in the bit sequence indicates the node may be on the path, while a “0” indicates that the node is definitely not on the path. This is an indirect representation because the snake path has to be chosen from the “1” valued nodes [6].

Figure 1.2 shows one of the longest possible snake paths through a 3-dimensional hypercube. The length of the snake is four, and there are five nodes on the path. Due to node adjacency constraints the snake may not travel from node six to four, nor from node six to two since that would cause the snake to be adjacent to node zero, which is already on the snake. The node sequence representation of the snake is {0,1,3,7,6}, while the transition sequence is {0,1,2,0} and the bit sequence is {1,1,0,1,0,0,1,1}. For the purposes of this thesis all indices will begin at zero.

The SIB problem is similar to the traveling salesperson problem (TSP) with adjacency restrictions. However, in a TSP problem the goal is to minimize the path length, while in the SIB problem the goal is to maximize the path length. The SIB problem suffers from combinatorial explosion because the search space grows exponentially as the dimensionality increases [24]. This may be hard to visualize since the number of nodes from a given n-dimensional hypercube to an $(n + 1)$-dimensional hypercube is simply double. However, the complexity is exponentially greater due to the increased number of paths from a given node to any other node as a result of the connections between the added nodes and the original nodes. Appendix A contains the longest maximal snake and coil records for dimensions 1–12.

1.3 Current Search Methods

Exhaustive search is only feasible in dimensions 1–7 [19, 25]. Therefore, more intelligent search methods are needed for solving the SIB problem. Current search methods include non-recursive construction [12], extremal optimization [7], neural networks [2], ant colony optimization [11], genetic algorithms [6, 15, 20], and hybrid methods [4, 24]. Although these search techniques are all very sophisticated, progress has been extremely slow in the last fourteen years, with boundaries only slightly changing every few years. This is likely due to the problem that optimal solutions are not always close to near-optimal solutions. Additionally, most of these methods use very little knowledge of the search space. Therefore, a more thorough understanding of the SIB problem search space could help to overcome any limitations in current methods and provide ideas for the creation of new methods.

The only domain knowledge that most search methods employ involves adherence to adjacency constraints in order to ensure that the validity of the snake path is maintained as much as possible while search is progressing. Although this knowledge is crucial to finding any snakes, the search heuristic has larger problems. Most search methods operate on the idea that the best solutions are near good solutions. However, in the SIB problem the best solutions are extremely sharp peaks in the search space, making it difficult for a search heuristic to converge on the optimal solution.

1.4 Goals

The goal of this thesis is to increase the domain knowledge available for the SIB problem. Therefore, this thesis examines various properties of all longest snake paths and the hypercubes they travel through in dimensions 1–7. First, properties of the hypercube and its structure will be collected and analyzed. Second, all longest snake paths in dimensions 1–7 will be generated and examined. Finally, applications utilizing the collected data are proposed. Some of the characteristics that will be examined include how snake paths travel through a given hypercube and its sub-hypercubes, what the spread and density of snake path nodes are within a given hypercube, and frequency of transition between various dimensions of a given hypercube. Additionally, patterns in the collected data will be identified wherever possible so that they may be used to develop or enhance heuristic search in higher dimensions.

Chapter 2

Hypercube Analysis

2.1 m-Dimensional Hypercubes in n-Dimensional Space

Most search methods treat every n-dimensional hypercube as a single shape, thereby making the search space the maximum size and complexity possible. Instead, it may be beneficial to consider the lower dimensional hypercube elements that are essentially within the higher dimensional hypercube. This would allow the SIB problem to be broken into smaller pieces that could allow for a divide-and-conquer approach to solving the SIB problem. Additionally, it would allow for analysis of snake paths based on interconnected shapes and partial lower-dimensional hypercube paths. This would provide a clearer picture of the relationship between the snake and the hypercube, such as the constraints that the hypercube places on the snake path that force the path to have the shape it does to be the longest snake possible. A complete understanding of the internal structure could potentially allow for the direct construction of the longest snakes possible without requiring any search method.

Equation 2.1 provides the formula for the number of dimension-m hypercubes within a given dimension-n hypercube, where $0 \leq m \leq n$.

$$2^{n-m} * \binom{n}{m} \tag{2.1}$$

Dimension-m hypercubes will be referred to as *m-faces*, while a vertex in any hypercube may be interchangeably referred to as a *node*.

Every node in a given dimension-n hypercube has n adjacent nodes connected by n edges. Since an edge is a dimension-1 hypercube, each node takes part in n dimension-1 hypercubes. If you imagine a 3-face (a cube), each node is connected to three other nodes and takes part in three edges. Extending this idea further, each node is a part of six 2-faces (squares) because for each 2-face the node will participate in two edges. Therefore, for the three edges that the node participates in, two of those edges are used per 2-face, so there are $\binom{3}{2}$ 2-faces that every node in the 3-face participates in (i.e. six 2-faces). Generalizing this, each node in a given dimension-n hypercube participates in $\binom{n}{m}$ m-faces, where $0 \leq m \leq n$. This accounts for the second term of Equation 2.1.

Increasing the dimensionality of a hypercube from k to $k+1$ essentially extrudes all vertices of the dimension-k hypercube into dimension-$(k+1)$ with the resulting dimension-$(k+1)$ hypercube containing twice as many vertices. Therefore, the number of vertices in a given dimension-n hypercube is 2^n, where dimension-0 represents the dimensionality of the vertex itself (i.e. a point in space with no area or length), dimension-1 represents a line or an edge with two vertices, dimension-2 represents a plane or a square with four vertices, etc.

If every node in a given dimension-n hypercube were considered separately as participating in various m-faces, then each of the 2^m nodes of a given m-face would contribute that same m-face to the total count of m-faces rather than counting it only once. Therefore, the product of the number of nodes 2^n in a given dimension-n hypercube and the second term in Equation 2.1 needs to be scaled by the number of nodes 2^m in the m-face so that each m-face is counted only once. This results in $\frac{2^n * \binom{n}{m}}{2^m}$, or $\frac{2^n}{2^m} * \binom{n}{m}$, which reduces to Equation 2.1. Table 2.1 contains counts of the number of m-faces in dimensions 1–12. Note that in every third dimension starting with dimension-2 there are two m-faces with the same count, implying a possible relationship or shared characteristic between these dimensions.

Table 2.1: n-Dimensional Hypercube m-Face Count

Dimension	m-Face												
n	0[a]	1[b]	2[c]	3[d]	4[e]	5	6	7	8	9	10	11	12
0[a]	1												
1[b]	2	1											
2[c]	4	4	1										
3[d]	8	12	6	1									
4[e]	16	32	24	8	1								
5	32	80	80	40	10	1							
6	64	192	240	160	60	12	1						
7	128	448	672	560	280	84	14	1					
8	256	1 024	1 792	1 792	1 120	448	112	16	1				
9	512	2 304	4 608	5 376	4 032	2 016	672	144	18	1			
10	1024	5 120	11 520	15 360	13 440	8 064	3 360	960	180	20	1		
11	2048	11 264	28 160	42 240	42 240	29 568	14 784	5 280	1320	220	22	1	
12	4096	24 576	67 584	112 640	126 720	101 376	59 136	25 344	7920	1760	264	24	1

[a] node or vertex [b] edge or line [c] square or face [d] cube or cell [e] tesseract

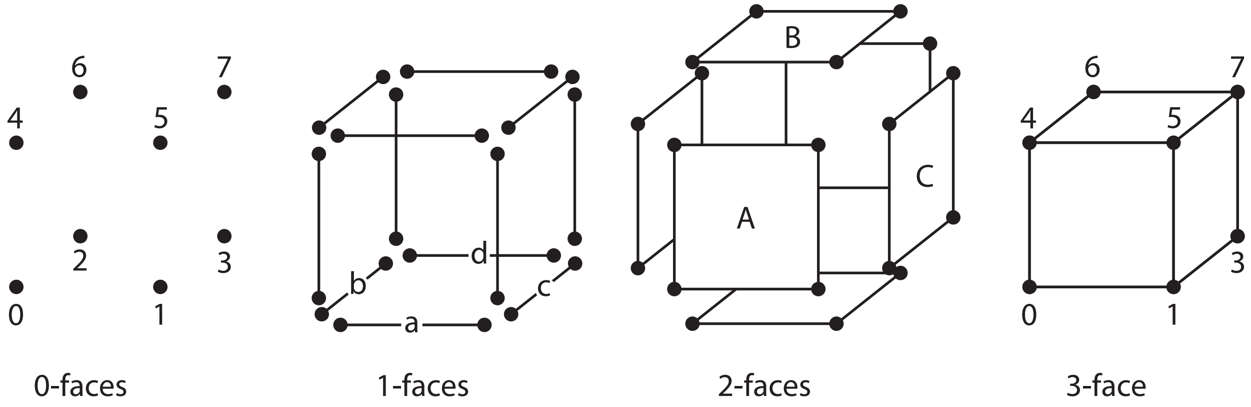

Figure 2.1: m-Faces within a 3-Dimensional Hypercube (some 1-faces and 2-faces are labeled)

Using the conventional hypercube numbering system, where the lowest node value is zero and the number for every node that is adjacent to a given node along an edge differs by only one bit to the given node (a transition), it is possible to generate all m-faces in any n-dimensional hypercube. This is done by using the binary value of the number assigned to each node and observing that all nodes in a given hypercube all have certain bits in their binary value that are the same. These bits shall be called *care bits*, while the bits that may differ between nodes shall be called *don't care bits*. This bit-wise relationship between nodes in a hypercube is easiest to see by looking at lower-dimensional hypercubes. Figure 2.1 shows all m-faces in a 3-dimensional hypercube, where there are eight 0-faces (nodes), twelve 1-faces (edges), six 2-faces, and one 3-face (the 3-dimensional hypercube itself).

For an edge, only a single bit differs between the two connected nodes. For a 2-face only two bits differ between the four nodes in the 2-face. For a 3-face (a cube) only 3 bits differ between all the nodes in the 3-face. Therefore, for a given n-dimensional hypercube there are n don't care bits, which makes sense when considering that the first node of the hypercube has no bits set (i.e. zero), while the last node of the hypercube has n bits set (i.e. $2^n - 1$). Generalizing this, for an n-dimensional hypercube with m-dimensional hypercubes inside, each m-dimensional hypercube has $(n - m)$ care bits and m don't care bits. These care bits are like a signature for the m-dimensional hypercube because they may be used to uniquely identify the m-face in the n-dimensional hypercube. For instance, 1-face “a” in Figure 2.1 has nodes “0” and “1”. Since “a” is in a 3-dimensional hypercube, each node has three bits. Therefore, nodes “0” and “1” have bits $\{0,0,0\}$ and $\{0,0,1\}$ respectively (where the bits are indexed from right to left). Since bit zero differs between “0” and “1”, bit zero is a don’t care bit and the other two bits are care bits. The signature for “a” can then be written as $\{0,0,X\}$, where X represents the don’t care bits (because they can be any value) and the care bits are identified by their actual value. The signature for the 1-face “b” would be $\{0,X,0\}$. This process also holds for the 2-faces. For instance, 2-face “C” has nodes “1”,“3”,“5”,“7” with bits $\{0,0,1\}$,$\{0,1,1\}$,$\{1,0,1\}$, and $\{1,1,1\}$. Therefore, the signature for “C” is $\{X,X,1\}$. Likewise, the signature for “B” is $\{1,X,X\}$. Note that 0-faces have only care bits, and the m-face where $m = n$ has only don’t care bits. For instance, in Figure 2.1 the 3-face only has don’t care bits since it is the 3-dimensional hypercube, so its signature would be $\{X,X,X\}$.

All nodes within each m-face may be calculated by starting with the care bits and generating all possible permutations for the don’t care bits. Note that the care bits and don’t care bits are only sometimes contiguous in the binary value for a given node, so calculation is not a simple matter of appending a permutation of the range zero to $(2^n - 1)$. Instead, the permutations of don’t care bits need to be inserted into the appropriate index position of the binary value to generate the nodes in the m-face.

2.2 2-Face and 3-Face Types

Rather than consider only m-face counts in a given dimension-n hypercube, it could be useful to classify the partial snake paths that could incorporate a 2-face or 3-face shape, both of which are building blocks of higher-dimensional hypercubes. Additionally, every snake path in a hypercube travels through a series of 2-face and 3-face shapes within the hypercube. Identifying all possible types of 2-face and 3-face shapes would allow the larger shape of the snake path to be identified, as well as any characteristics of the hypercube itself, such as proximity of certain types to each other, or type density. Appendix C.1 and C.2 contain images of the various 2-face and 3-face types respectively. Solov'eva first proposed (without images) the 2-face types as "partitions" of the set of "all 2-dimensional faces," with the exception of A_6 which has been added for completeness [23]. Sections 5.4.4 and 5.4.5 examine how the number of 2-faces and 3-faces change as various snake paths grow through hypercubes of dimensions 1–7.

2.3 sub-m-Dimensional Hypercubes

Just as every n-dimensional hypercube has smaller hypercube m-faces inside, those m-faces also have smaller hypercubes inside which shall be referred to as *sub-m-faces*. The easiest way to calculate the sub-m-faces in a given m-face is by iterating all k-faces, where $k \leq m \leq n$ and checking whether all the nodes in the k-face are within the m-face. This process could be done once and saved in an array for speed.

2.4 m-Dimensional Hypercube Vertex Participation

Section 2.1 derived the formula for calculating the number of m-faces that each node in a given n-dimensional hypercube participates in and found the number to be $\binom{n}{m}$. Table 2.2 contains the count of the number of m-faces a given node participates in for n-dimensional hypercubes in dimensions 1–12. Notice that the node participation counts match Pascal's triangle in Appendix D.1 where dimension n in Table 2.2 is equal to the row index in Pascal's triangle. This is probably a simple coincidence because $\binom{n}{m}$ is one of the methods for calculating Pascal's triangle, where n is the row and m is the column in that row. The simplest way to calculate the actual m-faces a given node participates in is by iterating over all m-faces calculated in the manner described in Section 2.1 and checking whether the given node is within the m-face. This process could be done once and saved in an array for speed.

Table 2.2: n-Dimensional Vertex m-Face Participation Count

Dimension	m-Face												
n	0[a]	1[b]	2[c]	3[d]	4[e]	5	6	7	8	9	10	11	12
0[a]	1												
1[b]	1	1											
2[c]	1	2	1										
3[d]	1	3	3	1									
4[e]	1	4	6	4	1								
5	1	5	10	10	5	1							
6	1	6	15	20	15	6	1						
7	1	7	21	35	35	21	7	1					
8	1	8	28	56	70	56	28	8	1				
9	1	9	36	84	126	126	84	36	9	1			
10	1	10	45	120	210	252	210	120	45	10	1		
11	1	11	55	165	330	462	462	330	165	55	11	1	
12	1	12	66	220	495	792	924	792	495	220	66	12	1

[a] node or vertex [b] edge or line [c] square or face [d] cube or cell [e] tesseract

Chapter 3

Level Structure Analysis

3.1 Initial Proposal

Observing that a hypercube may be represented in 2-dimensional space as a Petrie polygon projection [5, p. 24–25, 123, 223–230], the snake path through a 4-dimensional hypercube (a tesseract) can easily be visualized in pseudo-3-dimensional space as shown in Figure 3.1. The path is the bold line that begins at node zero and is the longest snake path possible in a 4-dimensional hypercube. By dimming the remaining lines on each of the cubes that the snake passes through, a 3-dimensional shape appears within the 2-dimensional projection of the 4-dimensional hypercube. If nodes 0–3 and 12–15 are considered surfaces, then those two surfaces form the lowest and highest levels of the initial level structure. The remaining level is then formed from the remaining nodes, and is shown as two intersecting squares in the center of the tesseract. Therefore, for a tesseract there are three levels of four, eight, and four nodes respectively. The 3-dimensional hypercube (a cube) in Figure 1.2 shows two levels with four nodes each.

If the hypercube is assumed to have a lowest and a highest level of four nodes each in successive dimensions, then a multiple of Pascal's triangle may be built as shown in Table 3.1. Since the initial level will contain four nodes, the multiplier will be four and every n-dimensional hypercube will correspond to row $(n-2)$ in Pascal's triangle. Each row in the triangle represents the distribution of hypercube nodes within the initial level structure. For example, in dimension four there are a total of sixteen nodes in three levels. This orientation reduces the search space by reducing the number of adjacent nodes that a search algorithm can see by restricting visible adjacencies to the given level.

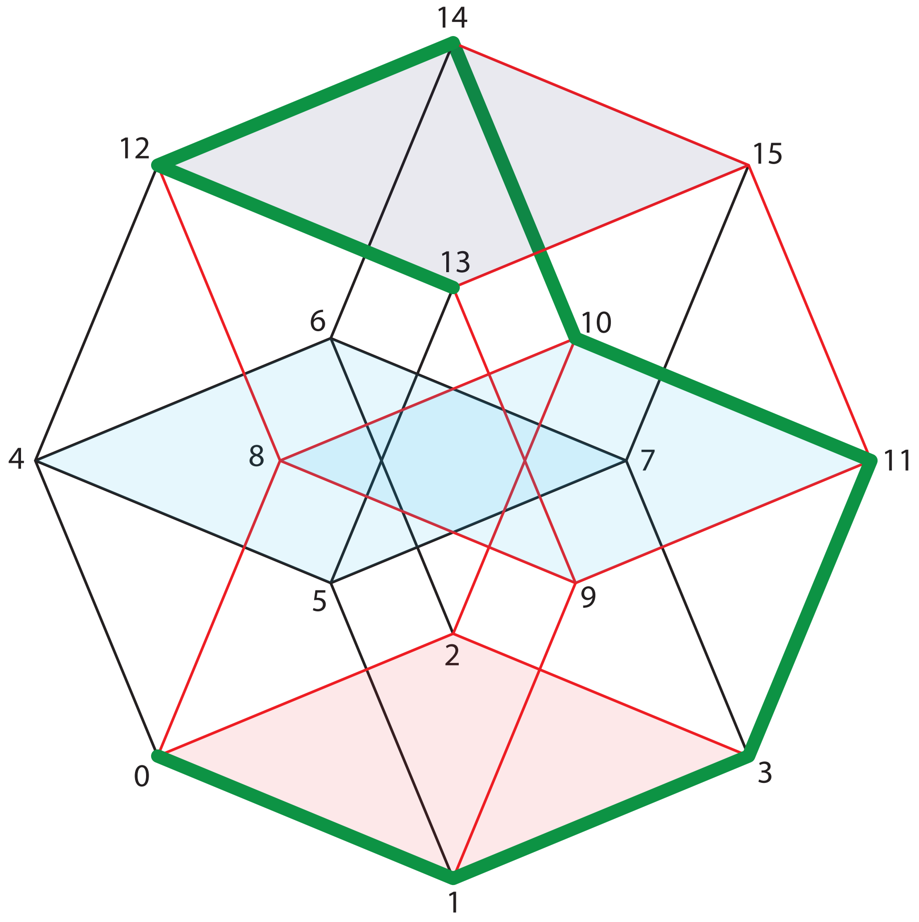

Figure 3.1: 4-Dimensional Hypercube with Levels and Snake Path

Table 3.1: Pascal's Triangle Multiplied by Four

Dimension		Triangle														
n	Nodes	Row	Sum													
2	4	0	4							4						
3	8	1	8						4		4					
4	16	2	16					4		8		4				
5	32	3	32				4		12		12		4			
6	64	4	64			4		16		24		16		4		
7	128	5	128		4		20		40		40		20		4	
8	256	6	256	4		24		60		80		60		24		4

Since this thesis uses a conventional representation by starting all snakes at node zero, observations based on Figure 1.2 and 3.1 are used to distribute the nodes into the levels. Therefore, the hypercube nodes will be assigned to levels in numerical order starting with node zero assigned to level zero and counting up to node $(2^n - 1)$, assigning each node to the given level until that level is full, and then moving to the next level.

With the level distribution completed, a guided random search of an 8-dimensional hypercube was performed. The search algorithm always began at node zero (level zero) and would add nodes onto the snake in a given level while there were still nodes available before moving on to the next level. The search algorithm essentially fills a level as completely as possible, which might normally be problematic except that the idea of distributing the nodes into levels was to reduce the search space such that a near-linear search will always find the longest snake possible.

After a few hours of performing the search a 93 length snake was found. Unfortunately, after two weeks and several billion runs, no further progress was made. The algorithm was then modified to allow the search to randomly leave some levels sparse (by not building the snake too densely in a given level), to allow the snake to search for the next node starting from the bottom and searching up, starting from the same level as the tail node, or from a random level. These changes had no effect on the search results, with 93 still the best length after several billion runs with each configuration. Finally, the level structure was altered to use a different multiplier (and a different row in Pascal's triangle). For a multiple of two, the appropriate row for an n-dimensional hypercube is $(n - 1)$, and for a multiple of one, the appropriate row is n. Although these new level distributions allowed the 93 length snake to be found faster, after several billion more runs each, no additional progress was made.

It is highly likely that this search method was only partially successful because the number of levels in the distribution increases at the same rate as the hypercube dimensionality, while each level gets much wider (i.e. the number of nodes in each level increases more quickly). The hardest portion of the search space is near the middle of the snake because a majority of the nodes in the hypercube are still available to grow the snake, which means that there are many different directions to explore. At the beginning the choices are few, and at the end there are even fewer choices since most available nodes have been eliminated by the snake path. Since values in Pascal's triangle mirror this observation, with values in the center of the row being larger than those on the ends, the level structure as it stands provides limited benefit because the greatest number of available nodes will exist near the middle. Therefore, a representation should work harder to reduce the search space by reducing the number of choices, so there should be more levels with fewer nodes per level. However, Section 4.3 shows that the sequentially numbered nodes in the hypercube often occur in blocks of a single type, which may prohibit any level structure that distributes nodes in a linear fashion, especially if additional levels with fewer nodes are added to the representation.

3.2 Hypercube Level Structure

Since linear assignment of nodes into levels failed to generate expected results, a different approach was taken that would allow a moderately reduced search space, while providing a new avenue for analysis of longest known snakes in any dimension. This time the adjacency of nodes is preserved by assigning nodes into levels based on the count of bits set to "1" in the binary value of the node's number [9]. Therefore, level zero will contain all numbers with zero bits set, level one will contain all numbers with one bit set, and level n will contain numbers with n bits set. As a result there will always be $(n+1)$ levels for an n-dimensional hypercube, which indicates that row n in Pascal's triangle may be used without multiplication. This distribution of nodes makes sense when realizing that the formula $\binom{n}{m}$ for calculating the value at a given row n and column m in Pascal's triangle is the same formula for calculating the number of permutations with m bits set to "1" in a bit sequence of width n. This novel distribution of nodes shall be termed the *hypercube level structure*.

Since nodes that differ by only a single bit are adjacent to each other in a given hypercube (a transition difference), a node on a given level is only adjacent to nodes that are exactly one level lower or higher, but never on the same level. This has the benefit that the level of a given node specifies the shortest distance (in edges or transitions) between any two nodes in the hypercube. For instance, if a given node is on level one and another node is on level four, the nodes are minimally three edges away from each other (therefore they must also have three bits that are different). As a result, level zero always (and only) contains node zero, and level n always (and only) contains node $(2^n - 1)$, the bitwise opposite of node zero. Additionally, the structure has the added effect that for a given node, all adjacent nodes in a lower level also have a lower numerical value, while adjacent nodes in higher levels have a higher value. See Appendix D.1 for the first 15 rows of Pascal's triangle and Appendix D.2 for the distribution of all nodes into the hypercube level structure for dimensions 1–7. Chapter 4 examines the way that snake paths travel through the hypercube level structure.

Table 3.2 splits the levels into *hypercube level groups* (HLGs) that identify what portion of the hypercube level structure a given level is in. For n-dimensional hypercubes where n is even, there are an odd number of levels so the center level is placed in "C" for center, while all the lower levels are placed in "L" and the higher levels are placed in "R". In odd dimensions the levels are broken in half and there is no "C" value. Section 4.8 utilizes the HLGs to examine snake paths through hypercube dimensions 1–7.

Table 3.2: Hypercube Level Group (HLG)

Dimension	Hypercube Level Group		
n	L	C	R
1	0		1
2	0	1	2
3	0,1		2,3
4	0,1	2	3,4
5	0,1,2		3,4,5
6	0,1,2	3	4,5,6
7	0,1,2,3		4,5,6,7
8	0,1,2,3	4	5,6,7,8
9	0,1,2,3,4		5,6,7,8,9
10	0,1,2,3,4	5	6,7,8,9,10
11	0,1,2,3,4,5		6,7,8,9,10,11
12	0,1,2,3,4,5	6	7,8,9,10,11,12

Chapter 4

Longest Maximal Snake Analysis

4.1 Maximal Snake

A *maximal snake* is a snake path that cannot be extended because there are no available nodes for the path to extend to. A subset of these paths are the *longest maximal snakes*, which are maximal snakes whose length is the longest possible snake length (known only through exhaustive search) in the given dimension. Being maximal or longest maximal does not imply that the path has exhausted all available nodes in the hypercube, nor does it inherently define a degree of tightness to the snake within a hypercube. Being maximal simply identifies that the path has reached a dead-end, and being longest maximal simply identifies the snake path as the longest possible in the given dimension.

Table 4.1 contains statistics for all shortest and longest maximal snakes in dimensions 1–7 obtained by exhaustive search of those dimensions. Within each dimension, all longest maximal snakes share the same hypercube node type distribution. *Snake nodes* are hypercube nodes that are connected by the snake path, while *skin nodes* are those that are adjacent to any snake node. An *available node* is neither a skin nor a snake node and represents a location in the hypercube that the snake could theoretically include if the node were reachable (i.e. the node does not violate any path constraints). An *unshared node* is a snake node that is adjacent to at most one skin node. An analysis of how the hypercube node type distribution changes as the longest maximal snakes grow is given in Section 5.4.

Table 4.1: Shortest and Longest Maximal Snake Statistics

		Longest Maximal Snake							
Dimension n	Shortest Maximal Snake Length (edges)	Length (edges)	Hypercube Node Type Distribution				Equivalence Class (EC)		
			Snake	Skin	Available	Unshared	Count	Snakes per EC ($n!$)[1]	Total Snakes
1	1	1	2	0	0	2	1	1	1
2	2	2	3	1	0	3	1	2	2
3	4	4	5	3	0	3	1	6	6
4	6	7	8	8	0	0	1	24	24
5	8	13	14	18	0	0	8	120	960
6	10	26	27	36	1	0	1	720	720
7	12	50	51	76	1	0	12	5040	60 480

[1] There are $n!$ snakes per EC starting from a single node in the hypercube (for example node zero). Therefore, there are actually $2^n * n!$ snakes per EC if snakes begin from any node and $(EC\ Count) * 2^n * n!$ total snakes in dimension-n.

Table 4.1 also describes the number of equivalence classes in each dimension. An equivalence class essentially represents a group of snakes. Once an equivalence class has been identified all snakes within the equivalence class can be generated. Therefore the value for "Total Snakes" is the complete number of longest maximal snakes in its corresponding dimension. Equivalence classes are described in more detail in Chapter 5.

Although the shortest maximal snake lengths appear to follow a predictable pattern in Table 4.1, an analysis of dimensions 8–12 should be performed to determine if the pattern remains. Currently there is no known formula to calculate the length of the longest maximal snakes in a given dimension, although it is known that the upper bound is at most (2^{n-1}) [1, 8]. The best estimate for the upper bound in dimensions greater than seven is $(2^{n-1} - \frac{2^n}{n^2+n+2})$, although there are better upper bound estimates for higher dimensions [8, 23]. It is interesting to note that all maximal snakes are also longest maximal snakes in dimensions 1–3. Note that the number of edges in a path length is also the same as the number of transitions in the path. See Appendix A for current longest maximal snake length records in dimensions greater than seven.

4.2 Distance from Head to Tail Node and Head to Mid-Point Node

The distance from the head to any given node is the number of edges (transitions) on the shortest possible path between the head and the given node. The number of edges between two nodes reveals not only how close the nodes are, but also the smallest hypercube that both nodes share. For instance, if two nodes are separated by a single edge, then they share a dimension-1 hypercube (a line). If they are two edges apart, then they share a dimension-2 hypercube (a square). If they are n edges apart, then they share a dimension-n hypercube. In all cases, the distance n between the given nodes is the greatest distance possible between any two nodes on the dimension-n hypercube they share (i.e. they are as far away as possible on the shared hypercube since the hypercube is the minimal dimensionality that can connect them together).

Table 4.2: Longest Maximal Snake Head to Tail Node and Head to Mid-Point Node Distance

Dimension		Distance (edges)	
n	NLP	Tail	Mid-Point
1		1	
2		2	1
3		2	2
4		3	3 (L) and 2 (R)
5		3	2 (L) and 3 (R)
6		2	3
7	1,3,4,5,9,12	2	3
	8,11	4	3
	2,7,10	6	3
	6	6	5

Table 4.2 shows all distances for dimensions 1–7 for all longest maximal snakes in the given dimension. The longest maximal snakes in dimension four and five have an even number of nodes, so there is no exact mid-point node. Therefore, the immediate-left and -right nodes of a virtual mid-point that splits the node sequence in half is indicated in Table 4.2 by (L) and (R) respectively. Dimension seven is unique in that there are different distances depending on the node level pattern (NLP) for a given longest maximal snake. The applicable NLPs from Table 4.6 are also provided when there is a difference between NLPs for distance in a given dimension.

Knowing the distance between the head node and both the tail node and the mid-point node is useful in determining a degree of compactness in the snake both as the snake grows and at completion. It is interesting to observe from Table 4.2 that most longest maximal snakes end very close to where they start, in many cases with both nodes on the same square or cube. Additionally, the mid-point node is generally very close to the starting node. These characteristics may be helpful in developing an intelligent direct-construction algorithm, as guidance in developing a repair operator for an evolutionary algorithm, or as part of a fitness function.

Table 4.3: Longest Maximal Snake Hypercube Map Characteristics

Dimension	Specific Hypercube Nodes That Are Always:		Contiguous Nodes (Canonical)				Contiguous Nodes (All LMS)			
			Skin		Snake		Skin		Snake	
n	Skin	Snake [snake index]	Min.	Max.	Min.	Max.	Min.	Max.	Min.	Max.
1		0 [0], 1 [1]	0	0	2	2	0	0	2	2
2		0 [0]	1	1	1	2	1	1	1	2
3		0 [0], 7 [3]	1	2	1	2	1	3	1	3
4	15	0 [0]	1	4	1	3	1	6	1	5
5	31	0 [0]	1	4	1	5	1	9	1	6
6		0 [0], 63 [16]	1	7	1	3	1	9	1	5
7		0 [0]	1	11	1	5	1	13	1	6

4.3 Hypercube Map

The *hypercube map* is a novel view of the hypercube that may be obtained by generating a vector of the same length as the number of nodes in the hypercube, with each position in the vector corresponding to a node in the hypercube. Therefore, node zero in the hypercube is position zero in the vector, node one is position one, etc. For each node, the hypercube map stores a value indicating the type of node. If the node is available or is a skin node then a character is used to indicate either. However, if the node is a snake node, the node's index in the node sequence is used. There are too many longest maximal snakes to show all of them (see *Total Count* in Table 4.1), but a small sample may be seen in Appendix B.1.

Table 4.3 collects two sets of data from the hypercube maps of all longest maximal snakes in dimensions 1–7. The first set of data is the specific nodes in the hypercube that are always skin or snake. Although not every dimension has a node that is always skin, when there is one it is always the highest node in the hypercube map ($2^n - 1$). Likewise, when a non-zero hypercube node is always a snake node, it occupies the exact same location on the snake (i.e. it has the same snake index, in all longest maximal snakes in that dimension). The second set of data is the minimum and maximum number of sequential nodes that occur as a contiguous block in the hypercube map that are all the same type. Note that in dimension-1 there cannot be any skin nodes. Whether any of these observations hold in higher dimensions remains to be seen.

4.4 Skin Density Pattern (SDP)

As discussed in Section 4.1, a skin node is any hypercube node that is adjacent to a snake path node but is not itself a snake node. In this way, skin nodes are literally the "skin" of the snake path through the hypercube since they are all nodes that surround the snake path through the hypercube. *Skin density* for a given skin node represents the number of snake nodes that the skin node is adjacent to. For instance, if a skin node is adjacent to two snake nodes, then its skin density is two. A skin node by definition cannot have a skin density of zero, nor can it have a skin density greater than n since every node in the hypercube has exactly n connections to other nodes. By extension, a *skin density pattern* (SDP) is a new representation that records the state of all skin nodes in a dimension-n hypercube (with a longest maximal snake running through it) by counting all skin nodes of skin density one to n.

Table 4.4 collects the SDPs for all longest maximal snakes in dimensions 1–7. If there is only one SDP for a given dimension then that SDP is not numbered. Note that dimension five and seven are the only dimensions with more than one SDP. Besides the skin density node counts, the minimum and maximum skin density and the average skin density are recorded. It is interesting to observe that, although the minimum and maximum skin density values may differ between SDP within the same dimension, the average skin density remains the same. This implies that even though the compactness or tightness of the snake path may vary, there are certain constraints forced by the geometry of the hypercube which only allow longest maximal snakes to occur under very specific conditions, thereby mandating a consistency in the "skin" of the snake path.

It is also interesting to observe from Table 4.4 that some dimensions have no nodes with a skin density of one (note that this is expected in dimension-1 since there can be no skin

Table 4.4: Longest Maximal Snake Skin Density Pattern (SDP)

Dimension		Skin Density Node Count							Skin Density			
n	SDP	1	2	3	4	5	6	7	Min.	Max.	Avg.	Avg./n
1		0							0	0	0.0000	0.0000
2		0	1						2	2	2.0000	1.0000
3		0	2	1					2	3	2.3333	0.7778
4		2	2	4	0				1	3	2.2500	0.5625
5	1	2	6	10	0	0			1	3	2.4444	0.4889
	2	1	9	7	1	0			1	4	2.4444	0.4889
	3	0	12	4	2	0			2	4	2.4444	0.4889
6		0	13	10	11	2	0		2	5	3.0556	0.5093
7	1	8	4	25	29	10	0	0	1	5	3.3816	0.4831
	2	7	8	21	29	11	0	0	1	5	3.3816	0.4831
	3	7	7	22	30	10	0	0	1	5	3.3816	0.4831
	4	7	5	24	32	8	0	0	1	5	3.3816	0.4831
	5	7	4	27	29	9	0	0	1	5	3.3816	0.4831
	6	6	7	24	30	9	0	0	1	5	3.3816	0.4831

nodes), and all dimensions above three have no nodes with a skin density of n. Additionally, dimension-5 and -7 have SDPs where no skin nodes have a skin density of $(n-1)$. Likewise, there are more skin nodes with a skin density near the median. These characteristics are reminiscent of a bell-shaped distribution of skin density and imply that a snake path cannot be too loose nor too tight within the hypercube in order to be a longest maximal snake, likely mandated by the hypercube geometry. Whether these distributions are predictable remains uncertain.

4.5 Transition Frequency Pattern (TFP)

When examining the transition sequences of all longest maximal snakes it becomes obvious that there is a repetitive pattern of transition frequency. This pattern shall be identified by the new term *transition frequency pattern* (TFP). The TFP does not explicitly define the number of specific occurrences of a given transition that a longest maximal snake must

Table 4.5: Longest Maximal Snake Transition Frequency Pattern (TFP)

Dimension									Permutations	
n	TFP	Bag of Transition Frequencies							Canonical	Total
1		1							1	1
2		1	1						1	1
3		2	1	1					1	3
4		3	2	1	1				1	12
5		4	3	3	2	1			3	60
6		6	6	5	5	2	2		1	90
7	1	16	8	8	8	5	3	2	2	840
	2	15	9	9	7	5	3	2	2	2520
	3	15	8	8	8	6	4	1	2	840
	4	14	9	8	7	7	4	1	2	2520
	5	13	9	9	7	7	4	1	2	1260

have. Instead, the TFP provides a bag of frequencies from which the transition counts of a given longest maximal snake must be a permutation. This property is due to the symmetric geometry of the hypercube and becomes more evident when equivalence classes and canonical snakes are discussed in Chapter 5.

Table 4.5 collects all transition frequency patterns for dimensions 1–7. If there is only one TFP for a given dimension then that TFP is not numbered. Dimension seven is oddly the only dimension with more than one TFP, which implies that the structure of the hypercube may have an unusual geometric property as compared to the lower dimensions. Since the TFP represents a bag (multiset) of frequency values, the total number of permutations is given by Equation 4.1, where K is the number of unique values in the TFP and m_i is the occurrence count of each value in the TFP.

$$\frac{n!}{\displaystyle\prod_{i=1}^{K} m_i!} \tag{4.1}$$

There is at least one longest maximal snake for each permutation of a given TFP, but the total number of permutations is not indicative of the total number of longest maximal snakes in a given dimension because that would require knowing the total number of equivalence classes. The number of canonical permutations is related to equivalence classes and is discussed further in Chapter 5.

4.6 Node Level Pattern (NLP)

A *Node Level Pattern* (NLP) is a new term for the path that a longest maximal snake takes through the level-based representation of the hypercube described in Section 3.2. The NLP is the same length as the node sequence representation of the snake path, where for each position on the snake the NLP stores the corresponding level of the hypercube level structure that the snake node resides in. Since node zero is always on level zero in this structure, and snakes conventionally start at node zero, all NLPs start at level zero. In a sense the NLP is like a road map because a exhaustive search algorithm can use the NLP to direct the snake growth by only extending the snake path to adjacent nodes in the level that the NLP indicates is next. Since each level in the level structure contains more than one node (except the first and last level; see Appendix D.2), there must be multiple longest maximal snakes per NLP.

Table 4.6 shows all NLPs for all longest maximal snakes in dimensions 1–7. It is interesting to observe that there is a one-to-one correspondence of NLP to equivalence class EC in dimension seven, while in dimension five the situation is much different. As Section 4.1 has shown, all ECs in a given dimension have the same number of longest maximal snakes, which implies that an NLP with more ECs provides more opportunities for snake growth, thereby leading to a greater number of longest maximal snakes for that NLP.

Table 4.6: Longest Maximal Snake Hypercube Node Level Pattern (NLP)

Dimension			Node Sequence Index																																																			
n	NLP	EC	0	1	2	3	4	5	6	7	8	9	10	11	12	13	14	15	16	17	18	19	20	21	22	23	24	25	26	27	28	29	30	31	32	33	34	35	36	37	38	39	40	41	42	43	44	45	46	47	48	49	50
1			0	1																																															
2			0	1	2																																														
3			0	1	2	3	2																																												
4			0	1	2	3	2	3	2	3																																									
5	1	2, 6, 7, 8	0	1	2	3	4	3	2	3	2	3	2	3	4	3																																			
	2	5	0	1	2	3	4	3	2	3	2	3	4	3	2	3																																			
	3	1, 3, 4	0	1	2	3	4	3	2	3	4	3	4	3	2	3																																			
6			0	1	2	3	4	3	2	3	2	3	4	3	2	3	4	5	6	5	4	3	2	3	2	3	2	3	2																						
7	1	1	0	1	2	3	2	3	2	3	4	3	4	3	2	3	4	3	4	3	2	3	2	3	4	3	2	3	2	3	4	5	6	5	4	5	6	5	4	3	4	5	6	5	6	5	4	5	6	5	4	3	2
	2	2	0	1	2	3	2	3	2	3	4	3	4	3	2	3	4	3	4	3	2	3	2	3	4	3	2	3	2	3	4	5	6	5	4	5	6	5	4	3	4	5	6	5	6	5	4	3	2	3	4	5	6
	3	3	0	1	2	3	2	3	2	3	4	3	4	3	2	3	2	3	4	3	2	3	2	3	4	3	2	3	2	3	4	5	6	5	4	5	6	5	4	3	4	5	6	5	6	5	4	5	6	5	4	3	2
	4	4	0	1	2	3	4	3	2	3	4	3	4	3	2	3	4	5	6	5	6	5	6	5	4	3	2	3	4	5	6	5	4	3	2	3	4	3	2	3	4	3	4	3	4	3	2	3	4	5	4	3	2
	5	5	0	1	2	3	4	3	2	3	4	3	4	3	2	3	4	5	6	5	6	5	6	5	4	3	2	3	4	5	6	5	4	3	2	3	4	3	4	3	4	3	4	3	4	3	2	3	4	5	4	3	2
	6	6	0	1	2	3	4	3	2	3	2	3	2	3	4	5	4	3	2	3	4	3	2	3	4	5	6	5	6	5	4	5	6	5	4	3	2	3	2	3	4	3	2	3	2	3	4	3	4	3	4	5	6
	7	7	0	1	2	3	4	3	4	3	2	3	2	3	4	3	2	3	2	3	4	5	6	5	4	3	2	3	2	3	4	3	2	3	4	5	6	5	6	5	4	5	6	5	4	3	2	3	2	3	4	5	6
	8	8	0	1	2	3	4	3	4	3	4	5	4	3	4	3	2	3	2	3	2	3	4	5	4	3	2	3	4	3	4	3	2	3	4	5	4	5	6	7	6	5	4	3	2	3	4	5	4	3	2	3	4
	9	9	0	1	2	3	4	3	4	3	4	5	4	5	4	3	2	3	2	3	2	3	4	5	4	3	2	3	4	5	4	5	4	3	2	3	4	5	4	3	4	3	4	5	6	7	6	5	4	5	4	3	2
	10	10	0	1	2	3	4	5	6	5	4	3	2	3	4	3	2	3	2	3	2	3	4	3	2	3	4	3	4	3	2	3	2	3	4	5	6	5	6	5	4	5	6	5	4	3	2	3	2	3	4	5	6
	11	11	0	1	2	3	4	5	6	5	4	3	2	3	4	3	2	3	2	3	2	3	2	3	2	3	4	3	4	3	2	3	2	3	4	5	6	5	4	5	4	5	6	5	4	3	2	3	4	5	6	5	4
	12	12	0	1	2	3	4	5	6	5	4	3	2	3	4	3	2	3	2	3	2	3	2	3	2	3	4	3	4	3	4	5	6	5	4	3	2	3	4	5	6	5	4	5	4	5	6	5	4	3	2	3	2

4.7 Node Level (Node Sequence) Less-/Greater-than Pattern (NLLGP)

Due to the connective nature of the hypercube level structure, a node can only be adjacent to other nodes that are a single level away, and never within the same level. This allows for the conversion of the NLP into a new representation that is called the *node level (node sequence) less-/greater-than pattern* (NLLGP). The NLLGP stores a value indicating whether the level at a given index is a single level less or greater than the previous level. In this way, the representation is similar to the relationship between a transition sequence and a node sequence, where a value in the transition sequence describes the next node value in the node sequence.

Table 4.7 contains the NLLGP for all NLP of all longest maximal snakes in dimensions 1–7, where a "G" is used to indicate that the level at a given index in the NLLGP is one greater than the previous level and an "L" is used to indicate that the level is one less than the previous level. Note that the NLLGP pattern for a given NLP also applies to the node sequences that follow that same NLP (due to the distribution of nodes in the level structure). In other words, the NLLGP describes whether the given position in the node sequence has a numerical value greater or lesser than the previous node. However, unlike the NLP, the NLLGP cannot give the exact value of the node in the node sequence.

Table 4.7: Hypercube Node Level (Node Sequence) Less-/Greater-than Pattern (NLLGP)

Dimension			Node Sequence Index																																																		
n	NSLGP	NLP	0	1	2	3	4	5	6	7	8	9	10	11	12	13	14	15	16	17	18	19	20	21	22	23	24	25	26	27	28	29	30	31	32	33	34	35	36	37	38	39	40	41	42	43	44	45	46	47	48	49	50
1			0	G																																																
2			0	G	G																																															
3			0	G	G	G	L																																													
4			0	G	G	G	L	G	L	G																																										
5	1	1	0	G	G	G	G	L	L	G	L	G	L	G	G	L																																		
	2	2	0	G	G	G	G	L	L	G	L	G	G	L	L	G																																		
	3	3	0	G	G	G	G	L	L	G	G	L	G	L	L	G																																		
6			0	G	G	G	G	L	L	G	L	G	G	L	L	G	G	G	G	L	L	L	L	G	L	G	L	G	L																							
7	1	1	0	G	G	G	L	G	L	G	G	L	G	L	L	G	G	L	G	L	L	G	L	G	G	L	L	G	L	G	G	G	G	L	L	G	G	L	L	L	G	G	G	L	G	L	L	G	G	L	L	L	L
	2	2	0	G	G	G	L	G	L	G	G	L	G	L	L	G	G	L	G	L	L	G	L	G	G	L	L	G	L	G	G	G	G	L	L	G	G	L	L	L	G	G	G	L	G	L	L	L	L	G	G	G	G
	3	3	0	G	G	G	L	G	L	G	G	L	G	L	L	G	L	G	G	L	L	G	L	G	G	L	L	G	L	G	G	G	G	L	L	G	G	L	L	L	G	G	G	L	G	L	L	G	G	L	L	L	L
	4	4	0	G	G	G	G	L	L	G	G	L	G	L	L	G	G	G	G	L	G	L	G	L	L	L	L	G	G	G	G	L	L	L	L	G	G	L	L	G	G	L	G	L	G	L	L	G	G	G	L	L	L
	5	5	0	G	G	G	G	L	L	G	G	L	G	L	L	G	G	G	G	L	G	L	G	L	L	L	L	G	G	G	G	L	L	L	L	G	G	L	G	L	G	L	G	L	G	L	L	G	G	G	L	L	L
	6	6	0	G	G	G	G	L	L	G	L	G	L	G	G	G	L	L	L	G	G	L	L	G	G	G	G	L	G	L	L	G	G	L	L	L	L	G	L	G	G	L	L	G	L	G	G	L	G	L	G	G	G
	7	7	0	G	G	G	G	L	G	L	L	G	L	G	G	L	L	G	L	G	G	G	G	L	L	L	L	G	L	G	G	L	L	G	G	G	G	L	G	L	L	G	G	L	L	L	L	G	L	G	G	G	G
	8	8	0	G	G	G	G	L	G	L	G	G	L	L	G	L	L	G	L	G	L	G	G	G	L	L	L	G	G	L	G	L	L	G	G	G	L	G	G	G	L	L	L	L	L	G	G	G	L	L	L	G	G
	9	9	0	G	G	G	G	L	G	L	G	G	L	G	L	L	L	G	L	G	L	G	G	G	L	L	L	G	G	G	L	G	L	L	L	G	G	G	L	L	G	L	G	G	G	G	L	L	L	G	L	L	L
	10	10	0	G	G	G	G	G	G	L	L	L	L	G	G	L	L	G	L	G	L	G	G	L	L	G	G	L	G	L	L	G	L	G	G	G	G	L	G	L	L	G	G	L	L	L	L	G	L	G	G	G	G
	11	11	0	G	G	G	G	G	G	L	L	L	L	G	G	L	L	G	L	G	L	G	L	G	L	G	G	L	G	L	L	G	L	G	G	G	G	L	L	G	L	G	G	L	L	L	L	G	G	G	G	L	L
	12	12	0	G	G	G	G	G	G	L	L	L	L	G	G	L	L	G	L	G	L	G	L	G	L	G	G	L	G	L	G	G	G	L	L	L	L	G	G	G	G	L	L	G	L	G	G	L	L	L	L	G	L

4.8 Node Level Group Pattern (NLGP)

The *node level group pattern* (NLGP) applies the HLGs shown in Table 3.2 to the NLP to identify whether every position in the NLP is on the left or right half of the hypercube level structure. In even dimensions there is also a center HLG due to the odd number of levels in even dimensions. The resulting NLGPs are shown in Table 4.8 for all NLPs in dimensions 1–7. From the NLGPs it is possible to quickly identify what region of the hypercube a given snake path is passing through at a given position.

Table 4.8: Hypercube Node Level Group Pattern (NLGP)

Dimension			Node Sequence Index																																															
n	NLGP	NLP	0	1	2	3	4	5	6	7	8	9	10	11	12	13	14	15	16	17	18	19	20	21	22	23	24	25	26	27	28	29	30	31	32	33	34	35	36	37	38	39	40	41	42	43	44	45	46	47	48	49	50
1			L	R																																															
2			L	C	R																																														
3			L	L	R	R	R																																												
4			L	L	C	R	C	R	C	R																																									
5	1	1	L	L	L	R	R	R	L	R	L	R	L	R	R	R																																			
	2	2	L	L	L	R	R	R	L	R	L	R	R	R	L	R																																			
	3	3	L	L	L	R	R	R	L	R	R	R	R	R	L	R																																			
6			L	L	L	C	R	C	L	C	L	C	R	C	L	C	R	R	R	R	R	C	L	C	L	C	L	C	L																							
7	1	1	L	L	L	L	L	L	L	L	R	L	R	L	L	L	R	L	R	L	L	L	L	L	R	L	L	L	L	L	R	R	R	R	R	R	R	R	R	L	R	R	R	R	R	R	R	R	R	R	R	L	L
	2	2	L	L	L	L	L	L	L	L	R	L	R	L	L	L	R	L	R	L	L	L	L	L	R	L	L	L	L	L	R	R	R	R	R	R	R	R	R	L	R	R	R	R	R	R	R	L	L	L	R	R	R
	3	3	L	L	L	L	L	L	L	L	R	L	R	L	L	L	L	L	R	L	L	L	L	L	R	L	L	L	L	L	R	R	R	R	R	R	R	R	R	L	R	R	R	R	R	R	R	R	R	R	R	L	L
	4	4	L	L	L	L	R	L	L	L	R	L	R	L	L	L	R	R	R	R	R	R	R	R	R	L	L	L	R	R	R	R	R	L	L	L	R	L	L	L	R	L	R	L	R	L	L	L	R	R	R	L	L
	5	5	L	L	L	L	R	L	L	L	R	L	R	L	L	L	R	R	R	R	R	R	R	R	R	L	L	L	R	R	R	R	R	L	L	L	R	L	R	L	R	L	R	L	R	L	L	L	R	R	R	L	L
	6	6	L	L	L	L	R	L	L	L	L	L	L	L	R	R	R	L	L	L	R	L	L	L	R	R	R	R	R	R	R	R	R	R	R	L	L	L	L	L	R	L	L	L	L	L	R	L	R	L	R	R	R
	7	7	L	L	L	L	R	L	R	L	L	L	L	L	R	L	L	L	L	L	R	R	R	R	R	L	L	L	L	L	R	L	L	L	R	R	R	R	R	R	R	R	R	R	R	L	L	L	L	L	R	R	R
	8	8	L	L	L	L	R	L	R	L	R	R	R	L	R	L	L	L	L	L	L	L	R	R	R	L	L	L	R	L	R	L	L	L	R	R	R	R	R	R	R	R	R	L	L	L	R	R	R	L	L	L	R
	9	9	L	L	L	L	R	L	R	L	R	R	R	R	R	L	L	L	L	L	L	L	R	R	R	L	L	L	R	R	R	R	R	L	L	L	R	R	R	L	R	L	R	R	R	R	R	R	R	R	R	L	L
	10	10	L	L	L	L	R	R	R	R	R	L	L	L	R	L	L	L	L	L	L	L	R	L	L	L	R	L	R	L	L	L	L	L	R	R	R	R	R	R	R	R	R	R	R	L	L	L	L	L	R	R	R
	11	11	L	L	L	L	R	R	R	R	R	L	L	L	R	L	L	L	L	L	L	L	L	L	L	L	R	L	R	L	L	L	L	L	R	R	R	R	R	R	R	R	R	R	R	L	L	L	R	R	R	R	R
	12	12	L	L	L	L	R	R	R	R	R	L	L	L	R	L	L	L	L	L	L	L	L	L	L	L	R	L	R	L	R	R	R	R	R	L	L	L	R	R	R	R	R	R	R	R	R	R	R	L	L	L	L

Table 4.9: Condensed Hypercube Node Level Group Pattern (NLGPC)

Dimension																									
n	NLPGC	NLGP																							
1			L	R																					
2			L	C	R																				
3			L2	R3																					
4			L2	C	R	C	R	C	R																
5	1	1	L3	R3	L	R	L	R	L	R3															
	2	2	L3	R3	L	R	L	R3	L	R															
	3	3	L3	R3	L	R5			L	R															
6			L3	C	R	C	L	C	L	C	R	C	L	C	R5	C	L	C	L	C	L	C	L		
7	1	1	L8			R	L	R	L3	R	L	R	L5	R	L5	R9					L	R11			L2
	2	2	L8			R	L	R	L3	R	L	R	L5	R	L5	R9					L	R7	L3	R3	
	3	3	L8			R	L	R	L5	R	L5	R	L5	R9							L	R11			L2
	4	4	L4	R	L3	R	L	R	L3	R9	L3	R5	L3	R	L3			R	L	R	L	R	L3	R3	L2
	5	5	L4	R	L3	R	L	R	L3	R9	L3	R5	L3	R	L	R	L	R	L	R	L	R	L3	R3	L2
	6	6	L4	R	L7	R3			L3	R	L3	R11	L5	R	L5					R	L	R	L	R3	
	7	7	L4			R	L	R	L5	R	L5	R5	L5	R	L3	R11							L5	R3	
	8	8	L4	R	L	R	L	R3	L	R	L7	R3	L3	R	L	R	L3			R9	L3	R3	L3	R	
	9	9	L4	R	L	R	L	R5	L7	R3	L3	R5	L3	R3			L	R	L	R9					L2
	10	10	L4	R5			L3	R	L7	R	L3	R	L	R	L5	R11							L5	R3	
	11	11	L4	R5			L3	R	L11			R	L	R	L5	R11							L3	R5	
	12	12	L4	R5			L3	R	L11			R	L	R	L	R5					L3	R11			L4

4.9 Condensed Node Level Group Pattern (NLGPC)

The NLGPs shown in Table 4.8 can be condensed by grouping sequential values that are the same, where a number is appended to the HLG to indicate how many of the given HLG occur in sequence. For instance, "L9 R2" indicates that there are nine sequential "L" levels followed by two "R" levels. The resulting condensed NLGPs (NLGPCs) are shown in Table 4.9. The various condensed values in each dimension have been aligned in an attempt to show a similarity between NLPGCs in a given dimension, although no significance is implied by the spacing.

4.10 Node Level Distribution (NLD)

A *node level distribution* (NLD) is a new term for the counts of how many times a given longest maximal snake passes through the levels in the hypercube level structure. Level zero

Table 4.10: Hypercube Node Level Distribution (NLD)

Dimension			Node Levels							
n	NLD	NLP	0	1	2	3	4	5	6	7
1			1	1						
2			1	1	1					
3			1	1	2	1				
4			1	1	3	3	0			
5	1	1,2	1	1	4	6	2	0		
	2	3	1	1	3	6	3	0		
6			1	1	8	10	4	2	1	
7	1	6	1	1	10	17	11	7	4	0
	2	7,10	1	1	10	16	10	8	5	0
	3	11,12	1	1	10	15	11	9	4	0
	4	3	1	1	10	15	10	9	5	0
	5	2	1	1	9	16	11	8	5	0
	6	1	1	1	9	15	11	9	5	0
	7	8	1	1	8	17	15	6	2	1
	8	4	1	1	8	17	13	7	4	0
	9	5	1	1	7	17	14	7	4	0
	10	9	1	1	7	14	16	9	2	1

and one will always have a count of only one. This is because level zero contains only node zero, where snakes typically start, and level one contains only nodes that are adjacent to node zero due to the design of the hypercube level structure. Therefore, only one node in level one may be on the snake path or a path violation would occur, invalidating the snake path. The last level in the level structure also contains only one node (the bit-wise inverse of zero, or $(2^n - 1)$). Therefore, if the last level in a given dimension has a value of one in the NLD, then the last node is always in the snake path for all longest maximal snakes with that NLD. Likewise, if the value of the last level is zero, then it is never in the snake path.

Table 4.10 collects the NLDs for all longest maximal snakes in dimensions 1–7. Essentially it is a condensed version the NLPs from Table 4.6. It is interesting to note that although every level in the hypercube level structure may not be visited, as shown in the Table 4.5 every transition is always used at least once, a fact that is related to equivalence classes and the number of snakes per equivalence class. This certainly provides only a small piece of knowledge if used as part of a search heuristic. However, it is useful in understanding the internal geometry of the hypercube and how it places constraints on the snake path. This will be discussed further in Chapter 5.

4.11 Node Level Group Distribution (NLGD)

A *node level group distribution* (NLGD) is a new term for the counts of how many times a given longest maximal snake passes through a level in one of the HLGs identified in Table 3.2 for the hypercube level structure. Due to the distribution of levels in the HLG framework, the snake path will visit every HLG at least once. NLGDs help to show what portion of the hypercube level structure the snake path primarily travels through.

Table 4.11 collects the NLGDs for all longest maximal snakes in dimensions 1–7. Essentially it is a very condensed version of the NLGPs from Table 4.8. The NLGDs show a fairly even distribution of snake nodes between HLGs, with a slightly higher focus on the left-hand levels in dimension six and seven and on the right-hand levels in dimension 3-5. In the lower dimensions this is mostly due to the lower two levels only allowing the snake to visit them once each (meaning the snake path has only one node from each of the lower two levels) which creates an apparent skew in the NLGD to the right-most HLGs. If the higher dimensions continue this trend it may be a helpful statistic to guide snake growth, especially in search algorithms that operate on entire snake paths because it will help the algorithm to quickly decide whether the snake path is a strong candidate for growth, or if it favors certain areas of the hypercube too much. The NLGDs may be very helpful in dimension eight, if the NLGD for dimension six is any indication, because dimension eight has a central HLG, so it may be possible to approximate how many nodes on the snake path should be from the middle level of the hypercube level structure.

Table 4.11: Hypercube Node Level Group Distribution (NLGD)

Dimension				Node Level Group		
n	NLGD	NLGP	NLD	L	C	R
1				1		1
2				1	1	1
3				2		3
4				2	3	3
5	1	1,2	1	6		8
	2	3	2	5		9
6				10	10	7
7	1	6	1	29		22
	2	7,10	2	28		23
	3	2,3,4,8,11,12	3,4,5,7,8	27		24
	4	1,5	6,9	26		25
	5	9	10	23		28

Chapter 5

Equivalence Class Analysis

5.1 Equivalence Class (Canonical Transition Sequence) (EC)

An *equivalence class* (EC) is essentially the set of all possible snake paths that have the exact same shape within the hypercube, where the total number of snakes for a given EC in dimension-n is given by Equation 5.1.

$$2^n * n! \tag{5.1}$$

Since the hypercube is a symmetrical shape, a snake starting from a given node in the hypercube is effectively identical if it starts from any other node in the hypercube (it is merely a *translation* of the snake), accounting for the first term in Equation 5.1. This makes sense by realizing that all nodes in the hypercube are identical and any label a node is given (such as by numbering all nodes in the hypercube) does not alter this identity.

Likewise, due to this symmetry, if the transition sequence was altered by swapping all occurrences of a single transition with all occurrences of a second transition then the snake shape is unaltered, it is simply rotated. For example, given transition sequence {2,1,0,2}, transition zero and two can be swapped so that the new transition sequence is {0,1,2,0}, which is the same snake, but simply rotated. A way to imagine this is by visualizing a square that has two adjacent edges highlighted. If the square is examined from above, the highlighted edges may resemble an "L", but from below they may look like "Γ". The snake has not been altered, only your perspective (you rotated the hypercube, i.e. the square). By swapping all transitions of one type for another, the snake *rotates* while the hypercube remains fixed. Therefore, the shape of the snake path is the same, and only the node sequence and transition sequence will be different.

The ECs this thesis is specifically concerned with are those of longest maximal snakes. Since there are n transitions in a dimension-n hypercube, and the transition sequence for every longest maximal snake in a given dimension includes every possible transition for that dimension as shown in Table 4.5, then there must be $n!$ ways to swap transitions (i.e. rotate the snake path) for a given longest maximal snake transition sequence. This accounts for the second term in Equation 5.1. See Table 4.1 for the number of longest maximal snakes starting from a single node.

Because translation and rotation of a snake path does not alter the shape of the snake, and because of the symmetry of a hypercube, all snakes in an EC have the exact same properties. For this reason, all snakes in an EC are *synonyms* of each other. Therefore, the entire EC can be represented by a single transition sequence called the *canonical* transition sequence (or *canonical form* of a snake path). The canonical transition sequence is a snake path transition sequence where every possible transition occurs in the transition sequence in increasing order (such that no lower dimensional transition occurs after a higher dimensional one). For instance, transition sequence {0,1,2,3} is a canonical transition sequence in dimension four, but {0,1,3,2} is not since three occurs before two. For this reason, every canonical transition sequence above dimension two will always start with {0,1,2} since {0,0}, {0,1,0}, and {0,1,1} are invalid snake paths. Likewise, since node sequences start from node zero by convention, the node sequence for a canonical snake always starts with {0,1,3,7}.

Table 5.1 contains the canonical transition sequences for all longest maximal snake ECs in dimensions 1–7, and Table 5.2 contains the node sequences for those transition sequences. If a given dimension has only one EC then that EC is not numbered. Currently dimension five and seven are the only dimensions known to have more than one longest maximal snake EC, but it is very likely that there are others in higher dimensions since every dimension builds upon every previous dimension. A better understanding of hypercube geometry may explain why some dimensions have multiple ECs and others don't. Additionally, since each EC has the same number of snake paths in a given dimension, some search techniques may have an easier time finding long snakes in dimensions with multiple ECs since there are effectively more snake paths possible (for instance in a node or transition sequence based search method). However, for a geometric (shape-based) search technique there would not be much difference because it would be searching the EC space. This is because the number of actual unique shapes (and by extension unique snakes) in the hypercube is the number of ECs in a given dimension (since all others are synonyms of the canonical snakes). Therefore, each EC in a given dimension has a different geometric shape than the others in its dimension. It is conceivable that a better understanding of the geometry of hypercubes would help both with search and with determining why some dimensions have a single EC (i.e. only one longest maximal snake length shape possible) and others have multiple ECs.

Table 5.1: Equivalence Class (Canonical Transition Sequence) (EC)

Dimension					Transition Sequence Index																																																	
n	EC	NLP	SDP	ECTFP	0	1	2	3	4	5	6	7	8	9	10	11	12	13	14	15	16	17	18	19	20	21	22	23	24	25	26	27	28	29	30	31	32	33	34	35	36	37	38	39	40	41	42	43	44	45	46	47	48	49
1					0																																																	
2					0	1																																															
3					0	1	2	0																																											
4					0	1	2	0	3	1	0																																							
5	1	3	2	1	0	1	2	3	0	1	4	0	2	1	0	3	2																																		
	2	1	2	2	0	1	2	3	0	1	4	3	1	2	3	0	1																																		
	3	3	3	1	0	1	2	3	0	2	4	0	1	2	0	3	1																																		
	4	3	2	1	0	1	2	3	0	2	4	0	1	2	3	0	1																																		
	5	2	1	1	0	1	2	3	0	2	4	1	0	2	3	0	1																																		
	6	1	2	3	0	1	2	3	0	2	4	3	2	1	0	3	2																																		
	7	1	3	3	0	1	2	3	0	2	4	3	2	1	3	0	2																																		
	8	1	1	2	0	1	2	3	1	0	4	3	1	2	3	0	1																																		
6					0	1	2	3	1	0	4	3	0	5	4	0	1	3	4	0	2	4	1	0	4	3	1	5	3	4																								
7	1	1	3	2	0	1	2	0	3	1	0	4	2	1	0	3	5	0	1	2	4	0	6	5	0	4	2	0	3	4	0	1	2	4	0	3	5	0	4	2	0	3	4	0	1	2	0	6	1	0	4	2	1	0
	2	2	2	3	0	1	2	0	3	1	0	4	2	1	0	3	5	0	1	2	4	0	6	5	0	4	2	0	3	4	0	1	2	4	0	3	5	0	4	2	0	3	4	0	1	2	0	6	2	4	0	1	2	4
	3	3	6	2	0	1	2	0	3	1	0	4	2	1	0	3	5	1	0	2	4	0	6	5	0	4	2	0	3	4	0	1	2	4	0	3	5	0	4	2	0	3	4	0	1	2	0	6	1	0	4	2	1	0
	4	4	6	1	0	1	2	3	0	1	4	0	2	1	0	3	5	0	2	3	0	6	5	0	3	2	1	0	3	5	0	2	3	0	6	4	0	3	2	0	1	6	5	0	1	2	3	0	1	5	0	2	1	0
	5	5	3	1	0	1	2	3	0	1	4	0	2	1	0	3	5	0	2	3	0	6	5	0	3	2	1	0	3	5	0	2	3	0	6	4	0	3	2	1	0	6	5	0	1	2	3	0	1	5	0	2	1	0
	6	6	2	5	0	1	2	3	0	1	4	3	1	2	3	0	5	3	1	0	3	6	5	3	0	1	2	3	0	5	3	1	0	3	6	4	3	0	1	2	3	6	5	3	2	1	0	3	2	5	3	1	2	3
	7	7	5	4	0	1	2	3	1	4	2	0	5	3	0	2	4	0	1	2	3	0	4	2	0	5	3	2	6	1	0	2	4	0	1	3	5	0	1	4	0	3	1	0	2	4	1	0	3	5	0	1	4	2
	8	8	4	8	0	1	2	3	1	4	2	1	5	3	1	2	4	0	1	2	3	1	4	2	1	5	3	2	6	0	1	2	4	0	1	3	5	1	0	4	1	3	0	1	2	4	0	1	3	5	1	0	4	2
	9	9	1	10	0	1	2	3	1	4	2	1	5	3	2	1	4	0	1	2	3	1	4	2	1	5	3	1	6	5	1	2	3	5	1	4	0	1	5	3	1	4	5	1	2	3	5	1	4	0	1	5	3	2
	10	10	5	6	0	1	2	3	4	5	3	2	1	0	3	2	5	3	1	2	3	4	5	2	3	1	0	3	2	6	0	5	4	3	0	1	3	5	0	2	3	1	0	3	5	4	3	0	1	2	5	0	2	3
	11	11	4	7	0	1	2	3	4	5	3	2	1	0	3	2	5	3	1	2	3	4	5	3	2	1	0	3	2	6	0	5	4	3	0	1	3	5	0	3	2	1	0	3	5	4	3	0	1	3	5	0	3	2
	12	12	1	9	0	1	2	3	4	5	3	2	1	0	3	2	5	3	1	2	3	4	5	3	2	1	0	3	2	6	3	1	2	3	0	5	3	1	0	3	4	5	3	0	1	2	3	0	5	3	1	0	3	4

Table 5.2: Equivalence Class Node Sequence (ECNS)

Dimension			Node Sequence Index																											
n	ECNS	EC	0	1	2	3	4	5	6	7	8	9	10	11	12	13	14	15	16	17	18	19	20	21	22	23	24	25	26	· · ·
1			0	1																										
2			0	1	3																									
3			0	1	3	7	6																							
4			0	1	3	7	6	14	12	13																				
5	1	1	0	1	3	7	15	14	12	28	29	25	27	26	18	22														
	2	2	0	1	3	7	15	14	12	28	20	22	18	26	27	25														
	3	3	0	1	3	7	15	14	10	26	27	25	29	28	20	22														
	4	4	0	1	3	7	15	14	10	26	27	25	29	21	20	22														
	5	5	0	1	3	7	15	14	10	26	24	25	29	21	20	22														
	6	6	0	1	3	7	15	14	10	26	18	22	20	21	29	25														
	7	7	0	1	3	7	15	14	10	26	18	22	20	28	29	25														
	8	8	0	1	3	7	15	13	12	28	20	22	18	26	27	25														
6			0	1	3	7	15	13	12	28	20	21	53	37	36	38	46	62	63	59	43	41	40	56	48	50	18	26	10	
7	1	1	0	1	3	7	6	14	12	13	29	25	27	26	18	50	51	49	53	37	36	100	68	69	85	81	80	88	72	
	2	2	0	1	3	7	6	14	12	13	29	25	27	26	18	50	51	49	53	37	36	100	68	69	85	81	80	88	72	
	3	3	0	1	3	7	6	14	12	13	29	25	27	26	18	50	48	49	53	37	36	100	68	69	85	81	80	88	72	
	4	4	0	1	3	7	15	14	12	28	29	25	27	26	18	50	51	55	63	62	126	94	95	87	83	81	80	88	120	
	5	5	0	1	3	7	15	14	12	28	29	25	27	26	18	50	51	55	63	62	126	94	95	87	83	81	80	88	120	
	6	6	0	1	3	7	15	14	12	28	20	22	18	26	27	59	51	49	48	56	120	88	80	81	83	87	95	94	126	
	7	7	0	1	3	7	15	13	29	25	24	56	48	49	53	37	36	38	34	42	43	59	63	62	30	22	18	82	80	
	8	8	0	1	3	7	15	13	29	25	27	59	51	49	53	37	36	38	34	42	40	56	60	62	30	22	18	82	83	
	9	9	0	1	3	7	15	13	29	25	27	59	51	55	53	37	36	38	34	42	40	56	60	62	30	22	20	84	116	
	10	10	0	1	3	7	15	31	63	55	51	49	48	56	60	28	20	22	18	26	10	42	46	38	36	37	45	41	105	
	11	11	0	1	3	7	15	31	63	55	51	49	48	56	60	28	20	22	18	26	10	42	34	38	36	37	45	41	105	
	12	12	0	1	3	7	15	31	63	55	51	49	48	56	60	28	20	22	18	26	10	42	34	38	36	37	45	41	105	

Table 5.2: Equivalence Class Node Sequence (ECNS) - cont.

Dimension			Node Sequence Index (cont.)																							
n	ECNS	EC	···	27	28	29	30	31	32	33	34	35	36	37	38	39	40	41	42	43	44	45	46	47	48	49	50
1																											
2																											
3																											
4																											
5	1	1																									
	2	2																									
	3	3																									
	4	4																									
	5	5																									
	6	6																									
	7	7																									
	8	8																									
6																											
7	1	1		73	75	79	95	94	86	118	119	103	99	98	106	122	123	121	125	124	60	62	63	47	43	41	40
	2	2		73	75	79	95	94	86	118	119	103	99	98	106	122	123	121	125	124	60	56	40	41	43	47	63
	3	3		73	75	79	95	94	86	118	119	103	99	98	106	122	123	121	125	124	60	62	63	47	43	41	40
	4	4		121	125	117	116	52	36	37	45	41	40	42	106	74	75	73	77	69	68	70	102	103	99	97	96
	5	5		121	125	117	116	52	36	37	45	41	43	42	106	74	75	73	77	69	68	70	102	103	99	97	96
	6	6		118	116	117	125	61	45	37	36	38	34	42	106	74	66	70	68	69	77	73	105	97	99	103	111
	7	7		81	85	69	68	70	78	110	111	109	125	124	116	118	119	115	99	97	96	104	72	73	75	91	95
	8	8		81	85	69	68	70	78	110	108	109	125	127	119	118	116	112	96	97	99	107	75	73	72	88	92
	9	9		118	114	122	90	88	72	73	75	107	99	97	113	81	83	87	95	127	125	109	108	110	78	70	66
	10	10		104	72	88	80	81	83	91	123	122	126	118	116	117	125	93	77	69	68	70	66	98	99	103	111
	11	11		104	72	88	80	81	83	91	123	122	114	118	116	117	125	93	77	69	68	70	78	110	111	103	99
	12	12		97	99	103	111	110	78	70	68	69	77	93	125	117	116	118	114	122	123	91	83	81	80	88	72

5.2 Equivalence Class Transition Frequency Pattern (ECTFP)

Using the TFPs identified in Table 4.5, the exact permutation that applies to each EC can be determined. Table 5.3 collects the TFPs for all canonical snakes in dimensions 1–7. In dimensions with multiple ECs, it appears that the ECTFPs with a larger number of transition-0 transitions also have a higher number of ECs. Additionally, the shape of the longest maximal snake determines what transitions are most common. For instance, since all canonical transition sequences begin {0,1,2} (in dimensions greater than 2) it is clear why transitions 0–2 generally have the greatest number of instances in the canonical snakes. Therefore, any search that forces a canonical start sequence should emphasize transition 0–2 (or if the transition sequence begins with a different three transition prefix then those three should be emphasized). However, note that transition three in ECTFP 7.5-7 and 7.9 has the highest number of transitions, which indicates that the geometry of the hypercube affords easy expansion in that transitional dimension.

The presence of more than one TFP in dimension seven implies that the hypercube structure may be much different starting with hypercubes greater than dimension seven. How the geometry of the hypercube affects the snake shape should be investigated further. A deeper understanding could allow the generation of an ECTFP in any dimension, which, coupled with known ordering constraints on transition sequences, would greatly reduce the search space.

5.3 Equivalence Class Hypercube Map (ECHM)

As discussed in Section 4.3, a hypercube map is a vector that reflects the state of a given hypercube with a snake path passing through it. Appendix B.1 contains tables with the hypercube maps for all ECs in dimensions 1–7. For each hypercube map, "|" is used to represent a snake node and "#" is used to represent available nodes. Snake path nodes are represented in the hypercube by the index value reflecting the position of that node in the

Table 5.3: Equivalence Class Transition Frequency Pattern (ECTFP)

Dimension				Transitions						
n	ECTFP	EC	TFP	0	1	2	3	4	5	6
1				1						
2				1	1					
3				2	1	1				
4				3	2	1	1			
5	1	1,3,4,5		4	3	3	2	1		
	2	2,8		3	4	2	3	1		
	3	6,7		3	2	4	3	1		
6				6	5	2	5	6	2	
7	1	4,5	1	16	8	8	8	2	5	3
	2	1,3	1	16	8	8	5	8	3	2
	3	2	2	15	7	9	5	9	3	2
	4	7	5	13	9	9	7	7	4	1
	5	6	2	9	9	7	15	2	5	3
	6	10	5	9	7	9	13	4	7	1
	7	11	4	9	7	8	14	4	7	1
	8	8	4	8	14	9	7	7	4	1
	9	12	3	8	8	8	15	4	6	1
	10	9	3	4	15	8	8	6	8	1

snake path. Statistics of all hypercube maps for all canonical and longest maximal snakes are available in Table 4.3.

5.4 Equivalence Class Growth Analysis

Section 5.1 observes that the ECs represent all possible shapes of longest maximal snakes. Therefore, an analysis of the properties of a hypercube and all canonical snakes as the snake paths grows through the hypercube is equivalent to analyzing all possible longest maximal snakes. This section provides node type, skin density, transition count, 2-face, and 3-face growth analysis. Note that all tables referenced by this section have a column without a heading immediately before transition sequence index zero. This column represents the initial state of a given n-dimensional hypercube with only the head node of the snake path chosen.

5.4.1 Node Type Growth Analysis

Appendix B.2 contains statistics on the number of nodes of certain types for all canonical snakes in dimensions 1–7 as the snake paths grow. The statistics begin at the head of the snake before growth starts and provides updated counts of available (indicated by "A"), unavailable (indicated by "U"), and skin nodes (indicated by "S"). Available nodes indicate which nodes the snake path could grow to if the tail node was adjacent to any of those nodes, whereas the unavailable nodes are the opposite. The number of available and unavailable nodes always sum to 2^n, where n is the dimensionality of the hypercube. Having both may appear redundant, but visualizing the numbers separately may help to identify a pattern in relation to other growth statistics.

The number of skin nodes indicates how tightly the snake is winding through the hypercube. If the number of skin nodes increases from one transition to the next, then the snake path is growing into area, where a large increase indicates that the snake is heading in a completely new direction (away from everything explored so far) and a small increase indicates that the snake is moving near an already explored area. No increase in skin density indicates that the snake path is moving in an area where it has already encountered its bounding skin nodes (in a sense, the path is looking for an exit). Note that there are no skin nodes counted before the transition sequence starts, even though a node (the head node) is unavailable. This is because at the beginning the head node is also the tail node and the snake path can grow to any of the tail node's adjacent nodes. If the adjacent nodes were already considered snake nodes then the path could not grow to anything. Therefore, the statistics really reflect the effect of a given transition on the *previous* node, even though they apply to current state of the hypercube after the transition. The number of skin nodes will always increase rapidly at the start of snake growth because none of the hypercube has been explored, so the first transition will always increase the snake density by $(n - 1)$ (the number of edges connected to the start node minus the node that the transition indicated the snake path should grow to).

5.4.2 Skin Density Growth Analysis

Appendix B.3 contains statistics on the skin density for all canonical snakes in dimensions 1–7 as the snake paths grow. The statistics begin at the head of the snake before growth starts and provides counts of the number of skin nodes with skin density one to n, as well as the minimum skin density and maximum skin density of any skin node, and the skin density sum. The skin density sum is not the sum of the *number* of skin nodes, but rather the sum of all skin densities.

The skin density counts show how tightly the snake is growing because the sum of all skin density counts is equal to the number of skin nodes. Therefore, if the number of skin nodes remains the same while the number of a lower skin density decreases and the number of a higher skin density increases, then the snake is traveling only within nodes it has already seen. The greater the skin density, the tighter the snake is traveling through a given hypercube. If only lower skin density value are appearing then the snake is growing into new areas of the hypercube.

5.4.3 Transition Count Growth Analysis

Appendix B.4 contains transition counts for all canonical snakes in dimensions 1–7 as the snake paths grow. The statistics begin at head of the snake before growth starts and provides counts of the number of each transition within the range 0 to $(n-1)$ up to and including the transition at the given index. This notation would allow the recreation of the transition sequence by examining which transition count increased and then recording that transition for the given index. These counts may help to show whether there is any pattern to how frequently a given transition is used. Since transitions essentially represent a move from a given dimension into the dimension indicated by the transition, the counts can show at what point the different dimensions are first visited or when they were last visited. This information may indicate either the shape or portion of the hypercube that the snake path is traveling through, or the a limitations placed on the snake path by the hypercube.

5.4.4 2-Face Growth Analysis

Appendix B.5 contains counts of the 2-face types given in C.1 for all canonical snakes in dimensions 1–7 as the snake paths grow. The statistics begin at the head of the snake before growth starts and provides counts of the number of each 2-face type in the n-dimensional hypercube at the given index. Note that there are no 2-faces in a 1-dimensional hypercube so all values will be zero.

Solov'eva observed that for the set of 2-faces A in the hypercube, the number of A_1 paths (denoted $|A_1|$) that are in a coil path is equal to the length of the path [23]. However, the paths used for this thesis are snake paths. Therefore, the length of $|A_1|$ for a snake path should be $|A_1| = (length_{path} - 1)$, which can be confirmed by the data. This makes sense when recalling that every node within a snake is connected to two other nodes, with the exception of the head and tail nodes, unlike a coil where every node is connected to two nodes. Additionally, Solov'eva stated that $|A_2| = (length_{path} * (n-3))$ for coils, where n is dimensionality of the hypercube [23]. For snakes, this number appears to be $|A_2| = 2 + (length_{path} * (n-3))$ where $n \geq 3$, which can also be confirmed by the data. This again makes sense for snakes because the head and tail nodes have a connectivity of only one adjacent node. The formula does not apply below dimension three because in a 2-dimensional hypercube there can only be an A_1 2-face. For A_3, Solov'eva gives a formula that is dependent on A_4, neither of which appear to be modifiable to apply to snakes. Because A_5 is a 2-face without any node in the path, $|A_5|$ is simply $\sum_{i=1}^{4} |A_i|$ subtracted from 2-faces in the n-dimensional hypercube $\binom{n}{2}$, which gives $|A_5| = \binom{n}{2} - \sum_{i=1}^{4} |A_i|$.

It is interesting to observe from Table B.17 for dimension-5 that even though there are ten different growth patterns for $|A_3|$ and $|A_4|$, the final values for both are the same in all patterns. However, Table B.19 and B.20 shows that there are three ending patterns even though each EC has its own growth pattern for $|A_3|$ and $|A_4|$. This indicates that the value of $|A_3|$ and $|A_4|$ is not dependent on length despite appearances in lower dimensions. Instead, the shape of the snake is what determines the number of A_3 and A_4 2-faces. Therefore, it is possible that a correlation could be determined between a given n-dimensional hypercube structure, $|A_3|$, and $|A_4|$ that would allow a search method to guide snake growth.

5.4.5 3-Face Growth Analysis

Appendix B.6 contains counts of the 3-face types given in C.2 for all canonical snakes in dimensions 1–7 as the snake paths grow. The statistics begin at the head of the snake before growth starts and provides counts of the number of each 3-face type in the n-dimensional hypercube at the given index. Note that dimension one and two have been omitted because there are no 3-faces in 1- and 2-dimensional hypercubes. Also, although the two shapes for B_2 may appear to be different since human's see in three dimensions, a hypercube may be rotated through itself (essentially turning the hypercube inside-out) which will transform one shape into the other. Therefore, these two shapes are treated as a single shape.

There does not appear to be any consistency among the data that would allow development of a formula based on length alone as was done in 5.4.4. With the 2-face data, $|A_1|$ and $|A_2|$ were the same among all ECs in a given dimension, and the other values were often equal as well. The 3-face data appears to be much different. However, in all dimensions $|B_{13}|$ is always zero by the end of the snake path, which indicates that all 3-faces in the entire hypercube for a given dimension has at least one node of the snake passing through it. Additionally, the value for $|B_{12}|$ is very low, indicating that most 3-faces have more than one node on the snake path. Interestingly, $|B_{10}|$ is always greater than $|B_{11}|$, suggesting that there are more 3-faces with two nodes where those two nodes occur on the same 2-face of the 3-face, rather than on opposite corners of the 3-face. This indicates that a snake path which travels through two corners of a 3-face is likely to block too many other nodes in surrounding 3-faces since a node on opposite corners will affect all 3-faces adjacent to the given 3-face.

If these observations hold in higher dimensions, then a search method that utilizes the 3-face types, such as the representation described in Section 6.2, will have a high likelihood of finding the longest maximal snake in a given dimension. Additionally, the observation that all 3-faces have at least one node on the snake path, and most have more than two, indicates that the longest maximal snake in a given dimension explores the hypercube very thoroughly. Regardless, the analysis of 3-faces and higher m-dimensional faces is the most promising direction of research because it will allow a much better understanding of how the snake path interacts with the a given hypercube based directly on utilization of space by the snake.

Chapter 6

Applications of Analysis for Search Algorithms

6.1 Node Level Representation

The creation of the hypercube level structure introduces the possibility for a new snake path representation, one which would contain a large group of paths rather than a single path, unlike the node sequence. Instead, the new representation identifies a path through the hypercube level structure by specifying the exact order in which to traverse the levels. This novel representation shall be called the *node level representation* (NLR).

The NLR can either be a binary or integer vector. In a binary NLR, a "0" would indicate that the next node on the snake should be on the previous level in the hypercube level structure, while a "1" would indicate that the next node should be on the next level. In an integer NLR the exact order of the levels to traverse is specified, including the initial level (this is different than the binary version which simply specifies the level change, similar to the difference between a transition sequence and a node sequence). However, an integer representation may run into problems with some search techniques where portions are swapped or replaced with new values because the order specified in the representation could become invalid, such as if a level that was not immediately before or after was specified. The binary NLR does not have this problem and is the recommended form of the representation when used in a search algorithm. Regardless, both of these representations reduce the search space by constraining the available nodes that the snake can grow to based on the next level in the representation.

Since the first level of the hypercube only contains one node, the search should always start from that node. Therefore, every NLR should immediately direct the search to the first level of the NLR. Additionally, since every node in level one is adjacent to the node in level zero, the search may never return to level one or it would violate adjacency restrictions. Therefore, every NLR should always continue to the second level. This means that all binary NLRs would begin with {1,1}, while all integer NLRs would begin with {0,1,2}.

Section 4.6 shows the node level patterns of all longest maximal snakes. The NLPs are very similar to the integer NLR except that they identify specific level patterns for known longest maximal snakes. When searching in a dimension whose longest maximal snake has not been found, these patterns are not known so it is assumptive to identify specific representations as patterns since a random NLR is unlikely to generate a longest maximal snake. As Section 4.6 shows, most dimensions only have a single NLP for all longest maximal snakes, and those that have more than one still only have a single NLP per EC. This indicates that a representation which directs what hypercube level the snake should traverse would provide a sufficient reduction in search space to make the representation viable.

The viability of the NLR was further confirmed by the use of an exhaustive search algorithm. The algorithm was a depth-first search that constrained the adjacent nodes available to the tail node to those within the next level specified by the NLR. The algorithm was then run using all NLPs for dimension seven that are given in 4.6. The exhaustive search was able to enumerate the entire search space for the NLPs and find all longest maximal snakes in dimension seven in less than thirty minutes each, with some NLPs taking less than five minutes. This is substantially faster than the weeks or months typically taken by a standard exhaustive search [19, 25].

In addition to the observation that the NLR should always start with {1,1} for binary and {0,1,2} for integer, a search algorithm needs to take other constraints into consideration. For binary NLR, the sequence may specify a level outside the level structure. In that case the search algorithm could ignore all repeated values until a new value indicates a level in the opposite direction, or the search algorithm could *repair* the NLR so that the order specified by the NLR is valid. The first method will decrease the length of the NLR by the amount of values skipped which not only reduces correlation between the NLR and the generated level pattern, but possibly the fitness of the NLR. The second method may be too destructive to any search method, making it difficult for the search method to converge on an optimal NLR. The search algorithm could keep track of any values skipped or repaired and use them as a penalty against the fitness of the NLR. For an integer NLR the algorithm would need to ensure that all values are constrained to the range of levels in the structure and also make sure that every value is only one greater or less than the previous. Similar actions and penalties like those on the binary NLR could be imposed.

The advantages of this representation are obvious since there is such a close correlation between the NLPs and the ECs, so an NLR search is not only guaranteed to find a longest maximal snake, but also reduce the search space. However, the requirements of an exhaustive search to analyze the fitness of the NLR is a serious problem, especially in higher dimensions. If an NLP takes thirty minutes to traverse in dimension seven, one in dimension eight may take much longer which would make a search algorithm extremely slow while the fitness of the NLRs are evaluated. Although, additional domain knowledge could be used by the search algorithm to better search the NLR. This could include restrictions on the transitions between nodes based on the ECTFPs in Table 5.3. Or it could constrain how frequently and when the levels are visited as an approximate constraint based on the NLDs in Table 4.10 or the NLGDs in Table 4.11. Or the search algorithm could restrict the skin density to promote an approximate bell curve as observed in 4.4. All of these additions could help to focus the search in order to improve the speed. Finally, the search algorithm could simply try a time-limited random search within the NLR and perform a statistical analysis of all maximal snakes found to estimate the quality of the NLR rather than performing a completely exhaustive search.

6.2 m-Face Pattern Representation

Another possible representation is based upon the 2-face and 3-face types identified in Appendix C.1 and C.2 respectively. A *2-face pattern representation* would contain a number of ordered pairs equal to the number of 2-faces in the n-dimensional hypercube, while a *3-face pattern representation* would contain a number equal to the number of 3-faces in the hypercube. Each ordered pair corresponds to a specific 2- or 3-face in the hypercube, where the first value of the ordered pair indicates which of the 2- or 3-face types is in that position, while the second value indicates the rotation of that type. For the 2-faces there are five types (ignoring the coil type) and four rotations (one for each node), while for the 3-faces there are fourteen types (ignoring the coil types) and eight rotations (one for each node). These representations are suitable for any search algorithm that can swap or alter values, either within a given representation, or between representations.

To initiate the search, the algorithm could initialize the representations with randomly chosen values from the valid range. Since the m-face pattern representations actually represent the entire hypercube, search for a snake will start at a given node (say node zero) and progress to nodes indicated as snake nodes by the face types. However, the representation may contain many unreachable areas at the beginning of the search because there may be conflicting nodes marked as snake nodes, or unreachable areas, causing the algorithm to have difficulty calculating the fitness of the representation. Therefore, the search algorithm would probably need to incorporate the ability to repair the representation, either by rotation of values or replacement of faces, so that no face marks a node as a snake path node when another face does not. The operation should progress in a linear fashion from one end of the representation, repairing as it went, or from a randomly chosen position on the representation and moving outward in both directions. These repair operations may be too slow or too disruptive to the search to allow it to converge on a longest maximal snake.

Regardless, the representation will theoretically allow finding the longest maximal snake in any dimension since each representation contains the entire hypercube. Domain knowledge could be added to the search algorithm by using the observations from Section 5.4.4 and 5.4.5. The added knowledge may increase accuracy and speed by helping to focus the search and constrain the search space.

6.3 Transition Chunk Representation

Transition chunk representation (TCR) is a novel representation based on the observation that the snake path is simply chunks of transition sequences put together. TCR is an arbitrarily long vector of integers that each correspond to a transition chunk. The vector must be long enough to generate snakes below the upper bound for longest maximal snakes in a given dimension. Each transition chunk is one of a set of unique transition sequences of a limited length generated from all possible transitions in the given dimension. For instance, it is arbitrary to calculate all possible transitions of length four in dimension eight. The set of chunks should at least include all transition sequences of length 2–4 because these are the fundamental building blocks of a snake path. The integer will indicate which transition chunk will appear at that position in the TCR, while the overall TCR can be interpreted as a transition sequence. The TCR is suitable for any search algorithm that can swap or alter values, either within a given representation, or between representations.

To initiate the search, the algorithm could initialize the TCRs with randomly chosen values from the set of chunks. Since the TCR represents a specific transition sequence, the representation may be largely unusable if the transition sequence leads the snake path to a dead end very quickly. However, standard transition sequence representation also suffers from the same problem. This will still cause difficulty in determining the fitness of a given TCR. To help mitigate this, the search algorithm could incorporate a method to repair the TCR either by rotation or replacement of values. Depending on how the set of chunks are calculated, values with a similar index may have similar transition sequences, which indicates that a small increase or decrease in value may fix a dead-end, while not altering the transition sequence too drastically. The repair operation should probably progress in a linear fashion from lowest index to higher since evaluation of the transition sequence is generally done in the same fashion. However, these repair operations may be too slow or disruptive to the search, preventing convergence on a longest maximal snake.

TCR will theoretically allow finding the longest maximal snake in any dimension since enumeration of the set of all possible transition sequence chunks of a given length could produce the transition sequence of any longest maximal snake. Domain knowledge could be added to the search algorithm by using the observations from Section 4.5, 5.4.4 and 5.4.5. The added knowledge may increase accuracy and speed by helping to focus the search and constrain the search space.

Chapter 7

Conclusion

The snake-in-the-box problem has shown itself to be extremely difficult despite being fully observable. The problem is that very little domain knowledge is used in search methods currently employed, which appears to be a drawback in the SIB problem. In order to avoid these pitfalls, this thesis has performed a thorough examination of all dimension 1–7 longest maximal snake paths as they traverse their given hypercubes in order to collect enough characteristics of these paths to properly inform search. The material presented in this thesis provides sufficient data for many new directions of research and experimentation for the snake-in-the-box problem.

A better understanding of the relationship between longest snake paths and the hypercubes they travel through in dimensions that can be exhaustively searched should make search heuristics more intelligent so that they are not easily led into local optima. For instance, knowledge about the spread and density of snake path nodes throughout the hypercube would provide a rough guideline for a search heuristic to ensure that nodes are not tight or too spread out while searching, thereby improving snake length by ensuring that the snake is not too conservative nor too greedy. Knowledge about how the snake travels over and through the sub-hypercubes within a given n-dimensional hypercube will also help search heuristics avoid dead-ends by maintaining an expected degree of tightness within the hypercube. Knowledge about the frequency with which transitions occur in the snake paths will ensure that the snake does not visit a dimension of the hypercube too little or too often.

The symmetry of hypercube space leads me to believe that a heuristic measure could be developed through analysis of the data and observations presented in this thesis to help guide the search for the longest maximal snakes for any n-dimensional hypercube. Additionally, I believe that this measure is possible using a representation based on near-longest maximal snakes of varying lengths that are connected via a small "bridge" sequence of zero to three nodes (which themselves are technically maximal snakes in dimensions less than three). Since an n-dimensional hypercube is essentially two $(n-1)$-dimensional hypercubes whose vertices are connected, I conjecture that the absolute bound of a longest maximal snake in a given dimension n will always fall within the range $2 * length(n-1) - 3 \leq length(n) \leq 2 * length(n-1)$.

There are many areas of research and analysis remaining for the SIB problem. The collected data should be analyzed further to determine if there is any correlation between the various statistics. The interaction between the m-faces and the n-dimensional hypercube should be examined closer to see if there is a predictable nature to the way the snake travels through various m-faces. Additionally, new search techniques can be implemented that utilize all the data collected in this thesis to improve search either as part of an intelligent operator to aid in choosing nodes or transitions on the snake path, or it could be used as a penalty term calculated by the search heuristic's fitness operator.

Bibliography

[1] H.L. Abbott and M. Katchalski, “On the Snake-in-the-Box Problem,” Journal of Combinatorial Theory, vol. 45, pp. 13-24, 1988.

[2] J. Bishop, “Investigating the Snake-in-the-box problem with Neuroevolution,” Technical report, Department of Computer Science, University of Texas, Austin.

[3] W.L. Black, “Electronic combination locks,” *Quarterly Progress Report of the Research Laboratory of Electronics*, No. 73, Massachusetts Institute of Technology, Cambridge, Massachusetts, pp. 232–233, April, 1964.

[4] D.A. Casella and W.D. Potter, “Using Evolutionary Techniques to Hunt for Snakes and Coils,” *Proceedings of 2005 IEEE Congress on Evolutionary Computing*, CEC’05, pp. 2499–2505, Edinburgh, Scotland, Sept. 2-5, 2005.

[5] H.S.M Coxeter, *Regular Polytopes.* 2nd Edition. New York, NY: The Macmillan Company, 1963.

[6] P. Diaz-Gomez and D. Hougen, “Genetic Algorithms for Hunting Snakes in Hypercubes: Fitness Function Analysis and Open Questions,” *Seventh ACIS International Conference on Software Engineering, Artificial Intelligence, Networking, and Parallel/Distributed Computing* (SNPD’06). IEEE, Computer Society, Los Alamitos, CA, pp. 389–394, 2006.

[7] E. Drucker, “Exploring applications of extremal optimization,” M.S. thesis, University of Georgia, Athens, GA, 2009.

[8] P.G. Emelyanov and A. Lukito, “On the Maximal Length of a Snake in Hypercubes of Small Dimension,” *Discrete Mathematics*, vol. 218, pp. 51-59, 2000.

[9] M.L. Gargano, J.F. Malerba, and M. Lewinter, “Hypercubes and Pascal’s Triangle: A Tale of Two Proofs,” *Mathematics Magazine*, vol. 76, no. 3, pp. 216–217, June, 2003.

[10] D.E. Goldberg, *Genetic Algorithms in Search, Optimization, and Machine Learning.* Boston, MA: Addison-Wesley Publishing Co., Inc., 1989.

[11] S. Hardas, “An ant colony approach to the snake-in-the-box problem,” M.S. thesis, University of Georgia, Athens, GA, 2005.

[12] L. Haryanto, “Constructing snake-in-the-box codes and families of such codes covering the hypercube,” Ph.D. dissertation (A.J. van Zanten, Adviser), Delft University of Technology, Delft, Netherlands, 2007.

[13] A.P. Hiltgen and K.G. Paterson, “Single Track Circuit Codes,” *IEEE Transactions on Information Theory*, vol. 47, pp. 2587–2595, 2000.

[14] Institute for Artificial Intelligence, “Latest Records for the Snake-in-the-Box Problem (November, 2009),” *IAI Snake-in-the-Box Site at UGA*, Nov. 2009. [Online]. Available: http://www.ai.uga.edu/sib/records/. [Accessed: Apr. 16, 2010].

[15] M. Juric, W.D. Potter, and M. Plaksin, “Using PVM for Hunting Snake In The Box Codes,” *Proceedings of the 1994 Transputer Research and Applications Conference* (NATUG-7), pp. 97-102, Athens, GA, October, 1994.

[16] W.H. Kautz, “Unit-Distance Error-Checking Codes,” *IRE Transactions on Electronic Computers*, vol. EC-7, pp. 179–180, June, 1958.

[17] S. Kim and D.L. Neuhoff, “Snake-In-The-Box Codes as Robust Quantizer Index Assignments,” *Proceedings of IEEE International Symposium on Information Theory*, pp. 402, June 25–30, 2000.

[18] V. Klee, "The Use of Circuit Codes in Analog-to-Digital Conversion," *Graph Theory and its Applications*, (B.Harris, ed.), Academic Press, New York, pp. 121–131, 1970.

[19] K.J. Kochut, "Snake-in-the-box codes for dimension 7, *Journal of Combinatorial Mathematics and Combinatorial Computations*, vol. 20, pp. 175–185, 1996.

[20] W.D. Potter, R.W. Robinson, J.A. Miller, and K.J. Kochut, "Using the Genetic Algorithm to Find Snake-In-The-Box Codes," *Proceedings of the 7th International Conference on Industrial & Engineering Applications of Artificial Intelligence and Expert Systems*, pp. 421–426, Austin, Texas, 1994.

[21] F. Preparata and J. Nievergelt, "Difference-preserving codes," *IEEE Transactions on Information Theory*, vol. 20, pp. 643–649, 1974.

[22] R.E. Smith, "Genetic and Evolutionary Systems," *Adaptive Computing: Mathematics, Electronics, and Optics*, vol. CR5, pp. 151–174, SPIE Press, 1994.

[23] F.I. Solov'eva, "An Upper Bound for the Length of a Cycle in an n-Dimensional Unit Cube," *Dickretnyj Analiz*, vol. 45, pp. 71–76, 1987.

[24] D.R. Tuohy, W.D. Potter, and D.A. Casella, "Searching for Snake-In-The-Box Codes With Evolved Pruning Models," *Proceedings of The 2007 International Conference on Genetic and Evolutionary Methods (GEM'2007)*, CSREA Press, pp. 3–9, 2007.

[25] C. Wong and J. Sawada, "Exhaustive search for maximal length coil-in-the-box codes," Technical report (TR-UG-CIS-2008-001), University of Guelph, Guelph, Ontario, Canada, June, 2008.

Appendix A

Known Longest Maximal Snake Lengths

Table A.1: Longest Maximal Snake Length Lower Bound [14]

Dimension	Snake	Coil
1*	1	0
2*	2	4
3*	4	6
4*	7	8
5*	13	14
6*	26	26
7*	50	48
8	98	96
9	190	186
10	363	344
11	680	630
12	1260	1238

* absolute bound

Appendix B

Equivalence Class (Canonical Snake) Data

B.1 Equivalence Class Hypercube Map (ECHM)

Table B.1: Equivalence Class Hypercube Map (ECHM) Dimension 1–5

Dimension		Hypercube Node																															
n	EC	0	1	2	3	4	5	6	7	8	9	10	11	12	13	14	15	16	17	18	19	20	21	22	23	24	25	26	27	28	29	30	31
1		0	1																														
2		0	1	|	2																												
3		0	1	|	2	|	|	4	3																								
4		0	1	|	2	|	|	4	3	|	|	|	|	6	7	5	|																
5	1	0	1	|	2	|	|	|	3	|	|	|	|	6	|	5	4	|	|	12	|	|	|	13	|	|	9	11	10	7	8	|	|
	2	0	1	|	2	|	|	|	3	|	|	|	|	6	|	5	4	|	|	10	|	8	|	9	|	|	13	11	12	7	|	|	|
	3	0	1	|	2	|	|	|	3	|	|	6	|	|	|	5	4	|	|	|	|	12	|	13	|	|	9	7	8	11	10	|	|
	4	0	1	|	2	|	|	|	3	|	|	6	|	|	|	5	4	|	|	|	|	12	11	13	|	|	9	7	8	|	10	|	|
	5	0	1	|	2	|	|	|	3	|	|	6	|	|	|	5	4	|	|	|	|	12	11	13	|	8	9	7	|	|	10	|	|
	6	0	1	|	2	|	|	|	3	|	|	6	|	|	|	5	4	|	|	8	|	10	11	9	|	|	13	7	|	|	12	|	|
	7	0	1	|	2	|	|	|	3	|	|	6	|	|	|	5	4	|	|	8	|	10	|	9	|	|	13	7	|	11	12	|	|
	8	0	1	|	2	|	|	|	3	|	|	|	|	6	5	|	4	|	|	10	|	8	|	9	|	|	13	11	12	7	|	|	|

Table B.2: Equivalence Class Hypercube Map (ECHM) Dimension 6–7

Dimension		Hypercube Node																										
n	EC	0	1	2	3	4	5	6	7	8	9	10	11	12	13	14	15	16	17	18	19	20	21	22	23	24	25	26	⋯
6		0	1	|	2	|	|	|	3	|	|	26	|	6	5	|	4	|	|	24	|	8	9	|	|	|	#	25	
7	1	0	1	|	2	|	|	4	3	|	|	|	|	6	7	5	|	|	|	12	|	#	|	|	|	|	9	11	
	2	0	1	|	2	|	|	4	3	|	|	|	|	6	7	5	|	|	|	12	|	#	|	|	|	|	9	11	
	3	0	1	|	2	|	|	4	3	|	|	|	|	6	7	5	|	|	|	12	|	#	|	|	|	|	9	11	
	4	0	1	|	2	|	|	|	3	|	|	|	|	6	|	5	4	|	|	12	|	|	|	|	|	|	9	11	
	5	0	1	|	2	|	|	|	3	|	|	|	|	6	|	5	4	|	|	12	|	|	|	|	|	|	9	11	
	6	0	1	|	2	|	|	|	3	|	|	|	|	6	|	5	4	|	|	10	|	8	|	9	|	|	|	11	
	7	0	1	|	2	|	|	|	3	|	|	|	|	|	5	|	4	|	|	24	|	|	|	23	|	8	7	|	
	8	0	1	|	2	|	|	|	3	|	|	|	|	|	5	|	4	|	|	24	|	|	|	23	|	|	7	|	
	9	0	1	|	2	|	|	|	3	|	|	|	|	|	5	|	4	|	|	|	|	24	|	23	|	|	7	|	
	10	0	1	|	2	|	|	|	3	|	|	18	|	|	|	|	4	|	|	16	|	14	|	15	|	|	#	17	
	11	0	1	|	2	|	|	|	3	|	|	18	|	|	|	|	4	|	|	16	|	14	|	15	|	|	#	17	
	12	0	1	|	2	|	|	|	3	|	|	18	|	|	|	|	4	|	|	16	|	14	|	15	|	|	#	17	

Dimension		Hypercube Node (cont.)																											
n	EC	⋯	27	28	29	30	31	32	33	34	35	36	37	38	39	40	41	42	43	44	45	46	47	48	49	50	51	52	⋯
6			|	7	|	|	|	|	|	|	|	12	11	13	|	20	19	|	18	|	|	14	|	22	|	23	|	|	
7	1		10	|	8	|	|	|	|	|	|	18	17	|	|	50	49	|	48	|	|	|	47	|	15	13	14	|	
	2		10	|	8	|	|	|	|	|	|	18	17	|	|	46	47	|	48	|	|	|	49	|	15	13	14	|	
	3		10	|	8	|	|	|	|	|	|	18	17	|	|	50	49	|	48	|	|	|	47	14	15	13	|	|	
	4		10	7	8	|	|	|	|	|	|	32	33	|	|	36	35	37	|	|	34	|	|	|	|	13	14	31	
	5		10	7	8	|	|	|	|	|	|	32	33	|	|	|	35	37	36	|	34	|	|	|	|	13	14	31	
	6		12	7	|	|	|	|	|	36	|	34	33	35	|	|	|	37	|	|	32	|	|	16	15	|	14	|	
	7		|	|	6	22	|	|	|	16	|	14	13	15	|	|	|	17	18	|	|	|	|	10	11	|	|	|	
	8		8	|	6	22	|	|	|	16	|	14	13	15	|	18	|	17	|	|	|	|	|	|	11	|	10	|	
	9		8	|	6	22	|	|	|	16	|	14	13	15	|	18	|	17	|	|	|	|	|	|	|	|	10	|	
	10		|	13	|	|	5	|	|	|	|	22	23	21	|	|	25	19	|	|	24	20	|	10	9	|	8	|	
	11		|	13	|	|	5	|	|	20	|	22	23	21	|	|	25	19	|	|	24	|	|	10	9	|	8	|	
	12		|	13	|	|	5	|	|	20	|	22	23	21	|	|	25	19	|	|	24	|	|	10	9	|	8	|	

Table B.2: Equivalence Class Hypercube Map (ECHM) Dimension 6–7 - cont.

Dimension		Hypercube Node (cont.)																											
n	EC	···	53	54	55	56	57	58	59	60	61	62	63	64	65	66	67	68	69	70	71	72	73	74	75	76	77	78	···
6			10	|	|	21	|	|	17	|	|	15	16																
7	1		16	|	|	|	|	|	|	44	|	45	46	|	|	|	|	20	21	|	|	26	27	|	28	|	|	|	
	2		16	|	|	45	|	|	|	44	|	|	50	|	|	|	|	20	21	|	|	26	27	|	28	|	|	|	
	3		16	|	|	|	|	|	|	44	|	45	46	|	|	|	|	20	21	|	|	26	27	|	28	|	|	|	
	4		|	|	15	|	|	|	|	|	|	17	16	|	|	|	|	44	43	45	|	|	41	39	40	|	42	|	
	5		|	|	15	|	|	|	|	|	|	17	16	|	|	|	|	44	43	45	|	|	41	39	40	|	42	|	
	6		|	|	|	17	|	|	13	|	31	|	|	|	|	40	|	42	43	41	|	|	45	39	|	|	44	|	
	7		12	|	|	9	|	|	19	|	|	21	20	|	|	|	|	30	29	31	|	46	47	|	48	|	|	32	
	8		12	|	|	19	|	|	9	20	|	21	|	|	|	|	|	30	29	31	|	48	47	|	46	|	|	32	
	9		12	|	11	19	|	|	9	20	|	21	|	|	|	50	|	|	#	49	|	32	33	|	34	|	|	48	
	10		|	|	7	11	|	|	|	12	|	|	6	|	|	46	|	44	43	45	|	28	|	|	|	|	42	|	
	11		|	|	7	11	|	|	|	12	|	|	6	|	|	|	|	44	43	45	|	28	|	|	|	|	42	46	
	12		|	|	7	11	|	|	|	12	|	|	6	|	|	|	|	34	35	33	|	50	|	|	|	|	36	32	

Dimension		Hypercube Node (cont.)																											
n	EC	···	79	80	81	82	83	84	85	86	87	88	89	90	91	92	93	94	95	96	97	98	99	100	101	102	103	104	···
6																													
7	1		29	24	23	|	|	|	22	32	|	25	|	|	|	|	|	31	30	|	|	37	36	19	|	|	35	|	
	2		29	24	23	|	|	|	22	32	|	25	|	|	|	|	|	31	30	|	|	37	36	19	|	|	35	|	
	3		29	24	23	|	|	|	22	32	|	25	|	|	|	|	|	31	30	|	|	37	36	19	|	|	35	|	
	4		|	24	23	|	22	|	|	|	21	25	|	|	|	|	|	19	20	50	49	|	48	|	|	46	47	|	
	5		|	24	23	|	22	|	|	|	21	25	|	|	|	|	|	19	20	50	49	|	48	|	|	46	47	|	
	6		|	20	21	|	22	|	|	|	23	19	|	|	|	|	|	25	24	|	47	|	48	|	|	|	49	|	
	7		|	26	27	25	|	|	28	|	|	|	|	|	49	|	|	|	50	44	43	|	42	|	|	|	|	45	
	8		|	|	27	25	26	|	28	|	|	49	|	|	|	50	|	|	|	42	43	|	44	|	|	|	|	|	
	9		|	|	39	|	40	25	|	|	41	31	|	30	|	|	|	|	42	|	37	|	36	|	|	|	|	|	
	10		|	30	31	|	32	|	|	|	|	29	|	|	33	|	41	|	|	|	|	47	48	|	|	|	49	27	
	11		|	30	31	|	32	|	|	|	|	29	|	|	33	|	41	|	|	|	|	|	50	|	|	|	49	27	
	12		|	48	47	|	46	|	|	|	|	49	|	|	45	|	37	|	|	|	27	|	28	|	|	|	29	|	

Table B.2: Equivalence Class Hypercube Map (ECHM) Dimension 6–7 - cont.

Dimension		Hypercube Node (cont.)																						
n	EC	···	105	106	107	108	109	110	111	112	113	114	115	116	117	118	119	120	121	122	123	124	125	126	127
6																									
7	1		|	38	|	|	|	|	|	|	|	|	|	|	|	33	34	|	41	39	40	43	42	|	|
7	2		|	38	|	|	|	|	|	|	|	|	|	|	|	33	34	|	41	39	40	43	42	|	|
7	3		|	38	|	|	|	|	|	|	|	|	|	|	|	33	34	|	41	39	40	43	42	|	|
7	4		|	38	|	#	|	|	|	|	|	|	|	30	29	|	|	26	27	|	|	|	28	18	|
7	5		|	38	|	#	|	|	|	|	|	|	|	30	29	|	|	26	27	|	|	|	28	18	|
7	6		46	38	|	#	|	|	50	|	|	|	|	28	29	27	|	18	|	|	|	|	30	26	|
7	7		|	|	|	|	35	33	34	|	|	|	41	38	|	39	40	|	|	#	|	37	36	|	|
7	8		|	|	45	34	35	33	|	41	|	|	|	40	|	39	38	|	|	#	|	|	36	|	37
7	9		|	|	35	46	45	47	|	|	38	28	|	26	|	27	|	|	|	29	|	|	44	|	43
7	10		26	|	|	|	|	|	50	|	|	|	|	38	39	37	|	|	|	35	34	|	40	36	|
7	11		26	|	|	|	|	47	48	|	|	36	|	38	39	37	|	|	|	35	34	|	40	|	|
7	12		26	|	|	|	|	31	30	|	|	42	|	40	39	41	|	|	|	43	44	|	38	|	|

B.2 Node Type Growth Analysis

Table B.3: Node Type Growth Pattern (ECNTGP) Dimension 1–6

Dimension		Node Type[1]	Transition Sequence Index																										
n	EC			0	1	2	3	4	5	6	7	8	9	10	11	12	13	14	15	16	17	18	19	20	21	22	23	24	25
1		A	1	0																									
		U	1	2																									
		S	0	0																									
2		A	3	1	0																								
		U	1	3	4																								
		S	0	1	1																								
3		A	7	4	2	1	0																						
		U	1	4	6	7	8																						
		S	0	2	3	3	3																						
4		A	15	11	8	6	4	3	1	0																			
		U	1	5	8	10	12	13	15	16																			
		S	0	3	5	6	7	7	8	8																			
5	1,2,5	A	31	26	22	19	16	13	10	9	6	4	3	2	1	0													
		U	1	6	10	13	16	19	22	23	26	28	29	30	31	32													
		S	0	4	7	9	11	13	15	15	17	18	18	18	18	18													
	3,4,6,7	A	31	26	22	19	16	13	10	9	6	5	4	2	1	0													
		U	1	6	10	13	16	19	22	23	26	27	28	30	31	32													
		S	0	4	7	9	11	13	15	15	17	17	17	18	18	18													
	8	A	31	26	22	19	16	13	11	10	7	5	4	3	1	0													
		U	1	6	10	13	16	19	21	22	25	27	28	29	31	32													
		S	0	4	7	9	11	13	14	14	16	17	17	17	18	18													
6		A	63	57	52	48	44	40	37	35	31	28	27	23	22	21	18	16	14	13	9	8	7	6	5	4	3	2	1
		U	1	7	12	16	20	24	27	29	33	36	37	41	42	43	46	48	50	51	55	56	57	58	59	60	61	62	63
		S	0	5	9	12	15	18	20	21	24	26	26	29	29	29	31	32	33	33	36	36	36	36	36	36	36	36	36

[1] "A" indicates *Available Nodes*, "U" indicates *Unavailable Nodes*, and "S" indicates *Skin Nodes*

Table B.4: Node Type Growth Pattern (ECNTGP) Dimension 7

Dimension		Node Type	Transition Sequence Index																									
n	EC		0	1	2	3	4	5	6	7	8	9	10	11	12	13	14	15	16	17	18	19	20	21	22	23	24	···
7	1,2	A	127	120	114	109	104	100	95	91	88	83	79	76	73	71	66	63	61	58	56	55	50	48	47	45	43	41	
		U	1	8	14	19	24	28	33	37	40	45	49	52	55	57	62	65	67	70	72	73	78	80	81	83	85	87	
		S	0	6	11	15	19	22	26	29	31	35	38	40	42	43	47	49	50	52	53	53	57	58	58	59	60	61	
	3	A	127	120	114	109	104	100	95	91	88	83	79	76	73	71	66	62	60	57	55	54	49	47	46	44	42	41	
		U	1	8	14	19	24	28	33	37	40	45	49	52	55	57	62	66	68	71	73	74	79	81	82	84	86	87	
		S	0	6	11	15	19	22	26	29	31	35	38	40	42	43	47	50	51	53	54	54	58	59	59	60	61	61	
	4	A	127	120	114	109	104	99	94	91	86	82	79	76	73	70	65	62	59	57	56	51	49	48	46	45	43	40	
		U	1	8	14	19	24	29	34	37	42	46	49	52	55	58	63	66	69	71	72	77	79	80	82	83	85	88	
		S	0	6	11	15	19	23	27	29	33	36	38	40	42	44	48	50	52	53	53	57	58	58	59	59	60	62	
	5	A	127	120	114	109	104	99	94	91	86	82	79	76	73	70	65	62	59	57	56	51	49	48	46	45	43	40	
		U	1	8	14	19	24	29	34	37	42	46	49	52	55	58	63	66	69	71	72	77	79	80	82	83	85	88	
		S	0	6	11	15	19	23	27	29	33	36	38	40	42	44	48	50	52	53	53	57	58	58	59	59	60	62	
	6	A	127	120	114	109	104	99	94	91	86	82	79	76	73	70	65	62	59	57	55	50	47	46	44	43	41	38	
		U	1	8	14	19	24	29	34	37	42	46	49	52	55	58	63	66	69	71	73	78	81	82	84	85	87	90	
		S	0	6	11	15	19	23	27	29	33	36	38	40	42	44	48	50	52	53	54	58	60	60	61	61	62	64	
	7	A	127	120	114	109	104	99	95	90	86	83	78	74	71	68	66	63	59	57	54	51	49	47	45	43	40	39	
		U	1	8	14	19	24	29	33	38	42	45	50	54	57	60	62	65	69	71	74	77	79	81	83	85	88	89	
		S	0	6	11	15	19	23	26	30	33	35	39	42	44	46	47	49	52	53	55	57	58	59	60	61	63	63	
	8	A	127	120	114	109	104	99	95	90	86	83	78	74	71	68	66	63	59	57	54	51	49	47	45	43	40	39	
		U	1	8	14	19	24	29	33	38	42	45	50	54	57	60	62	65	69	71	74	77	79	81	83	85	88	89	
		S	0	6	11	15	19	23	26	30	33	35	39	42	44	46	47	49	52	53	55	57	58	59	60	61	63	63	
	9	A	127	120	114	109	104	99	95	90	86	83	78	74	71	68	66	63	60	58	55	52	49	47	45	43	40	39	
		U	1	8	14	19	24	29	33	38	42	45	50	54	57	60	62	65	68	70	73	76	79	81	83	85	88	89	
		S	0	6	11	15	19	23	26	30	33	35	39	42	44	46	47	49	51	52	54	56	58	59	60	61	63	63	
	10	A	127	120	114	109	104	99	94	89	85	82	79	76	71	68	65	62	60	58	56	54	50	48	46	44	42	40	
		U	1	8	14	19	24	29	34	39	43	46	49	52	57	60	63	66	68	70	72	74	78	80	82	84	86	88	
		S	0	6	11	15	19	23	27	31	34	36	38	40	44	46	48	50	51	52	53	54	57	58	59	60	61	62	
	11	A	127	120	114	109	104	99	94	89	85	82	79	76	71	68	65	62	60	58	56	54	50	48	46	44	42	40	
		U	1	8	14	19	24	29	34	39	43	46	49	52	57	60	63	66	68	70	72	74	78	80	82	84	86	88	
		S	0	6	11	15	19	23	27	31	34	36	38	40	44	46	48	50	51	52	53	54	57	58	59	60	61	62	
	12	A	127	120	114	109	104	99	94	89	85	82	79	76	71	68	65	62	60	58	56	54	50	48	46	44	42	40	
		U	1	8	14	19	24	29	34	39	43	46	49	52	57	60	63	66	68	70	72	74	78	80	82	84	86	88	
		S	0	6	11	15	19	23	27	31	34	36	38	40	44	46	48	50	51	52	53	54	57	58	59	60	61	62	

Table B.4: Node Type Growth Pattern (ECNTGP) Dimension 7 - cont.

Dimension		Node Type	Transition Sequence Index (cont.)																									
n	EC		…	25	26	27	28	29	30	31	32	33	34	35	36	37	38	39	40	41	42	43	44	45	46	47	48	49
7	1,2	A		38	35	33	31	29	27	25	24	23	22	21	19	17	14	13	12	11	9	8	6	5	4	3	2	1
		U		90	93	95	97	99	101	103	104	105	106	107	109	111	114	115	116	117	119	120	122	123	124	125	126	127
		S		63	65	66	67	68	69	70	70	70	70	70	71	72	74	74	74	74	75	75	76	76	76	76	76	76
	3	A		38	35	33	31	29	27	25	24	23	21	20	18	16	13	12	11	10	8	7	6	5	4	3	2	1
		U		90	93	95	97	99	101	103	104	105	107	108	110	112	115	116	117	118	120	121	122	123	124	125	126	127
		S		63	65	66	67	68	69	70	70	70	71	71	72	73	75	75	75	75	76	76	76	76	76	76	76	76
	4	A		38	35	32	30	28	26	25	23	22	21	19	18	17	14	12	11	10	9	8	7	6	5	3	2	1
		U		90	93	96	98	100	102	103	105	106	107	109	110	111	114	116	117	118	119	120	121	122	123	125	126	127
		S		63	65	67	68	69	70	70	71	71	71	72	72	72	74	75	75	75	75	75	75	75	75	76	76	76
	5	A		38	35	32	30	28	26	25	23	22	21	19	17	16	14	12	11	10	9	8	7	6	5	3	2	1
		U		90	93	96	98	100	102	103	105	106	107	109	111	112	114	116	117	118	119	120	121	122	123	125	126	127
		S		63	65	67	68	69	70	70	71	71	71	72	73	73	74	75	75	75	75	75	75	75	75	76	76	76
	6	A		37	34	31	29	27	25	24	22	21	20	19	17	16	14	12	11	10	9	8	7	6	5	3	2	1
		U		91	94	97	99	101	103	104	106	107	108	109	111	112	114	116	117	118	119	120	121	122	123	125	126	127
		S		64	66	68	69	70	71	71	72	72	72	72	73	73	74	75	75	75	75	75	75	75	75	76	76	76
	7	A		34	32	31	29	28	26	25	23	21	19	17	15	13	12	11	10	9	8	7	6	5	4	3	2	1
		U		94	96	97	99	100	102	103	105	107	109	111	113	115	116	117	118	119	120	121	122	123	124	125	126	127
		S		67	68	68	69	69	70	70	71	72	73	74	75	76	76	76	76	76	76	76	76	76	76	76	76	76
	8	A		34	32	31	29	28	26	25	23	21	20	18	16	14	12	11	10	9	8	7	6	5	4	3	2	1
		U		94	96	97	99	100	102	103	105	107	108	110	112	114	116	117	118	119	120	121	122	123	124	125	126	127
		S		67	68	68	69	69	70	70	71	72	72	73	74	75	76	76	76	76	76	76	76	76	76	76	76	76
	9	A		34	32	31	29	28	26	25	23	21	20	18	16	14	12	11	10	9	8	7	6	5	4	3	2	1
		U		94	96	97	99	100	102	103	105	107	108	110	112	114	116	117	118	119	120	121	122	123	124	125	126	127
		S		67	68	68	69	69	70	70	71	72	72	73	74	75	76	76	76	76	76	76	76	76	76	76	76	76
	10	A		39	34	31	29	27	26	24	22	20	19	17	15	14	13	12	11	10	9	8	7	5	4	3	2	1
		U		89	94	97	99	101	102	104	106	108	109	111	113	114	115	116	117	118	119	120	121	123	124	125	126	127
		S		62	66	68	69	70	70	71	72	73	73	74	75	75	75	75	75	75	75	75	75	76	76	76	76	76
	11	A		39	34	31	29	27	26	24	22	20	19	17	16	15	14	13	12	11	10	9	8	6	4	3	2	1
		U		89	94	97	99	101	102	104	106	108	109	111	112	113	114	115	116	117	118	119	120	122	124	125	126	127
		S		62	66	68	69	70	70	71	72	73	73	74	74	74	74	74	74	74	74	74	74	75	76	76	76	76
	12	A		39	34	32	31	30	29	26	23	21	20	18	17	15	14	13	12	11	10	9	8	6	4	3	2	1
		U		89	94	96	97	98	99	102	105	107	108	110	111	113	114	115	116	117	118	119	120	122	124	125	126	127
		S		62	66	67	67	67	67	69	71	72	72	73	73	74	74	74	74	74	74	74	74	75	76	76	76	76

B.3 Skin Density Growth Analysis

Table B.5: Skin Density Growth Pattern (ECSDGP) Dimension 1–4

Dimension		Skin	Transition Sequence Index							
n	EC	Density		0	1	2	3	4	5	6
1		1	0	0						
		Min	0	0						
		Max	0	0						
		Sum	0	0						
2		1	0	1	0					
		2	0	0	1					
		Min	0	1	2					
		Max	0	1	2					
		Sum	0	1	2					
3		1	0	2	2	1	0			
		2	0	0	1	2	2			
		3	0	0	0	0	1			
		Min	0	1	1	1	2			
		Max	0	1	2	2	3			
		Sum	0	2	4	5	7			
4		1	0	3	4	4	4	3	3	2
		2	0	0	1	2	2	3	3	2
		3	0	0	0	0	1	1	2	4
		4	0	0	0	0	0	0	0	0
		Min	0	1	1	1	1	1	1	1
		Max	0	1	2	2	3	3	3	3
		Sum	0	3	6	8	11	12	15	18

Table B.6: Skin Density Growth Pattern (ECSDGP) Dimension 5

Dimension		Skin Density	Transition Sequence Index													
n	EC			0	1	2	3	4	5	6	7	8	9	10	11	12
5	1	1	0	4	6	7	8	9	8	7	8	6	5	4	3	1
		2	0	0	1	2	3	4	7	8	8	11	10	9	8	9
		3	0	0	0	0	0	0	0	0	1	1	3	5	7	7
		4	0	0	0	0	0	0	0	0	0	0	0	0	0	1
		5	0	0	0	0	0	0	0	0	0	0	0	0	0	0
		Min	0	1	1	1	1	1	1	1	1	1	1	1	1	1
		Max	0	1	2	2	2	2	2	2	3	3	3	3	3	4
		Sum	0	4	8	11	14	17	22	23	27	31	34	37	40	44
	2	1	0	4	6	7	8	9	8	7	8	8	7	5	4	1
		2	0	0	1	2	3	4	7	8	8	7	6	8	7	9
		3	0	0	0	0	0	0	0	0	1	3	5	4	6	7
		4	0	0	0	0	0	0	0	0	0	0	0	1	1	1
		5	0	0	0	0	0	0	0	0	0	0	0	0	0	0
		Min	0	1	1	1	1	1	1	1	1	1	1	1	1	1
		Max	0	1	2	2	2	2	2	2	3	3	3	4	4	4
		Sum	0	4	8	11	14	17	22	23	27	31	34	37	40	44
	3	1	0	4	6	7	8	9	10	9	9	6	5	5	2	0
		2	0	0	1	2	3	4	3	4	6	9	9	8	11	12
		3	0	0	0	0	0	0	2	2	1	1	2	4	4	4
		4	0	0	0	0	0	0	0	0	1	1	1	1	1	2
		5	0	0	0	0	0	0	0	0	0	0	0	0	0	0
		Min	0	1	1	1	1	1	1	1	1	1	1	1	1	2
		Max	0	1	2	2	2	2	3	3	4	4	4	4	4	4
		Sum	0	4	8	11	14	17	22	23	28	31	33	37	40	44
	4	1	0	4	6	7	8	9	10	9	9	6	5	5	2	1
		2	0	0	1	2	3	4	3	4	6	9	9	8	11	9
		3	0	0	0	0	0	0	2	2	1	1	2	4	4	7
		4	0	0	0	0	0	0	0	0	1	1	1	1	1	1
		5	0	0	0	0	0	0	0	0	0	0	0	0	0	0
		Min	0	1	1	1	1	1	1	1	1	1	1	1	1	1
		Max	0	1	2	2	2	2	3	3	4	4	4	4	4	4
		Sum	0	4	8	11	14	17	22	23	28	31	33	37	40	44

Table B.6: Skin Density Growth Pattern (ECSDGP) Dimension 5 - cont.

Dimension		Skin Density	Transition Sequence Index													
n	EC			0	1	2	3	4	5	6	7	8	9	10	11	12
5	5	1	0	4	6	7	8	9	10	9	10	8	5	4	3	2
		2	0	0	1	2	3	4	3	4	4	7	10	9	8	6
		3	0	0	0	0	0	0	2	2	3	3	3	5	7	10
		4	0	0	0	0	0	0	0	0	0	0	0	0	0	0
		5	0	0	0	0	0	0	0	0	0	0	0	0	0	0
		Min	0	1	1	1	1	1	1	1	1	1	1	1	1	1
		Max	0	1	2	2	2	2	3	3	3	3	3	3	3	3
		Sum	0	4	8	11	14	17	22	23	27	31	34	37	40	44
	6	1	0	4	6	7	8	9	10	9	9	8	7	7	4	1
		2	0	0	1	2	3	4	3	4	6	5	5	4	7	9
		3	0	0	0	0	0	0	2	2	1	3	4	6	6	7
		4	0	0	0	0	0	0	0	0	1	1	1	1	1	1
		5	0	0	0	0	0	0	0	0	0	0	0	0	0	0
		Min	0	1	1	1	1	1	1	1	1	1	1	1	1	1
		Max	0	1	2	2	2	2	3	3	4	4	4	4	4	4
		Sum	0	4	8	11	14	17	22	23	28	31	33	37	40	44
	7	1	0	4	6	7	8	9	10	9	9	8	7	6	3	0
		2	0	0	1	2	3	4	3	4	6	5	5	7	10	12
		3	0	0	0	0	0	0	2	2	1	3	4	3	3	4
		4	0	0	0	0	0	0	0	0	1	1	1	2	2	2
		5	0	0	0	0	0	0	0	0	0	0	0	0	0	0
		Min	0	1	1	1	1	1	1	1	1	1	1	1	1	2
		Max	0	1	2	2	2	2	3	3	4	4	4	4	4	4
		Sum	0	4	8	11	14	17	22	23	28	31	33	37	40	44
	8	1	0	4	6	7	8	9	7	6	7	5	4	3	3	2
		2	0	0	1	2	3	3	6	7	7	10	9	9	8	6
		3	0	0	0	0	0	1	1	1	2	2	4	5	7	10
		4	0	0	0	0	0	0	0	0	0	0	0	0	0	0
		5	0	0	0	0	0	0	0	0	0	0	0	0	0	0
		Min	0	1	1	1	1	1	1	1	1	1	1	1	1	1
		Max	0	1	2	2	2	3	3	3	3	3	3	3	3	3
		Sum	0	4	8	11	14	18	22	23	27	31	34	36	40	44

Table B.7: Skin Density Growth Pattern (ECSDGP) Dimension 6

Dimension		Skin Density	Transition Sequence Index																										
n	EC			0	1	2	3	4	5	6	7	8	9	10	11	12	13	14	15	16	17	18	19	20	21	22	23	24	25
6		1	0	5	8	10	12	14	13	13	15	15	14	14	12	11	12	10	8	7	8	7	7	6	5	3	1	0	0
		2	0	0	1	2	3	3	6	7	7	8	9	12	13	13	12	15	17	18	19	17	14	12	12	13	14	13	13
		3	0	0	0	0	0	1	1	1	2	2	2	2	2	3	5	5	6	6	6	9	11	14	13	13	13	15	10
		4	0	0	0	0	0	0	0	0	0	1	1	0	1	1	1	1	1	1	2	2	3	3	5	6	7	6	11
		5	0	0	0	0	0	0	0	0	0	0	0	1	1	1	1	1	1	1	1	1	1	1	1	1	1	2	2
		6	0	0	0	0	0	0	0	0	0	0	0	0	0	0	0	0	0	0	0	0	0	0	0	0	0	0	0
		Min	0	1	1	1	1	1	1	1	1	1	1	1	1	1	1	1	1	1	1	1	1	1	1	1	1	2	2
		Max	0	1	2	2	2	3	3	3	3	4	4	5	5	5	5	5	5	5	5	5	5	5	5	5	5	5	5
		Sum	0	5	10	14	18	23	28	30	35	41	42	49	53	55	60	64	69	70	77	81	85	89	93	97	101	105	110

Table B.8: Skin Density Growth Pattern (ECSDGP) Dimension 7 EC 1–3

Dimension		Skin Density	Transition Sequence Index																									
n	EC			0	1	2	3	4	5	6	7	8	9	10	11	12	13	14	15	16	17	18	19	20	21	22	23	24 ···
7	1	1	0	6	10	13	16	18	21	23	24	27	27	26	26	26	28	27	25	25	22	21	22	20	17	16	16	16
		2	0	0	1	2	2	3	3	2	3	3	6	9	10	11	13	15	18	19	23	24	27	29	31	32	30	29
		3	0	0	0	0	1	1	2	4	4	5	5	5	5	5	4	5	5	5	4	4	4	5	6	6	9	11
		4	0	0	0	0	0	0	0	0	0	0	0	0	1	1	2	2	2	3	4	4	3	2	2	3	3	3
		5	0	0	0	0	0	0	0	0	0	0	0	0	0	0	0	0	0	0	0	0	1	2	2	2	2	2
		6	0	0	0	0	0	0	0	0	0	0	0	0	0	0	0	0	0	0	0	0	0	0	0	0	0	0
		7	0	0	0	0	0	0	0	0	0	0	0	0	0	0	0	0	0	0	0	0	0	0	0	0	0	0
		Min	0	1	1	1	1	1	1	1	1	1	1	1	1	1	1	1	1	1	1	1	1	1	1	1	1	1
		Max	0	1	2	2	3	3	3	3	3	3	3	3	4	4	4	4	4	4	4	4	5	5	5	5	5	5
		Sum	0	6	12	17	23	27	33	39	42	48	54	59	65	67	74	80	84	90	96	97	105	111	115	120	125	129
	2	1	0	6	10	13	16	18	21	23	24	27	27	26	26	26	28	27	25	25	22	21	22	20	17	16	16	16
		2	0	0	1	2	2	3	3	2	3	3	6	9	10	11	13	15	18	19	23	24	27	29	31	32	30	29
		3	0	0	0	0	1	1	2	4	4	5	5	5	5	5	4	5	5	5	4	4	4	5	6	6	9	11
		4	0	0	0	0	0	0	0	0	0	0	0	0	1	1	2	2	2	3	4	4	3	2	2	3	3	3
		5	0	0	0	0	0	0	0	0	0	0	0	0	0	0	0	0	0	0	0	0	1	2	2	2	2	2
		6	0	0	0	0	0	0	0	0	0	0	0	0	0	0	0	0	0	0	0	0	0	0	0	0	0	0
		7	0	0	0	0	0	0	0	0	0	0	0	0	0	0	0	0	0	0	0	0	0	0	0	0	0	0
		Min	0	1	1	1	1	1	1	1	1	1	1	1	1	1	1	1	1	1	1	1	1	1	1	1	1	1
		Max	0	1	2	2	3	3	3	3	3	3	3	3	4	4	4	4	4	4	4	4	5	5	5	5	5	5
		Sum	0	6	12	17	23	27	33	39	42	48	54	59	65	67	74	80	84	90	96	97	105	111	115	120	125	129
	3	1	0	6	10	13	16	18	21	23	24	27	27	26	26	26	29	29	27	27	26	25	26	24	21	20	19	18
		2	0	0	1	2	2	3	3	2	3	3	6	9	10	11	11	13	16	17	17	18	21	23	25	26	26	25
		3	0	0	0	0	1	1	2	4	4	5	5	5	5	5	6	7	7	7	8	8	8	9	10	10	11	13
		4	0	0	0	0	0	0	0	0	0	0	0	0	1	1	1	1	1	2	3	3	2	1	1	2	3	3
		5	0	0	0	0	0	0	0	0	0	0	0	0	0	0	0	0	0	0	0	0	1	2	2	2	2	2
		6	0	0	0	0	0	0	0	0	0	0	0	0	0	0	0	0	0	0	0	0	0	0	0	0	0	0
		7	0	0	0	0	0	0	0	0	0	0	0	0	0	0	0	0	0	0	0	0	0	0	0	0	0	0
		Min	0	1	1	1	1	1	1	1	1	1	1	1	1	1	1	1	1	1	1	1	1	1	1	1	1	1
		Max	0	1	2	2	3	3	3	3	3	3	3	3	4	4	4	4	4	4	4	4	5	5	5	5	5	5
		Sum	0	6	12	17	23	27	33	39	42	48	54	59	65	67	73	80	84	90	96	97	105	111	115	120	126	129

Table B.8: Skin Density Growth Pattern (ECSDGP) Dimension 7 EC 1–3 - cont.

Dimension		Skin Density	Transition Sequence Index (cont.)																									
n	EC		. . .	25	26	27	28	29	30	31	32	33	34	35	36	37	38	39	40	41	42	43	44	45	46	47	48	49
7	1	1		18	20	18	18	18	18	19	14	12	11	10	9	9	10	10	9	9	9	9	9	9	9	8	8	7
		2		27	26	28	28	26	24	20	25	25	24	22	23	22	21	19	17	16	15	12	12	12	9	10	9	7
		3		12	10	11	10	13	16	19	19	20	20	23	23	25	25	24	27	25	25	27	26	23	25	23	21	22
		4		4	7	7	9	9	9	10	10	11	13	13	14	14	16	19	18	21	23	24	25	26	26	26	28	30
		5		2	2	2	2	2	2	2	2	2	2	2	2	2	2	2	3	3	3	3	4	6	7	9	10	10
		6		0	0	0	0	0	0	0	0	0	0	0	0	0	0	0	0	0	0	0	0	0	0	0	0	0
		7		0	0	0	0	0	0	0	0	0	0	0	0	0	0	0	0	0	0	0	0	0	0	0	0	0
		Min		1	1	1	1	1	1	1	1	1	1	1	1	1	1	1	1	1	1	1	1	1	1	1	1	1
		Max		5	5	5	5	5	5	5	5	5	5	5	5	5	5	5	5	5	5	5	5	5	5	5	5	5
		Sum		134	140	145	150	155	160	166	171	176	181	185	190	194	201	206	211	215	221	225	231	236	241	246	251	257
	2	1		18	20	18	18	18	18	19	14	12	11	10	9	9	10	10	9	9	9	9	10	9	9	9	8	7
		2		27	26	28	28	26	24	20	25	25	24	22	23	22	21	19	17	16	15	12	11	10	8	7	7	8
		3		12	10	11	10	13	16	19	19	20	20	23	23	25	25	24	27	25	25	27	25	25	26	24	23	21
		4		4	7	7	9	9	9	10	10	11	13	13	14	14	16	19	18	21	23	24	26	28	27	29	30	29
		5		2	2	2	2	2	2	2	2	2	2	2	2	2	2	2	3	3	3	3	4	4	6	7	8	11
		6		0	0	0	0	0	0	0	0	0	0	0	0	0	0	0	0	0	0	0	0	0	0	0	0	0
		7		0	0	0	0	0	0	0	0	0	0	0	0	0	0	0	0	0	0	0	0	0	0	0	0	0
		Min		1	1	1	1	1	1	1	1	1	1	1	1	1	1	1	1	1	1	1	1	1	1	1	1	1
		Max		5	5	5	5	5	5	5	5	5	5	5	5	5	5	5	5	5	5	5	5	5	5	5	5	5
		Sum		134	140	145	150	155	160	166	171	176	181	185	190	194	201	206	211	215	221	225	231	236	241	246	251	257
	3	1		20	22	20	20	20	20	21	16	14	14	11	10	10	11	10	9	9	9	8	7	7	7	6	6	6
		2		23	22	24	24	22	20	16	21	22	21	23	24	23	22	21	19	18	17	16	16	14	11	11	10	7
		3		14	12	13	12	15	18	21	21	21	21	22	22	24	24	24	27	25	25	25	24	25	27	26	24	24
		4		4	7	7	9	9	9	10	10	11	13	13	14	14	16	18	17	20	22	24	25	24	24	25	27	30
		5		2	2	2	2	2	2	2	2	2	2	2	2	2	2	2	3	3	3	3	4	6	7	8	9	9
		6		0	0	0	0	0	0	0	0	0	0	0	0	0	0	0	0	0	0	0	0	0	0	0	0	0
		7		0	0	0	0	0	0	0	0	0	0	0	0	0	0	0	0	0	0	0	0	0	0	0	0	0
		Min		1	1	1	1	1	1	1	1	1	1	1	1	1	1	1	1	1	1	1	1	1	1	1	1	1
		Max		5	5	5	5	5	5	5	5	5	5	5	5	5	5	5	5	5	5	5	5	5	5	5	5	5
		Sum		134	140	145	150	155	160	166	171	175	181	185	190	194	201	206	211	215	221	226	231	236	241	246	251	257

Table B.9: Skin Density Growth Pattern (ECSDGP) Dimension 7 EC 4–6

Dimension		Skin Density	Transition Sequence Index																										
n	EC			0	1	2	3	4	5	6	7	8	9	10	11	12	13	14	15	16	17	18	19	20	21	22	23	24	···
7	4	1	0	6	10	13	16	19	20	21	24	24	25	26	27	28	30	29	29	28	27	28	26	23	21	18	18	20	
		2	0	0	1	2	3	4	7	8	8	11	10	9	8	9	11	14	15	15	16	19	21	23	25	27	26	23	
		3	0	0	0	0	0	0	0	0	1	1	3	5	7	7	6	6	6	7	7	7	8	9	10	11	13	15	
		4	0	0	0	0	0	0	0	0	0	0	0	0	0	0	1	1	2	3	3	2	1	1	0	0	0	1	
		5	0	0	0	0	0	0	0	0	0	0	0	0	0	0	0	0	0	0	0	1	2	2	3	3	3	3	
		6	0	0	0	0	0	0	0	0	0	0	0	0	0	0	0	0	0	0	0	0	0	0	0	0	0	0	
		7	0	0	0	0	0	0	0	0	0	0	0	0	0	0	0	0	0	0	0	0	0	0	0	0	0	0	
		Min	0	1	1	1	1	1	1	1	1	1	1	1	1	1	1	1	1	1	1	1	1	1	1	1	1	1	
		Max	0	1	2	2	2	2	2	2	3	3	3	3	3	3	4	4	4	4	4	5	5	5	5	5	5	5	
		Sum	0	6	12	17	22	27	34	37	43	49	54	59	64	67	74	79	85	91	92	100	106	110	116	120	124	130	
	5	1	0	6	10	13	16	19	20	21	24	24	25	26	27	28	30	29	29	28	27	28	26	23	21	18	18	20	
		2	0	0	1	2	3	4	7	8	8	11	10	9	8	9	11	14	15	15	16	19	21	23	25	27	26	23	
		3	0	0	0	0	0	0	0	0	1	1	3	5	7	7	6	6	6	7	7	7	8	9	10	11	13	15	
		4	0	0	0	0	0	0	0	0	0	0	0	0	0	0	1	1	2	3	3	2	1	1	0	0	0	1	
		5	0	0	0	0	0	0	0	0	0	0	0	0	0	0	0	0	0	0	0	1	2	2	3	3	3	3	
		6	0	0	0	0	0	0	0	0	0	0	0	0	0	0	0	0	0	0	0	0	0	0	0	0	0	0	
		7	0	0	0	0	0	0	0	0	0	0	0	0	0	0	0	0	0	0	0	0	0	0	0	0	0	0	
		Min	0	1	1	1	1	1	1	1	1	1	1	1	1	1	1	1	1	1	1	1	1	1	1	1	1	1	
		Max	0	1	2	2	2	2	2	2	3	3	3	3	3	3	4	4	4	4	4	5	5	5	5	5	5	5	
		Sum	0	6	12	17	22	27	34	37	43	49	54	59	64	67	74	79	85	91	92	100	106	110	116	120	124	130	
	6	1	0	6	10	13	16	19	20	21	24	26	27	27	28	29	31	30	30	30	30	32	31	28	26	23	23	24	
		2	0	0	1	2	3	4	7	8	8	7	6	8	7	8	10	13	14	12	13	15	17	19	21	23	22	20	
		3	0	0	0	0	0	0	0	0	1	3	5	4	6	6	5	5	5	8	8	7	8	9	10	11	13	16	
		4	0	0	0	0	0	0	0	0	0	0	0	1	1	1	2	2	3	3	3	4	3	3	2	2	2	1	
		5	0	0	0	0	0	0	0	0	0	0	0	0	0	0	0	0	0	0	0	0	1	1	2	2	2	3	
		6	0	0	0	0	0	0	0	0	0	0	0	0	0	0	0	0	0	0	0	0	0	0	0	0	0	0	
		7	0	0	0	0	0	0	0	0	0	0	0	0	0	0	0	0	0	0	0	0	0	0	0	0	0	0	
		Min	0	1	1	1	1	1	1	1	1	1	1	1	1	1	1	1	1	1	1	1	1	1	1	1	1	1	
		Max	0	1	2	2	2	2	2	2	3	3	3	4	4	4	4	4	4	4	4	4	5	5	5	5	5	5	
		Sum	0	6	12	17	22	27	34	37	43	49	54	59	64	67	74	79	85	90	92	99	106	110	116	120	124	131	

Table B.9: Skin Density Growth Pattern (ECSDGP) Dimension 7 EC 4–6 - cont.

Dimension		Skin Density	Transition Sequence Index (cont.)																									
n	EC		. . .	25	26	27	28	29	30	31	32	33	34	35	36	37	38	39	40	41	42	43	44	45	46	47	48	49
7	4	1		18	18	20	20	19	18	15	14	13	12	11	9	8	9	9	9	8	8	8	7	5	5	6	6	6
		2		26	28	25	23	24	24	26	26	25	23	23	23	22	22	21	18	18	16	12	11	11	11	7	7	7
		3		15	14	16	19	19	20	21	22	22	25	26	27	29	28	28	30	29	28	31	31	32	29	32	29	24
		4		1	2	3	3	4	5	5	6	8	8	9	10	10	12	14	14	15	18	19	21	22	24	25	26	30
		5		3	3	3	3	3	3	3	3	3	3	3	3	3	3	3	4	5	5	5	5	5	6	6	8	9
		6		0	0	0	0	0	0	0	0	0	0	0	0	0	0	0	0	0	0	0	0	0	0	0	0	0
		7		0	0	0	0	0	0	0	0	0	0	0	0	0	0	0	0	0	0	0	0	0	0	0	0	0
		Min		1	1	1	1	1	1	1	1	1	1	1	1	1	1	1	1	1	1	1	1	1	1	1	1	1
		Max		5	5	5	5	5	5	5	5	5	5	5	5	5	5	5	5	5	5	5	5	5	5	5	5	5
		Sum		134	139	145	150	155	161	165	171	176	180	186	191	194	200	206	211	216	221	226	231	236	240	246	251	257
	5	1		18	18	20	20	19	18	15	14	13	12	13	12	9	9	10	10	9	9	9	8	6	6	7	7	7
		2		26	28	25	23	24	24	26	26	25	23	22	22	24	24	21	18	18	16	12	11	11	11	9	9	7
		3		15	14	16	19	19	20	21	22	22	25	23	24	25	24	26	28	27	26	29	29	30	27	26	23	22
		4		1	2	3	3	4	5	5	6	8	8	11	12	12	14	14	14	15	18	19	21	22	24	27	28	30
		5		3	3	3	3	3	3	3	3	3	3	3	3	3	3	4	5	6	6	6	6	6	7	7	9	10
		6		0	0	0	0	0	0	0	0	0	0	0	0	0	0	0	0	0	0	0	0	0	0	0	0	0
		7		0	0	0	0	0	0	0	0	0	0	0	0	0	0	0	0	0	0	0	0	0	0	0	0	0
		Min		1	1	1	1	1	1	1	1	1	1	1	1	1	1	1	1	1	1	1	1	1	1	1	1	1
		Max		5	5	5	5	5	5	5	5	5	5	5	5	5	5	5	5	5	5	5	5	5	5	5	5	5
		Sum		134	139	145	150	155	161	165	171	176	180	185	191	195	200	206	211	216	221	226	231	236	240	246	251	257
	6	1		21	21	23	23	22	21	18	17	16	14	14	13	10	10	11	11	10	10	10	8	6	6	7	7	7
		2		23	25	22	20	21	21	23	23	22	22	21	21	23	23	20	18	18	16	12	12	12	12	10	10	8
		3		16	15	17	20	20	21	22	23	23	24	22	23	24	23	25	26	25	24	27	28	29	26	25	22	21
		4		1	2	3	3	4	5	5	6	8	9	12	13	13	15	15	14	15	18	19	20	21	23	26	27	29
		5		3	3	3	3	3	3	3	3	3	3	3	3	3	3	4	6	7	7	7	7	7	8	8	10	11
		6		0	0	0	0	0	0	0	0	0	0	0	0	0	0	0	0	0	0	0	0	0	0	0	0	0
		7		0	0	0	0	0	0	0	0	0	0	0	0	0	0	0	0	0	0	0	0	0	0	0	0	0
		Min		1	1	1	1	1	1	1	1	1	1	1	1	1	1	1	1	1	1	1	1	1	1	1	1	1
		Max		5	5	5	5	5	5	5	5	5	5	5	5	5	5	5	5	5	5	5	5	5	5	5	5	5
		Sum		134	139	145	150	155	161	165	171	176	181	185	191	195	200	206	211	216	221	226	231	236	240	246	251	257

Table B.10: Skin Density Growth Pattern (ECSDGP) Dimension 7 EC 7–9

Dimension		Skin Density	Transition Sequence Index																									
n	EC			0	1	2	3	4	5	6	7	8	9	10	11	12	13	14	15	16	17	18	19	20	21	22	23	24 ···
7	7	1	0	6	10	13	16	19	21	24	24	25	28	30	29	29	29	30	31	29	30	30	30	29	28	28	29	28
		2	0	0	1	2	3	3	4	4	7	8	8	7	10	11	10	10	11	14	13	14	12	13	14	13	12	13
		3	0	0	0	0	0	1	1	2	2	2	3	5	5	5	7	8	8	8	10	10	13	13	13	15	15	15
		4	0	0	0	0	0	0	0	0	0	0	0	0	0	1	1	1	2	2	2	3	3	4	5	5	7	7
		5	0	0	0	0	0	0	0	0	0	0	0	0	0	0	0	0	0	0	0	0	0	0	0	0	0	0
		6	0	0	0	0	0	0	0	0	0	0	0	0	0	0	0	0	0	0	0	0	0	0	0	0	0	0
		7	0	0	0	0	0	0	0	0	0	0	0	0	0	0	0	0	0	0	0	0	0	0	0	0	0	0
		Min	0	1	1	1	1	1	1	1	1	1	1	1	1	1	1	1	1	1	1	1	1	1	1	1	1	1
		Max	0	1	2	2	2	3	3	3	3	3	3	3	3	4	4	4	4	4	4	4	4	4	4	4	4	4
		Sum	0	6	12	17	22	28	32	38	44	47	53	59	64	70	74	78	85	89	94	100	105	110	115	119	126	127
	8	1	0	6	10	13	16	19	21	24	26	27	30	32	31	31	29	30	32	30	30	30	30	29	28	28	29	28
		2	0	0	1	2	3	3	4	4	3	4	4	3	6	7	10	10	8	11	13	14	12	13	14	13	12	13
		3	0	0	0	0	0	1	1	2	4	4	5	7	7	7	7	8	11	11	10	10	13	13	13	15	15	15
		4	0	0	0	0	0	0	0	0	0	0	0	0	0	1	1	1	1	1	2	3	3	4	5	5	7	7
		5	0	0	0	0	0	0	0	0	0	0	0	0	0	0	0	0	0	0	0	0	0	0	0	0	0	0
		6	0	0	0	0	0	0	0	0	0	0	0	0	0	0	0	0	0	0	0	0	0	0	0	0	0	0
		7	0	0	0	0	0	0	0	0	0	0	0	0	0	0	0	0	0	0	0	0	0	0	0	0	0	0
		Min	0	1	1	1	1	1	1	1	1	1	1	1	1	1	1	1	1	1	1	1	1	1	1	1	1	1
		Max	0	1	2	2	2	3	3	3	3	3	3	3	3	4	4	4	4	4	4	4	4	4	4	4	4	4
		Sum	0	6	12	17	22	28	32	38	44	47	53	59	64	70	74	78	85	89	94	100	105	110	115	119	126	127
	9	1	0	6	10	13	16	19	21	24	26	27	30	30	29	29	27	27	28	26	26	27	28	29	28	29	30	29
		2	0	0	1	2	3	3	4	4	3	4	4	7	10	11	14	16	14	17	19	18	16	13	14	12	11	12
		3	0	0	0	0	0	1	1	2	4	4	5	5	5	5	5	4	7	7	6	8	11	13	13	14	14	14
		4	0	0	0	0	0	0	0	0	0	0	0	0	0	1	1	2	2	2	3	3	3	4	5	6	8	8
		5	0	0	0	0	0	0	0	0	0	0	0	0	0	0	0	0	0	0	0	0	0	0	0	0	0	0
		6	0	0	0	0	0	0	0	0	0	0	0	0	0	0	0	0	0	0	0	0	0	0	0	0	0	0
		7	0	0	0	0	0	0	0	0	0	0	0	0	0	0	0	0	0	0	0	0	0	0	0	0	0	0
		Min	0	1	1	1	1	1	1	1	1	1	1	1	1	1	1	1	1	1	1	1	1	1	1	1	1	1
		Max	0	1	2	2	2	3	3	3	3	3	3	3	3	4	4	4	4	4	4	4	4	4	4	4	4	4
		Sum	0	6	12	17	22	28	32	38	44	47	53	59	64	70	74	79	85	89	94	99	105	110	115	119	126	127

Table B.10: Skin Density Growth Pattern (ECSDGP) Dimension 7 EC 7–9 - cont.

Dimension		Skin Density	Transition Sequence Index (cont.)																									
n	EC		...	25	26	27	28	29	30	31	32	33	34	35	36	37	38	39	40	41	42	43	44	45	46	47	48	49
7	7	1		29	26	23	21	20	19	16	15	14	14	15	15	16	15	13	12	10	9	9	9	8	8	8	7	7
		2		16	20	22	24	22	22	24	25	26	24	21	19	17	18	19	16	16	17	16	12	10	9	7	6	4
		3		15	14	15	16	19	20	21	21	21	24	26	29	28	24	24	28	29	25	23	26	29	27	26	26	27
		4		6	7	7	6	6	7	7	8	9	9	10	10	13	17	17	17	18	22	24	25	24	26	29	31	29
		5		1	1	1	2	2	2	2	2	2	2	2	2	2	2	3	3	3	3	4	4	5	6	6	6	9
		6		0	0	0	0	0	0	0	0	0	0	0	0	0	0	0	0	0	0	0	0	0	0	0	0	0
		7		0	0	0	0	0	0	0	0	0	0	0	0	0	0	0	0	0	0	0	0	0	0	0	0	0
		Min		1	1	1	1	1	1	1	1	1	1	1	1	1	1	1	1	1	1	1	1	1	1	1	1	1
		Max		5	5	5	5	5	5	5	5	5	5	5	5	5	5	5	5	5	5	5	5	5	5	5	5	5
		Sum		135	141	145	151	155	161	165	170	175	180	185	190	196	201	206	211	216	221	226	231	236	241	246	251	257
	8	1		29	26	23	21	18	17	14	13	12	11	12	12	13	13	13	12	11	10	9	9	8	8	8	7	7
		2		16	20	22	24	26	26	28	29	29	27	24	22	19	20	19	16	15	16	15	11	10	9	7	6	5
		3		15	14	15	16	17	18	19	19	20	23	25	28	30	26	24	28	30	26	26	29	29	27	26	26	24
		4		6	7	7	6	6	7	7	8	9	9	10	10	11	15	17	17	15	19	21	22	24	26	29	31	32
		5		1	1	1	2	2	2	2	2	2	2	2	2	2	2	3	3	5	5	5	5	5	6	6	6	8
		6		0	0	0	0	0	0	0	0	0	0	0	0	0	0	0	0	0	0	0	0	0	0	0	0	0
		7		0	0	0	0	0	0	0	0	0	0	0	0	0	0	0	0	0	0	0	0	0	0	0	0	0
		Min		1	1	1	1	1	1	1	1	1	1	1	1	1	1	1	1	1	1	1	1	1	1	1	1	1
		Max		5	5	5	5	5	5	5	5	5	5	5	5	5	5	5	5	5	5	5	5	5	5	5	5	5
		Sum		135	141	145	151	155	161	165	170	176	180	185	190	195	201	206	211	216	221	226	231	236	241	246	251	257
	9	1		30	28	25	23	20	18	15	14	13	12	13	13	14	14	14	13	12	11	10	10	9	9	9	8	8
		2		15	17	19	21	23	24	26	27	27	25	22	20	17	16	15	14	13	14	13	9	8	7	5	5	4
		3		14	15	16	17	18	20	21	21	22	25	27	30	32	32	30	30	32	28	28	31	31	29	28	27	25
		4		7	6	6	5	5	5	5	6	7	7	8	8	9	11	13	15	13	17	19	20	22	24	27	28	29
		5		1	2	2	3	3	3	3	3	3	3	3	3	3	3	4	4	6	6	6	6	6	7	7	8	10
		6		0	0	0	0	0	0	0	0	0	0	0	0	0	0	0	0	0	0	0	0	0	0	0	0	0
		7		0	0	0	0	0	0	0	0	0	0	0	0	0	0	0	0	0	0	0	0	0	0	0	0	0
		Min		1	1	1	1	1	1	1	1	1	1	1	1	1	1	1	1	1	1	1	1	1	1	1	1	1
		Max		5	5	5	5	5	5	5	5	5	5	5	5	5	5	5	5	5	5	5	5	5	5	5	5	5
		Sum		135	141	145	151	155	161	165	170	176	180	185	190	195	201	206	211	216	221	226	231	236	241	246	251	257

Table B.11: Skin Density Growth Pattern (ECSDGP) Dimension 7 EC 10–12

Dimension		Skin Density	Transition Sequence Index																									
n	EC			0	1	2	3	4	5	6	7	8	9	10	11	12	13	14	15	16	17	18	19	20	21	22	23	24 ···
7	10	1	0	6	10	13	16	19	22	25	25	24	23	24	25	24	25	25	26	25	24	24	26	26	27	28	28	27
		2	0	0	1	2	3	4	5	5	8	11	14	15	18	21	20	21	18	19	20	20	18	16	13	10	10	10
		3	0	0	0	0	0	0	0	1	1	1	1	1	1	1	3	3	5	5	5	6	9	12	14	16	15	16
		4	0	0	0	0	0	0	0	0	0	0	0	0	0	0	0	1	2	3	4	4	4	4	5	6	8	9
		5	0	0	0	0	0	0	0	0	0	0	0	0	0	0	0	0	0	0	0	0	0	0	0	0	0	0
		6	0	0	0	0	0	0	0	0	0	0	0	0	0	0	0	0	0	0	0	0	0	0	0	0	0	0
		7	0	0	0	0	0	0	0	0	0	0	0	0	0	0	0	0	0	0	0	0	0	0	0	0	0	0
		Min	0	1	1	1	1	1	1	1	1	1	1	1	1	1	1	1	1	1	1	1	1	1	1	1	1	1
		Max	0	1	2	2	2	2	2	3	3	3	3	3	3	3	3	4	4	4	4	4	4	4	4	4	4	4
		Sum	0	6	12	17	22	27	32	38	44	49	54	57	64	69	74	80	85	90	95	98	105	110	115	120	125	131
	11	1	0	6	10	13	16	19	22	25	25	24	23	24	25	24	25	25	26	25	24	24	27	27	27	28	28	27
		2	0	0	1	2	3	4	5	5	8	11	14	15	18	21	20	21	18	19	20	20	18	16	16	13	11	11
		3	0	0	0	0	0	0	0	1	1	1	1	1	1	1	3	3	5	5	5	6	7	10	9	11	14	15
		4	0	0	0	0	0	0	0	0	0	0	0	0	0	0	0	1	2	3	4	4	4	4	6	7	7	8
		5	0	0	0	0	0	0	0	0	0	0	0	0	0	0	0	0	0	0	0	0	1	1	1	1	1	1
		6	0	0	0	0	0	0	0	0	0	0	0	0	0	0	0	0	0	0	0	0	0	0	0	0	0	0
		7	0	0	0	0	0	0	0	0	0	0	0	0	0	0	0	0	0	0	0	0	0	0	0	0	0	0
		Min	0	1	1	1	1	1	1	1	1	1	1	1	1	1	1	1	1	1	1	1	1	1	1	1	1	1
		Max	0	1	2	2	2	2	2	3	3	3	3	3	3	3	3	4	4	4	4	4	5	5	5	5	5	5
		Sum	0	6	12	17	22	27	32	38	44	49	54	57	64	69	74	80	85	90	95	98	105	110	115	120	125	131
	12	1	0	6	10	13	16	19	22	25	25	24	23	24	25	24	25	25	26	25	24	24	27	27	27	28	28	27
		2	0	0	1	2	3	4	5	5	8	11	14	15	18	21	20	21	18	19	20	20	18	16	16	13	11	11
		3	0	0	0	0	0	0	0	1	1	1	1	1	1	1	3	3	5	5	5	6	7	10	9	11	14	15
		4	0	0	0	0	0	0	0	0	0	0	0	0	0	0	0	1	2	3	4	4	4	4	6	7	7	8
		5	0	0	0	0	0	0	0	0	0	0	0	0	0	0	0	0	0	0	0	0	1	1	1	1	1	1
		6	0	0	0	0	0	0	0	0	0	0	0	0	0	0	0	0	0	0	0	0	0	0	0	0	0	0
		7	0	0	0	0	0	0	0	0	0	0	0	0	0	0	0	0	0	0	0	0	0	0	0	0	0	0
		Min	0	1	1	1	1	1	1	1	1	1	1	1	1	1	1	1	1	1	1	1	1	1	1	1	1	1
		Max	0	1	2	2	2	2	2	3	3	3	3	3	3	3	3	4	4	4	4	4	5	5	5	5	5	5
		Sum	0	6	12	17	22	27	32	38	44	49	54	57	64	69	74	80	85	90	95	98	105	110	115	120	125	131

Table B.11: Skin Density Growth Pattern (ECSDGP) Dimension 7 EC 10–12 - cont.

Dimension		Skin Density	Transition Sequence Index (cont.)																									
n	EC		. . .	25	26	27	28	29	30	31	32	33	34	35	36	37	38	39	40	41	42	43	44	45	46	47	48	49
7	10	1		26	28	27	26	24	21	20	20	18	18	17	14	13	11	11	11	9	8	8	8	9	8	7	7	7
		2		11	13	15	16	18	20	21	19	20	19	20	24	22	22	20	16	16	15	13	10	8	7	6	6	4
		3		16	15	16	16	17	18	18	21	23	21	21	20	23	24	23	26	27	27	26	28	29	29	29	26	27
		4		9	10	10	11	10	10	11	11	11	14	15	16	15	16	19	20	21	23	26	27	26	28	30	31	29
		5		0	0	0	0	1	1	1	1	1	1	1	1	2	2	2	2	2	2	2	2	4	4	4	6	9
		6		0	0	0	0	0	0	0	0	0	0	0	0	0	0	0	0	0	0	0	0	0	0	0	0	0
		7		0	0	0	0	0	0	0	0	0	0	0	0	0	0	0	0	0	0	0	0	0	0	0	0	0
		Min		1	1	1	1	1	1	1	1	1	1	1	1	1	1	1	1	1	1	1	1	1	1	1	1	1
		Max		4	4	4	4	5	5	5	5	5	5	5	5	5	5	5	5	5	5	5	5	5	5	5	5	5
		Sum		132	139	145	150	156	160	165	170	176	180	185	191	196	201	206	211	216	221	226	230	236	241	246	251	257
	11	1		26	28	27	26	24	21	20	20	18	18	18	14	12	10	10	10	8	7	7	7	8	8	8	8	7
		2		12	14	16	17	19	21	22	20	21	20	20	24	25	25	21	17	17	16	14	11	8	7	6	6	5
		3		15	14	15	15	16	17	17	20	22	20	19	18	18	19	22	25	26	26	25	27	29	29	27	24	24
		4		8	9	9	10	9	9	10	10	10	13	14	15	15	16	17	18	19	21	24	25	26	28	30	31	32
		5		1	1	1	1	2	2	2	2	2	2	3	3	4	4	4	4	4	4	4	4	4	4	5	7	8
		6		0	0	0	0	0	0	0	0	0	0	0	0	0	0	0	0	0	0	0	0	0	0	0	0	0
		7		0	0	0	0	0	0	0	0	0	0	0	0	0	0	0	0	0	0	0	0	0	0	0	0	0
		Min		1	1	1	1	1	1	1	1	1	1	1	1	1	1	1	1	1	1	1	1	1	1	1	1	1
		Max		5	5	5	5	5	5	5	5	5	5	5	5	5	5	5	5	5	5	5	5	5	5	5	5	5
		Sum		132	139	145	150	156	160	165	170	176	180	186	191	196	201	206	211	216	221	226	230	235	241	246	251	257
	12	1		26	27	24	21	19	18	19	20	17	17	17	14	13	13	12	11	10	8	8	7	8	9	9	9	8
		2		12	15	19	21	21	20	19	19	23	22	21	23	24	21	19	19	17	17	15	13	11	9	8	6	4
		3		15	15	14	15	16	18	20	19	18	16	16	17	17	19	22	21	24	25	24	27	28	27	25	24	25
		4		8	7	8	7	8	8	8	10	11	14	16	16	16	16	15	16	15	16	19	19	19	22	24	27	29
		5		1	2	2	3	3	3	3	3	3	3	3	3	4	5	6	7	8	8	8	8	9	9	10	10	10
		6		0	0	0	0	0	0	0	0	0	0	0	0	0	0	0	0	0	0	0	0	0	0	0	0	0
		7		0	0	0	0	0	0	0	0	0	0	0	0	0	0	0	0	0	0	0	0	0	0	0	0	0
		Min		1	1	1	1	1	1	1	1	1	1	1	1	1	1	1	1	1	1	1	1	1	1	1	1	1
		Max		5	5	5	5	5	5	5	5	5	5	5	5	5	5	5	5	5	5	5	5	5	5	5	5	5
		Sum		132	140	146	151	156	159	164	170	176	180	186	190	196	201	206	211	216	221	226	230	235	241	246	251	257

B.4 Transition Count Growth Analysis

Table B.12: Transition Count Growth Pattern (ECTCGP) Dimension 1–4

Dimension			Transition Sequence Index							
n	EC	Transition		0	1	2	3	4	5	6
1		0	0	1						
2		0	0	1	1					
		1	0	0	1					
3		0	0	1	1	1	2			
		1	0	0	1	1	1			
		2	0	0	0	1	1			
4		0	0	1	1	1	2	2	2	3
		1	0	0	1	1	1	1	2	2
		2	0	0	0	1	1	1	1	1
		3	0	0	0	0	0	1	1	1

Table B.13: Transition Count Growth Pattern (ECTCGP) Dimension 5

Dimension			Transition Sequence Index													
n	EC	Transition		0	1	2	3	4	5	6	7	8	9	10	11	12
5	1	0	0	1	1	1	1	2	2	2	3	3	3	4	4	4
		1	0	0	1	1	1	1	2	2	2	2	3	3	3	3
		2	0	0	0	1	1	1	1	1	1	2	2	2	2	3
		3	0	0	0	0	1	1	1	1	1	1	1	1	2	2
		4	0	0	0	0	0	0	0	1	1	1	1	1	1	1
	2	0	0	1	1	1	1	2	2	2	2	2	2	2	3	3
		1	0	0	1	1	1	1	2	2	2	3	3	3	3	4
		2	0	0	0	1	1	1	1	1	1	1	2	2	2	2
		3	0	0	0	0	1	1	1	1	2	2	2	3	3	3
		4	0	0	0	0	0	0	0	1	1	1	1	1	1	1
	3	0	0	1	1	1	1	2	2	2	3	3	3	4	4	4
		1	0	0	1	1	1	1	1	1	1	2	2	2	2	3
		2	0	0	0	1	1	1	2	2	2	2	3	3	3	3
		3	0	0	0	0	1	1	1	1	1	1	1	1	2	2
		4	0	0	0	0	0	0	0	1	1	1	1	1	1	1
	4	0	0	1	1	1	1	2	2	2	3	3	3	3	4	4
		1	0	0	1	1	1	1	1	1	1	2	2	2	2	3
		2	0	0	0	1	1	1	2	2	2	2	3	3	3	3
		3	0	0	0	0	1	1	1	1	1	1	1	2	2	2
		4	0	0	0	0	0	0	0	1	1	1	1	1	1	1
	5	0	0	1	1	1	1	2	2	2	2	3	3	3	4	4
		1	0	0	1	1	1	1	1	1	2	2	2	2	2	3
		2	0	0	0	1	1	1	2	2	2	2	3	3	3	3
		3	0	0	0	0	1	1	1	1	1	1	1	2	2	2
		4	0	0	0	0	0	0	0	1	1	1	1	1	1	1
	6	0	0	1	1	1	1	2	2	2	2	2	2	3	3	3
		1	0	0	1	1	1	1	1	1	1	1	2	2	2	2
		2	0	0	0	1	1	1	2	2	2	3	3	3	3	4
		3	0	0	0	0	1	1	1	1	2	2	2	2	3	3
		4	0	0	0	0	0	0	0	1	1	1	1	1	1	1
	7	0	0	1	1	1	1	2	2	2	2	2	2	2	3	3
		1	0	0	1	1	1	1	1	1	1	1	2	2	2	2
		2	0	0	0	1	1	1	2	2	2	3	3	3	3	4
		3	0	0	0	0	1	1	1	1	2	2	2	3	3	3
		4	0	0	0	0	0	0	0	1	1	1	1	1	1	1
	8	0	0	1	1	1	1	1	2	2	2	2	2	2	3	3
		1	0	0	1	1	1	2	2	2	2	3	3	3	3	4
		2	0	0	0	1	1	1	1	1	1	1	2	2	2	2
		3	0	0	0	0	1	1	1	1	2	2	2	3	3	3
		4	0	0	0	0	0	0	0	1	1	1	1	1	1	1

Table B.14: Transition Count Growth Pattern (ECTCGP) Dimension 6

Dimension			Transition Sequence Index																										
n	EC	Transition		0	1	2	3	4	5	6	7	8	9	10	11	12	13	14	15	16	17	18	19	20	21	22	23	24	25
6		0	0	1	1	1	1	1	2	2	2	3	3	3	4	4	4	4	5	5	5	5	6	6	6	6	6	6	6
		1	0	0	1	1	1	2	2	2	2	2	2	2	2	3	3	3	3	3	3	4	4	4	4	5	5	5	5
		2	0	0	0	1	1	1	1	1	1	1	1	1	1	1	1	1	1	2	2	2	2	2	2	2	2	2	2
		3	0	0	0	0	1	1	1	1	2	2	2	2	2	2	3	3	3	3	3	3	3	3	4	4	4	5	5
		4	0	0	0	0	0	0	0	1	1	1	1	2	2	2	2	3	3	3	4	4	4	5	5	5	5	5	6
		5	0	0	0	0	0	0	0	0	0	0	1	1	1	1	1	1	1	1	1	1	1	1	1	1	2	2	2

Table B.15: Transition Count Growth Pattern (ECTCGP) Dimension 7

Dimension			Transition Sequence Index																																																	
n	EC	Transition		0	1	2	3	4	5	6	7	8	9	10	11	12	13	14	15	16	17	18	19	20	21	22	23	24	25	26	27	28	29	30	31	32	33	34	35	36	37	38	39	40	41	42	43	44	45	46	47	48	49
7	1	0	0	1	1	1	2	2	2	3	3	3	3	4	4	4	5	5	5	5	6	6	6	7	7	7	8	8	8	9	9	9	9	10	10	10	11	11	11	12	12	12	13	13	13	14	14	14	15	15	15	15	16
		1	0	0	1	1	1	1	2	2	2	2	3	3	3	3	3	4	4	4	4	4	4	4	4	4	4	4	4	4	5	5	5	5	5	5	5	5	5	5	5	5	5	6	6	6	6	7	7	7	7	8	8
		2	0	0	0	1	1	1	1	1	1	2	2	2	2	2	2	2	3	3	3	3	3	3	3	4	4	4	4	4	4	5	5	5	5	5	5	5	6	6	6	6	6	6	7	7	7	7	7	7	8	8	8
		3	0	0	0	0	0	1	1	1	1	1	1	1	2	2	2	2	2	2	2	2	2	2	2	2	2	3	3	3	3	3	3	3	4	4	4	4	4	4	5	5	5	5	5	5	5	5	5	5	5	5	5
		4	0	0	0	0	0	0	0	0	1	1	1	1	1	1	1	1	1	2	2	2	2	2	3	3	3	3	4	4	4	4	5	5	5	5	5	6	6	6	6	7	7	7	7	7	7	7	7	8	8	8	8
		5	0	0	0	0	0	0	0	0	0	0	0	0	0	1	1	1	1	1	1	1	2	2	2	2	2	2	2	2	2	2	2	2	2	3	3	3	3	3	3	3	3	3	3	3	3	3	3	3	3	3	3
		6	0	0	0	0	0	0	0	0	0	0	0	0	0	0	0	0	0	0	0	1	1	1	1	1	1	1	1	1	1	1	1	1	1	1	1	1	1	1	1	1	1	1	1	2	2	2	2	2	2	2
	2	0	0	1	1	1	2	2	2	3	3	3	3	4	4	4	5	5	5	5	6	6	6	7	7	7	8	8	8	9	9	9	9	10	10	10	11	11	11	12	12	12	13	13	13	14	14	14	14	15	15	15	15
		1	0	0	1	1	1	1	2	2	2	2	3	3	3	3	3	4	4	4	4	4	4	4	4	4	4	4	4	4	5	5	5	5	5	5	5	5	5	5	5	5	5	6	6	6	6	6	6	6	7	7	7
		2	0	0	0	1	1	1	1	1	1	2	2	2	2	2	2	2	3	3	3	3	3	3	3	4	4	4	4	4	4	5	5	5	5	5	5	5	6	6	6	6	6	6	7	7	7	8	8	8	8	9	9
		3	0	0	0	0	0	1	1	1	1	1	1	1	2	2	2	2	2	2	2	2	2	2	2	2	2	3	3	3	3	3	3	3	4	4	4	4	4	4	5	5	5	5	5	5	5	5	5	5	5	5	5
		4	0	0	0	0	0	0	0	0	1	1	1	1	1	1	1	1	1	2	2	2	2	2	3	3	3	3	4	4	4	4	5	5	5	5	5	6	6	6	6	7	7	7	7	7	7	7	8	8	8	8	9
		5	0	0	0	0	0	0	0	0	0	0	0	0	0	1	1	1	1	1	1	1	2	2	2	2	2	2	2	2	2	2	2	2	2	3	3	3	3	3	3	3	3	3	3	3	3	3	3	3	3	3	3
		6	0	0	0	0	0	0	0	0	0	0	0	0	0	0	0	0	0	0	0	1	1	1	1	1	1	1	1	1	1	1	1	1	1	1	1	1	1	1	1	1	1	1	1	2	2	2	2	2	2	2
	3	0	0	1	1	1	2	2	2	3	3	3	3	4	4	4	4	5	5	5	6	6	6	7	7	7	8	8	8	9	9	9	9	10	10	10	11	11	11	12	12	12	13	13	13	14	14	14	15	15	15	15	16
		1	0	0	1	1	1	1	2	2	2	2	3	3	3	3	4	4	4	4	4	4	4	4	4	4	4	4	4	4	5	5	5	5	5	5	5	5	5	5	5	5	5	6	6	6	6	7	7	7	7	8	8
		2	0	0	0	1	1	1	1	1	1	2	2	2	2	2	2	2	3	3	3	3	3	3	3	4	4	4	4	4	4	5	5	5	5	5	5	5	6	6	6	6	6	6	7	7	7	7	7	7	8	8	8
		3	0	0	0	0	0	1	1	1	1	1	1	1	2	2	2	2	2	2	2	2	2	2	2	2	2	3	3	3	3	3	3	3	4	4	4	4	4	4	5	5	5	5	5	5	5	5	5	5	5	5	5
		4	0	0	0	0	0	0	0	0	1	1	1	1	1	1	1	1	1	2	2	2	2	2	3	3	3	3	4	4	4	4	5	5	5	5	5	6	6	6	6	7	7	7	7	7	7	7	7	8	8	8	8
		5	0	0	0	0	0	0	0	0	0	0	0	0	0	1	1	1	1	1	1	1	2	2	2	2	2	2	2	2	2	2	2	2	2	3	3	3	3	3	3	3	3	3	3	3	3	3	3	3	3	3	3
		6	0	0	0	0	0	0	0	0	0	0	0	0	0	0	0	0	0	0	0	1	1	1	1	1	1	1	1	1	1	1	1	1	1	1	1	1	1	1	1	1	1	1	1	2	2	2	2	2	2	2
	4	0	0	1	1	1	1	2	2	2	3	3	3	4	4	4	5	5	5	6	6	6	7	7	7	7	8	8	8	9	9	9	10	10	10	11	11	11	12	12	12	12	13	13	13	13	14	14	14	15	15	15	16
		1	0	0	1	1	1	1	2	2	2	2	3	3	3	3	3	3	3	3	3	3	3	3	3	4	4	4	4	4	4	4	4	4	4	4	4	4	4	5	5	5	5	6	6	6	6	7	7	7	7	8	8
		2	0	0	0	1	1	1	1	1	1	2	2	2	2	2	2	3	3	3	3	3	3	3	4	4	4	4	4	4	5	5	5	5	5	5	5	6	6	6	6	6	6	6	7	7	7	7	7	7	8	8	8
		3	0	0	0	0	1	1	1	1	1	1	1	1	2	2	2	2	3	3	3	3	3	4	4	4	4	5	5	5	5	6	6	6	6	6	7	7	7	7	7	7	7	7	7	8	8	8	8	8	8	8	8
		4	0	0	0	0	0	0	0	1	1	1	1	1	1	1	1	1	1	1	1	1	1	1	1	1	1	1	1	1	1	1	1	1	2	2	2	2	2	2	2	2	2	2	2	2	2	2	2	2	2	2	2
		5	0	0	0	0	0	0	0	0	0	0	0	0	0	1	1	1	1	1	1	2	2	2	2	2	2	2	3	3	3	3	3	3	3	3	3	3	3	3	3	4	4	4	4	4	4	4	5	5	5	5	5
		6	0	0	0	0	0	0	0	0	0	0	0	0	0	0	0	0	0	0	1	1	1	1	1	1	1	1	1	1	1	1	1	2	2	2	2	2	2	2	3	3	3	3	3	3	3	3	3	3	3	3	3

Table B.15

Dimension				Transition Sequence Index																																																	
n	EC	Transition		0	1	2	3	4	5	6	7	8	9	10	11	12	13	14	15	16	17	18	19	20	21	22	23	24	25	26	27	28	29	30	31	32	33	34	35	36	37	38	39	40	41	42	43	44	45	46	47	48	49
7	5	0	0	1	1	1	1	2	2	2	3	3	3	4	4	4	5	5	5	6	6	6	7	7	7	7	8	8	8	9	9	9	10	10	10	11	11	11	11	12	12	12	13	13	13	13	14	14	14	15	15	15	16
		1	0	0	1	1	1	1	2	2	2	2	3	3	3	3	3	3	3	3	3	3	3	3	3	4	4	4	4	4	4	4	4	4	4	4	4	4	5	5	5	5	5	6	6	6	6	7	7	7	7	8	8
		2	0	0	0	1	1	1	1	1	1	2	2	2	2	2	2	3	3	3	3	3	3	3	4	4	4	4	4	4	5	5	5	5	5	5	5	6	6	6	6	6	6	6	7	7	7	7	7	7	8	8	8
		3	0	0	0	0	1	1	1	1	1	1	1	1	2	2	2	2	3	3	3	3	3	4	4	4	4	5	5	5	5	6	6	6	6	6	7	7	7	7	7	7	7	7	7	8	8	8	8	8	8	8	8
		4	0	0	0	0	0	0	0	1	1	1	1	1	1	1	1	1	1	1	1	1	1	1	1	1	1	1	1	1	1	1	1	1	2	2	2	2	2	2	2	2	2	2	2	2	2	2	2	2	2	2	2
		5	0	0	0	0	0	0	0	0	0	0	0	0	0	1	1	1	1	1	1	2	2	2	2	2	2	2	3	3	3	3	3	3	3	3	3	3	3	3	3	4	4	4	4	4	4	4	5	5	5	5	5
		6	0	0	0	0	0	0	0	0	0	0	0	0	0	0	0	0	0	0	1	1	1	1	1	1	1	1	1	1	1	1	1	2	2	2	2	2	2	2	3	3	3	3	3	3	3	3	3	3	3	3	3
	6	0	0	1	1	1	1	2	2	2	2	2	2	2	3	3	3	3	4	4	4	4	4	5	5	5	5	6	6	6	6	7	7	7	7	7	8	8	8	8	8	8	8	8	8	9	9	9	9	9	9	9	9
		1	0	0	1	1	1	1	2	2	2	3	3	3	3	3	3	4	4	4	4	4	4	4	5	5	5	5	5	5	6	6	6	6	6	6	6	7	7	7	7	7	7	7	8	8	8	8	8	8	9	9	9
		2	0	0	0	1	1	1	1	1	1	1	2	2	2	2	2	2	2	2	2	2	2	2	2	3	3	3	3	3	3	3	3	3	3	3	3	3	4	4	4	4	4	5	5	5	5	6	6	6	6	7	7
		3	0	0	0	0	1	1	1	1	2	2	2	3	3	3	4	4	4	5	5	5	6	6	6	6	7	7	7	8	8	8	9	9	9	10	10	10	10	11	11	11	12	12	12	12	13	13	13	14	14	14	15
		4	0	0	0	0	0	0	0	1	1	1	1	1	1	1	1	1	1	1	1	1	1	1	1	1	1	1	1	1	1	1	1	1	2	2	2	2	2	2	2	2	2	2	2	2	2	2	2	2	2	2	2
		5	0	0	0	0	0	0	0	0	0	0	0	0	0	1	1	1	1	1	1	2	2	2	2	2	2	2	3	3	3	3	3	3	3	3	3	3	3	3	3	4	4	4	4	4	4	4	5	5	5	5	5
		6	0	0	0	0	0	0	0	0	0	0	0	0	0	0	0	0	0	0	1	1	1	1	1	1	1	1	1	1	1	1	1	2	2	2	2	2	2	2	3	3	3	3	3	3	3	3	3	3	3	3	3
	7	0	0	1	1	1	1	1	1	1	2	2	2	3	3	3	4	4	4	4	5	5	5	6	6	6	6	6	6	7	7	7	8	8	8	8	9	9	9	10	10	10	11	11	11	11	12	12	12	13	13	13	13
		1	0	0	1	1	1	2	2	2	2	2	2	2	2	2	2	3	3	3	3	3	3	3	3	3	3	3	4	4	4	4	4	5	5	5	5	6	6	6	6	7	7	7	7	8	8	8	8	8	9	9	9
		2	0	0	0	1	1	1	1	2	2	2	2	2	3	3	3	3	4	4	4	4	5	5	5	5	6	6	6	6	7	7	7	7	7	7	7	7	7	7	7	7	7	8	8	8	8	8	8	8	8	8	9
		3	0	0	0	0	1	1	1	1	1	1	2	2	2	2	2	2	2	3	3	3	3	3	3	4	4	4	4	4	4	4	4	4	5	5	5	5	5	5	6	6	6	6	6	6	6	7	7	7	7	7	7
		4	0	0	0	0	0	0	1	1	1	1	1	1	1	2	2	2	2	2	2	3	3	3	3	3	3	3	3	3	3	4	4	4	4	4	4	4	5	5	5	5	5	5	6	6	6	6	6	6	6	7	7
		5	0	0	0	0	0	0	0	0	0	1	1	1	1	1	1	1	1	1	1	1	1	1	2	2	2	2	2	2	2	2	2	2	2	3	3	3	3	3	3	3	3	3	3	3	3	3	4	4	4	4	4
		6	0	0	0	0	0	0	0	0	0	0	0	0	0	0	0	0	0	0	0	0	0	0	0	0	0	1	1	1	1	1	1	1	1	1	1	1	1	1	1	1	1	1	1	1	1	1	1	1	1	1	1
	8	0	0	1	1	1	1	1	1	1	1	1	1	1	1	1	2	2	2	2	2	2	2	2	2	2	2	2	3	3	3	3	4	4	4	4	4	5	5	5	5	6	6	6	6	7	7	7	7	7	8	8	8
		1	0	0	1	1	1	2	2	2	3	3	3	4	4	4	4	5	5	5	6	6	6	7	7	7	7	7	7	8	8	8	8	9	9	9	10	10	10	11	11	11	12	12	12	12	13	13	13	14	14	14	14
		2	0	0	0	1	1	1	1	2	2	2	2	2	3	3	3	3	4	4	4	4	5	5	5	5	6	6	6	6	7	7	7	7	7	7	7	7	7	7	7	7	7	8	8	8	8	8	8	8	8	8	9
		3	0	0	0	0	1	1	1	1	1	1	2	2	2	2	2	2	2	3	3	3	3	3	3	4	4	4	4	4	4	4	4	4	5	5	5	5	5	5	6	6	6	6	6	6	6	7	7	7	7	7	7
		4	0	0	0	0	0	0	1	1	1	1	1	1	1	2	2	2	2	2	2	3	3	3	3	3	3	3	3	3	3	4	4	4	4	4	4	4	5	5	5	5	5	5	6	6	6	6	6	6	6	7	7
		5	0	0	0	0	0	0	0	0	0	1	1	1	1	1	1	1	1	1	1	1	1	1	2	2	2	2	2	2	2	2	2	2	2	3	3	3	3	3	3	3	3	3	3	3	3	3	4	4	4	4	4
		6	0	0	0	0	0	0	0	0	0	0	0	0	0	0	0	0	0	0	0	0	0	0	0	0	0	1	1	1	1	1	1	1	1	1	1	1	1	1	1	1	1	1	1	1	1	1	1	1	1	1	1

Table B.15

Dimension			Transition Sequence Index																																																	
n	EC	Transition	0	1	2	3	4	5	6	7	8	9	10	11	12	13	14	15	16	17	18	19	20	21	22	23	24	25	26	27	28	29	30	31	32	33	34	35	36	37	38	39	40	41	42	43	44	45	46	47	48	49
7	9	0	0	1	1	1	1	1	1	1	1	1	1	1	1	2	2	2	2	2	2	2	2	2	2	2	2	2	2	2	2	2	2	2	3	3	3	3	3	3	3	3	3	3	3	3	3	4	4	4	4	4
		1	0	0	1	1	1	2	2	3	3	3	3	4	4	4	5	5	5	6	6	6	7	7	7	8	8	8	9	9	9	9	10	10	10	11	11	11	12	12	12	13	13	13	13	14	14	14	15	15	15	15
		2	0	0	0	1	1	1	2	2	2	2	3	3	3	3	3	4	4	4	4	5	5	5	5	5	5	5	5	6	6	6	6	6	6	6	6	6	6	6	6	6	7	7	7	7	7	7	7	7	7	8
		3	0	0	0	0	1	1	1	1	1	2	2	2	2	2	2	2	3	3	3	3	3	3	4	4	4	4	4	4	5	5	5	5	5	5	5	6	6	6	6	6	6	7	7	7	7	7	7	7	8	8
		4	0	0	0	0	0	0	1	1	1	1	1	1	2	2	2	2	2	2	3	3	3	3	3	3	3	3	3	3	3	3	3	4	4	4	4	4	4	5	5	5	5	5	5	5	6	6	6	6	6	6
		5	0	0	0	0	0	0	0	0	1	1	1	1	1	1	1	1	1	1	1	1	1	2	2	2	2	3	3	3	3	4	4	4	4	4	5	5	5	5	6	6	6	6	7	7	7	7	7	8	8	8
		6	0	0	0	0	0	0	0	0	0	0	0	0	0	0	0	0	0	0	0	0	0	0	0	0	1	1	1	1	1	1	1	1	1	1	1	1	1	1	1	1	1	1	1	1	1	1	1	1	1	1
	10	0	0	1	1	1	1	1	1	1	1	2	2	2	2	2	2	2	2	2	2	2	2	2	3	3	3	3	4	4	4	4	5	5	5	5	6	6	6	6	7	7	7	7	7	8	8	8	8	9	9	9
		1	0	0	1	1	1	1	1	1	2	2	2	2	2	2	3	3	3	3	3	3	3	4	4	4	4	4	4	4	4	4	4	5	5	5	5	5	5	6	6	6	6	6	6	6	7	7	7	7	7	7
		2	0	0	0	1	1	1	1	2	2	2	2	3	3	3	3	4	4	4	4	5	5	5	5	5	6	6	6	6	6	6	6	6	6	6	6	7	7	7	7	7	7	7	7	7	7	8	8	8	9	9
		3	0	0	0	0	1	1	2	2	2	2	3	3	3	4	4	4	5	5	5	5	6	6	6	7	7	7	7	7	7	8	8	8	9	9	9	9	10	10	10	11	11	11	12	12	12	12	12	12	12	13
		4	0	0	0	0	0	1	1	1	1	1	1	1	1	1	1	1	1	2	2	2	2	2	2	2	2	2	2	2	3	3	3	3	3	3	3	3	3	3	3	3	3	4	4	4	4	4	4	4	4	4
		5	0	0	0	0	0	0	1	1	1	1	1	1	2	2	2	2	2	2	3	3	3	3	3	3	3	3	3	4	4	4	4	4	4	5	5	5	5	5	5	5	6	6	6	6	6	6	7	7	7	7
		6	0	0	0	0	0	0	0	0	0	0	0	0	0	0	0	0	0	0	0	0	0	0	0	0	0	1	1	1	1	1	1	1	1	1	1	1	1	1	1	1	1	1	1	1	1	1	1	1	1	1
	11	0	0	1	1	1	1	1	1	1	1	2	2	2	2	2	2	2	2	2	2	2	2	2	3	3	3	3	4	4	4	4	5	5	5	5	6	6	6	6	7	7	7	7	7	8	8	8	8	9	9	9
		1	0	0	1	1	1	1	1	1	2	2	2	2	2	2	3	3	3	3	3	3	3	4	4	4	4	4	4	4	4	4	4	5	5	5	5	5	5	6	6	6	6	6	6	6	7	7	7	7	7	7
		2	0	0	0	1	1	1	1	2	2	2	2	3	3	3	3	4	4	4	4	4	5	5	5	5	6	6	6	6	6	6	6	6	6	6	6	6	7	7	7	7	7	7	7	7	7	7	7	7	7	8
		3	0	0	0	0	1	1	2	2	2	2	3	3	3	4	4	4	5	5	5	6	6	6	6	7	7	7	7	7	7	8	8	8	9	9	9	10	10	10	10	11	11	11	12	12	12	13	13	13	14	14
		4	0	0	0	0	0	1	1	1	1	1	1	1	1	1	1	1	1	2	2	2	2	2	2	2	2	2	2	2	3	3	3	3	3	3	3	3	3	3	3	3	3	4	4	4	4	4	4	4	4	4
		5	0	0	0	0	0	0	1	1	1	1	1	1	2	2	2	2	2	2	3	3	3	3	3	3	3	3	3	4	4	4	4	4	4	5	5	5	5	5	5	5	6	6	6	6	6	6	7	7	7	7
		6	0	0	0	0	0	0	0	0	0	0	0	0	0	0	0	0	0	0	0	0	0	0	0	0	0	1	1	1	1	1	1	1	1	1	1	1	1	1	1	1	1	1	1	1	1	1	1	1	1	1
	12	0	0	1	1	1	1	1	1	1	1	2	2	2	2	2	2	2	2	2	2	2	2	2	3	3	3	3	3	3	3	3	4	4	4	4	5	5	5	5	5	6	6	6	6	7	7	7	7	8	8	8
		1	0	0	1	1	1	1	1	1	2	2	2	2	2	2	3	3	3	3	3	3	3	4	4	4	4	4	4	5	5	5	5	5	5	6	6	6	6	6	6	6	7	7	7	7	7	7	8	8	8	8
		2	0	0	0	1	1	1	1	2	2	2	2	3	3	3	3	4	4	4	4	4	5	5	5	5	6	6	6	6	7	7	7	7	7	7	7	7	7	7	7	7	7	8	8	8	8	8	8	8	8	8
		3	0	0	0	0	1	1	2	2	2	2	3	3	3	4	4	4	5	5	5	6	6	6	6	7	7	7	8	8	8	9	9	9	10	10	10	11	11	11	12	12	12	12	13	13	13	14	14	14	15	15
		4	0	0	0	0	0	1	1	1	1	1	1	1	1	1	1	1	1	2	2	2	2	2	2	2	2	2	2	2	2	2	2	2	2	2	2	2	3	3	3	3	3	3	3	3	3	3	3	3	3	4
		5	0	0	0	0	0	0	1	1	1	1	1	1	2	2	2	2	2	2	3	3	3	3	3	3	3	3	3	3	3	3	3	4	4	4	4	4	4	5	5	5	5	5	5	5	6	6	6	6	6	6
		6	0	0	0	0	0	0	0	0	0	0	0	0	0	0	0	0	0	0	0	0	0	0	0	0	0	1	1	1	1	1	1	1	1	1	1	1	1	1	1	1	1	1	1	1	1	1	1	1	1	1

B.5 2-Face Growth Analysis

Table B.16: 2-Face Type Growth Pattern (EC2FGP) Dimension 1–4

Dimension		2-Face	Transition Sequence Index							
n	EC	Type		0	1	2	3	4	5	6
1		A_1	0	0	0					
		A_2	0	0	0					
		A_3	0	0	0					
		A_4	0	0	0					
		A_5	0	0	0					
2		A_1	0	0	1					
		A_2	0	1	0					
		A_3	0	0	0					
		A_4	1	0	0					
		A_5	0	0	0					
3		A_1	0	0	1	2	3			
		A_2	0	2	2	2	2			
		A_3	0	0	0	0	1			
		A_4	3	2	2	2	0			
		A_5	3	2	1	0	0			
4		A_1	0	0	1	2	3	4	5	6
		A_2	0	3	4	5	6	7	8	9
		A_3	0	0	0	0	1	1	2	4
		A_4	6	6	7	8	7	8	7	4
		A_5	18	15	12	9	7	4	2	1

Table B.17: 2-Face Type Growth Pattern (EC2FGP) Dimension 5

Dimension		2-Face	Transition Sequence Index													
n	EC	Type		0	1	2	3	4	5	6	7	8	9	10	11	12
5	1	A_1	0	0	1	2	3	4	5	6	7	8	9	10	11	12
		A_2	0	4	6	8	10	12	14	16	18	20	22	24	26	28
		A_3	0	0	0	0	0	0	1	1	2	3	5	7	9	12
		A_4	10	12	15	18	21	24	25	28	29	30	29	28	27	24
		A_5	70	64	58	52	46	40	35	29	24	19	15	11	7	4
	2	A_1	0	0	1	2	3	4	5	6	7	8	9	10	11	12
		A_2	0	4	6	8	10	12	14	16	18	20	22	24	26	28
		A_3	0	0	0	0	0	0	1	1	2	4	6	8	10	12
		A_4	10	12	15	18	21	24	25	28	29	28	27	26	25	24
		A_5	70	64	58	52	46	40	35	29	24	20	16	12	8	4
	3,4	A_1	0	0	1	2	3	4	5	6	7	8	9	10	11	12
		A_2	0	4	6	8	10	12	14	16	18	20	22	24	26	28
		A_3	0	0	0	0	0	0	2	2	4	5	6	8	9	12
		A_4	10	12	15	18	21	24	23	26	25	26	27	26	27	24
		A_5	70	64	58	52	46	40	36	30	26	21	16	12	7	4
	5	A_1	0	0	1	2	3	4	5	6	7	8	9	10	11	12
		A_2	0	4	6	8	10	12	14	16	18	20	22	24	26	28
		A_3	0	0	0	0	0	0	2	2	3	4	5	7	9	12
		A_4	10	12	15	18	21	24	23	26	27	28	29	28	27	24
		A_5	70	64	58	52	46	40	36	30	25	20	15	11	7	4
	6,7	A_1	0	0	1	2	3	4	5	6	7	8	9	10	11	12
		A_2	0	4	6	8	10	12	14	16	18	20	22	24	26	28
		A_3	0	0	0	0	0	0	2	2	4	6	7	9	10	12
		A_4	10	12	15	18	21	24	23	26	25	24	25	24	25	24
		A_5	70	64	58	52	46	40	36	30	26	22	17	13	8	4
	8	A_1	0	0	1	2	3	4	5	6	7	8	9	10	11	12
		A_2	0	4	6	8	10	12	14	16	18	20	22	24	26	28
		A_3	0	0	0	0	0	1	2	2	3	4	6	7	9	12
		A_4	10	12	15	18	21	22	23	26	27	28	27	28	27	24
		A_5	70	64	58	52	46	41	36	30	25	20	16	11	7	4

Table B.18: 2-Face Type Growth Pattern (EC2FGP) Dimension 6

Dimension		2-Face Type	Transition Sequence Index																										
n	EC			0	1	2	3	4	5	6	7	8	9	10	11	12	13	14	15	16	17	18	19	20	21	22	23	24	25
6		A_1	0	0	1	2	3	4	5	6	7	8	9	10	11	12	13	14	15	16	17	18	19	20	21	22	23	24	25
		A_2	0	5	8	11	14	17	20	23	26	29	32	35	38	41	44	47	50	53	56	59	62	65	68	71	74	77	80
		A_3	0	0	0	0	0	1	2	2	3	6	6	9	12	13	15	16	18	18	21	24	28	31	35	38	41	45	52
		A_4	15	20	26	32	38	42	46	52	56	56	62	62	62	66	68	72	74	80	80	80	78	78	76	76	76	74	66
		A_5	225	215	205	195	185	176	167	157	148	141	131	124	117	108	100	91	83	73	66	59	53	46	40	33	26	20	17

Table B.19: 2-Face Type Growth Pattern (EC2FGP) Dimension 7 EC 1–6

Dimension		3-Face Type	Transition Sequence Index																									
n	EC		0	1	2	3	4	5	6	7	8	9	10	11	12	13	14	15	16	17	18	19	20	21	22	23	24	···
7	1	A_1	0	0	1	2	3	4	5	6	7	8	9	10	11	12	13	14	15	16	17	18	19	20	21	22	23	24	
		A_2	0	6	10	14	18	22	26	30	34	38	42	46	50	54	58	62	66	70	74	78	82	86	90	94	98	102	
		A_3	0	0	0	0	1	1	2	4	4	5	6	7	10	10	12	14	15	18	21	21	24	28	30	33	36	38	
		A_4	21	30	40	50	58	68	76	82	92	100	108	116	120	130	136	142	150	154	158	168	172	174	180	184	188	194	
		A_5	651	636	621	606	592	577	563	550	535	521	507	493	481	466	453	440	426	414	402	387	375	364	351	339	327	314	
	2	A_1	0	0	1	2	3	4	5	6	7	8	9	10	11	12	13	14	15	16	17	18	19	20	21	22	23	24	
		A_2	0	6	10	14	18	22	26	30	34	38	42	46	50	54	58	62	66	70	74	78	82	86	90	94	98	102	
		A_3	0	0	0	0	1	1	2	4	4	5	6	7	10	10	12	14	15	18	21	21	24	28	30	33	36	38	
		A_4	21	30	40	50	58	68	76	82	92	100	108	116	120	130	136	142	150	154	158	168	172	174	180	184	188	194	
		A_5	651	636	621	606	592	577	563	550	535	521	507	493	481	466	453	440	426	414	402	387	375	364	351	339	327	314	
	3	A_1	0	0	1	2	3	4	5	6	7	8	9	10	11	12	13	14	15	16	17	18	19	20	21	22	23	24	
		A_2	0	6	10	14	18	22	26	30	34	38	42	46	50	54	58	62	66	70	74	78	82	86	90	94	98	102	
		A_3	0	0	0	0	1	1	2	4	4	5	6	7	10	10	11	13	14	17	21	21	24	28	30	33	37	39	
		A_4	21	30	40	50	58	68	76	82	92	100	108	116	120	130	138	144	152	156	158	168	172	174	180	184	186	192	
		A_5	651	636	621	606	592	577	563	550	535	521	507	493	481	466	452	439	425	413	402	387	375	364	351	339	328	315	
	4	A_1	0	0	1	2	3	4	5	6	7	8	9	10	11	12	13	14	15	16	17	18	19	20	21	22	23	24	
		A_2	0	6	10	14	18	22	26	30	34	38	42	46	50	54	58	62	66	70	74	78	82	86	90	94	98	102	
		A_3	0	0	0	0	0	0	1	1	2	3	5	7	9	9	11	12	15	19	19	22	26	28	32	34	36	40	
		A_4	21	30	40	50	60	70	78	88	96	104	110	116	122	132	138	146	150	152	162	166	168	174	176	182	188	190	
		A_5	651	636	621	606	591	576	562	547	533	519	506	493	480	465	452	438	426	415	400	388	377	364	353	340	327	316	
	5	A_1	0	0	1	2	3	4	5	6	7	8	9	10	11	12	13	14	15	16	17	18	19	20	21	22	23	24	
		A_2	0	6	10	14	18	22	26	30	34	38	42	46	50	54	58	62	66	70	74	78	82	86	90	94	98	102	
		A_3	0	0	0	0	0	0	1	1	2	3	5	7	9	9	11	12	15	19	19	22	26	28	32	34	36	40	
		A_4	21	30	40	50	60	70	78	88	96	104	110	116	122	132	138	146	150	152	162	166	168	174	176	182	188	190	
		A_5	651	636	621	606	591	576	562	547	533	519	506	493	480	465	452	438	426	415	400	388	377	364	353	340	327	316	
	6	A_1	0	0	1	2	3	4	5	6	7	8	9	10	11	12	13	14	15	16	17	18	19	20	21	22	23	24	
		A_2	0	6	10	14	18	22	26	30	34	38	42	46	50	54	58	62	66	70	74	78	82	86	90	94	98	102	
		A_3	0	0	0	0	0	0	1	1	2	4	6	8	10	10	12	13	16	19	19	21	25	27	31	33	35	40	
		A_4	21	30	40	50	60	70	78	88	96	102	108	114	120	130	136	144	148	152	162	168	170	176	178	184	190	190	
		A_5	651	636	621	606	591	576	562	547	533	520	507	494	481	466	453	439	427	415	400	387	376	363	352	339	326	316	

Table B.19: 2-Face Type Growth Pattern (EC2FGP) Dimension 7 EC 1–6 - cont.

Dimension		3-Face Type	Transition Sequence Index (cont.)																									
n	EC		…	25	26	27	28	29	30	31	32	33	34	35	36	37	38	39	40	41	42	43	44	45	46	47	48	49
7	1	A_1		25	26	27	28	29	30	31	32	33	34	35	36	37	38	39	40	41	42	43	44	45	46	47	48	49
		A_2		106	110	114	118	122	126	130	134	138	142	146	150	154	158	162	166	170	174	178	182	186	190	194	198	202
		A_3		41	46	48	52	55	58	63	65	69	74	77	80	82	87	93	98	103	108	112	118	126	132	139	146	152
		A_4		198	198	204	206	210	214	214	220	222	222	226	230	236	236	234	234	234	234	236	234	228	226	222	218	216
		A_5		302	292	279	268	256	244	234	221	210	200	188	176	163	153	144	134	124	114	103	94	87	78	70	62	53
	2	A_1		25	26	27	28	29	30	31	32	33	34	35	36	37	38	39	40	41	42	43	44	45	46	47	48	49
		A_2		106	110	114	118	122	126	130	134	138	142	146	150	154	158	162	166	170	174	178	182	186	190	194	198	202
		A_3		41	46	48	52	55	58	63	65	69	74	77	80	82	87	93	98	103	108	112	119	124	131	138	144	153
		A_4		198	198	204	206	210	214	214	220	222	222	226	230	236	236	234	234	234	234	236	232	232	228	224	222	214
		A_5		302	292	279	268	256	244	234	221	210	200	188	176	163	153	144	134	124	114	103	95	85	77	69	60	54
	3	A_1		25	26	27	28	29	30	31	32	33	34	35	36	37	38	39	40	41	42	43	44	45	46	47	48	49
		A_2		106	110	114	118	122	126	130	134	138	142	146	150	154	158	162	166	170	174	178	182	186	190	194	198	202
		A_3		42	47	49	53	56	59	64	66	69	74	76	79	81	86	91	96	101	106	111	117	124	130	136	143	150
		A_4		196	196	202	204	208	212	212	218	222	222	228	232	238	238	238	238	238	238	238	236	232	230	228	224	220
		A_5		303	293	280	269	257	245	235	222	210	200	187	175	162	152	142	132	122	112	102	93	85	76	67	59	51
	4	A_1		25	26	27	28	29	30	31	32	33	34	35	36	37	38	39	40	41	42	43	44	45	46	47	48	49
		A_2		106	110	114	118	122	126	130	134	138	142	146	150	154	158	162	166	170	174	178	182	186	190	194	198	202
		A_3		41	43	47	50	53	57	59	63	68	71	75	79	81	85	90	96	102	108	113	118	122	128	133	141	150
		A_4		198	204	206	210	214	216	222	224	224	228	230	232	238	240	240	238	236	234	234	234	236	234	234	228	220
		A_5		302	289	278	266	254	243	230	219	209	197	186	175	162	151	141	132	123	114	104	94	83	74	64	57	51
	5	A_1		25	26	27	28	29	30	31	32	33	34	35	36	37	38	39	40	41	42	43	44	45	46	47	48	49
		A_2		106	110	114	118	122	126	130	134	138	142	146	150	154	158	162	166	170	174	178	182	186	190	194	198	202
		A_3		41	43	47	50	53	57	59	63	68	71	76	80	82	86	92	98	104	110	115	120	124	130	136	144	152
		A_4		198	204	206	210	214	216	222	224	224	228	228	230	236	238	236	234	232	230	230	230	232	230	228	222	216
		A_5		302	289	278	266	254	243	230	219	209	197	187	176	163	152	143	134	125	116	106	96	85	76	67	60	53
	6	A_1		25	26	27	28	29	30	31	32	33	34	35	36	37	38	39	40	41	42	43	44	45	46	47	48	49
		A_2		106	110	114	118	122	126	130	134	138	142	146	150	154	158	162	166	170	174	178	182	186	190	194	198	202
		A_3		41	43	47	50	53	57	59	63	68	72	77	81	83	87	93	100	106	112	117	121	125	131	137	145	153
		A_4		198	204	206	210	214	216	222	224	224	226	226	228	234	236	234	230	228	226	226	228	230	228	226	220	214
		A_5		302	289	278	266	254	243	230	219	209	198	188	177	164	153	144	136	127	118	108	97	86	77	68	61	54

Table B.20: 2-Face Type Growth Pattern (EC2FGP) Dimension 7 EC 7–12

Dimension		3-Face Type	Transition Sequence Index																									
n	EC		0	1	2	3	4	5	6	7	8	9	10	11	12	13	14	15	16	17	18	19	20	21	22	23	24	···
7	7	A_1	0	0	1	2	3	4	5	6	7	8	9	10	11	12	13	14	15	16	17	18	19	20	21	22	23	24	
		A_2	0	6	10	14	18	22	26	30	34	38	42	46	50	54	58	62	66	70	74	78	82	86	90	94	98	102	
		A_3	0	0	0	0	0	1	1	2	3	3	4	6	7	10	12	13	16	17	19	22	25	28	31	33	38	38	
		A_4	21	30	40	50	60	68	78	86	94	104	112	118	126	130	136	144	148	156	162	166	170	174	178	184	184	194	
		A_5	651	636	621	606	591	577	562	548	534	519	505	492	478	466	453	439	427	413	400	388	376	364	352	339	329	314	
	8	A_1	0	0	1	2	3	4	5	6	7	8	9	10	11	12	13	14	15	16	17	18	19	20	21	22	23	24	
		A_2	0	6	10	14	18	22	26	30	34	38	42	46	50	54	58	62	66	70	74	78	82	86	90	94	98	102	
		A_3	0	0	0	0	0	1	1	2	4	4	5	7	8	11	12	13	16	17	19	22	25	28	31	33	38	38	
		A_4	21	30	40	50	60	68	78	86	92	102	110	116	124	128	136	144	148	156	162	166	170	174	178	184	184	194	
		A_5	651	636	621	606	591	577	562	548	535	520	506	493	479	467	453	439	427	413	400	388	376	364	352	339	329	314	
	9	A_1	0	0	1	2	3	4	5	6	7	8	9	10	11	12	13	14	15	16	17	18	19	20	21	22	23	24	
		A_2	0	6	10	14	18	22	26	30	34	38	42	46	50	54	58	62	66	70	74	78	82	86	90	94	98	102	
		A_3	0	0	0	0	0	1	1	2	4	4	5	6	7	10	11	13	16	17	19	21	24	28	31	34	39	39	
		A_4	21	30	40	50	60	68	78	86	92	102	110	118	126	130	138	144	148	156	162	168	172	174	178	182	182	192	
		A_5	651	636	621	606	591	577	562	548	535	520	506	492	478	466	452	439	427	413	400	387	375	364	352	340	330	315	
	10	A_1	0	0	1	2	3	4	5	6	7	8	9	10	11	12	13	14	15	16	17	18	19	20	21	22	23	24	
		A_2	0	6	10	14	18	22	26	30	34	38	42	46	50	54	58	62	66	70	74	78	82	86	90	94	98	102	
		A_3	0	0	0	0	0	0	0	1	2	3	4	4	5	6	8	11	15	18	21	22	25	28	32	36	40	44	
		A_4	21	30	40	50	60	70	80	88	96	104	112	122	130	138	144	148	150	154	158	166	170	174	176	178	180	182	
		A_5	651	636	621	606	591	576	561	547	533	519	505	490	476	462	449	437	426	414	402	388	376	364	353	342	331	320	
	11	A_1	0	0	1	2	3	4	5	6	7	8	9	10	11	12	13	14	15	16	17	18	19	20	21	22	23	24	
		A_2	0	6	10	14	18	22	26	30	34	38	42	46	50	54	58	62	66	70	74	78	82	86	90	94	98	102	
		A_3	0	0	0	0	0	0	0	1	2	3	4	4	5	6	8	11	15	18	21	22	27	30	34	38	41	45	
		A_4	21	30	40	50	60	70	80	88	96	104	112	122	130	138	144	148	150	154	158	166	166	170	172	174	178	180	
		A_5	651	636	621	606	591	576	561	547	533	519	505	490	476	462	449	437	426	414	402	388	378	366	355	344	332	321	
	12	A_1	0	0	1	2	3	4	5	6	7	8	9	10	11	12	13	14	15	16	17	18	19	20	21	22	23	24	
		A_2	0	6	10	14	18	22	26	30	34	38	42	46	50	54	58	62	66	70	74	78	82	86	90	94	98	102	
		A_3	0	0	0	0	0	0	0	1	2	3	4	4	5	6	8	11	15	18	21	22	27	30	34	38	41	45	
		A_4	21	30	40	50	60	70	80	88	96	104	112	122	130	138	144	148	150	154	158	166	166	170	172	174	178	180	
		A_5	651	636	621	606	591	576	561	547	533	519	505	490	476	462	449	437	426	414	402	388	378	366	355	344	332	321	

Table B.20: 2-Face Type Growth Pattern (EC2FGP) Dimension 7 EC 7–12 - cont.

Dimension		3-Face Type	Transition Sequence Index (cont.)																									
n	EC		…	25	26	27	28	29	30	31	32	33	34	35	36	37	38	39	40	41	42	43	44	45	46	47	48	49
7	7	A_1		25	26	27	28	29	30	31	32	33	34	35	36	37	38	39	40	41	42	43	44	45	46	47	48	49
		A_2		106	110	114	118	122	126	130	134	138	142	146	150	154	158	162	166	170	174	178	182	186	190	194	198	202
		A_3		41	44	46	50	53	57	59	62	65	68	72	75	81	87	92	96	100	106	113	118	123	130	136	141	150
		A_4		198	202	208	210	214	216	222	226	230	234	236	240	238	236	236	238	240	238	234	234	234	230	228	228	220
		A_5		302	290	277	266	254	243	230	218	206	194	183	171	162	153	143	132	121	112	104	94	84	76	67	57	51
	8	A_1		25	26	27	28	29	30	31	32	33	34	35	36	37	38	39	40	41	42	43	44	45	46	47	48	49
		A_2		106	110	114	118	122	126	130	134	138	142	146	150	154	158	162	166	170	174	178	182	186	190	194	198	202
		A_3		41	44	46	50	52	56	58	61	65	68	72	75	79	85	92	96	102	108	113	118	123	130	136	141	150
		A_4		198	202	208	210	216	218	224	228	230	234	236	240	242	240	236	238	236	234	234	234	234	230	228	228	220
		A_5		302	290	277	266	253	242	229	217	206	194	183	171	160	151	143	132	123	114	104	94	84	76	67	57	51
	9	A_1		25	26	27	28	29	30	31	32	33	34	35	36	37	38	39	40	41	42	43	44	45	46	47	48	49
		A_2		106	110	114	118	122	126	130	134	138	142	146	150	154	158	162	166	170	174	178	182	186	190	194	198	202
		A_3		42	46	48	52	54	57	59	62	66	69	73	76	80	85	92	97	103	109	114	119	124	131	137	143	152
		A_4		196	198	204	206	212	216	222	226	228	232	234	238	240	240	236	236	234	232	232	232	232	228	226	224	216
		A_5		303	292	279	268	255	243	230	218	207	195	184	172	161	151	143	133	124	115	105	95	85	77	68	59	53
	10	A_1		25	26	27	28	29	30	31	32	33	34	35	36	37	38	39	40	41	42	43	44	45	46	47	48	49
		A_2		106	110	114	118	122	126	130	134	138	142	146	150	154	158	162	166	170	174	178	182	186	190	194	198	202
		A_3		44	46	48	51	55	57	60	63	66	71	74	77	82	86	92	97	101	106	112	116	123	128	133	141	150
		A_4		192	198	204	208	210	216	220	224	228	228	232	236	236	238	236	236	238	238	236	238	234	234	234	228	220
		A_5		305	292	279	267	256	243	231	219	207	197	185	173	163	152	143	133	122	112	103	92	84	74	64	57	51
	11	A_1		25	26	27	28	29	30	31	32	33	34	35	36	37	38	39	40	41	42	43	44	45	46	47	48	49
		A_2		106	110	114	118	122	126	130	134	138	142	146	150	154	158	162	166	170	174	178	182	186	190	194	198	202
		A_3		45	47	49	52	56	58	61	64	67	72	78	81	86	90	95	100	104	109	115	119	123	128	135	143	150
		A_4		190	196	202	206	208	214	218	222	226	226	224	228	228	230	230	230	232	232	230	232	234	234	230	224	220
		A_5		306	293	280	268	257	244	232	220	208	198	189	177	167	156	146	136	125	115	106	95	84	74	66	59	51
	12	A_1		25	26	27	28	29	30	31	32	33	34	35	36	37	38	39	40	41	42	43	44	45	46	47	48	49
		A_2		106	110	114	118	122	126	130	134	138	142	146	150	154	158	162	166	170	174	178	182	186	190	194	198	202
		A_3		45	48	51	55	59	61	63	67	70	75	80	82	87	93	98	104	109	113	119	122	127	133	140	146	152
		A_4		190	194	198	200	202	208	214	216	220	220	220	226	226	224	224	222	222	224	222	226	226	224	220	218	216
		A_5		306	294	282	271	260	247	234	223	211	201	191	178	168	159	149	140	130	119	110	98	88	79	71	62	53

B.6 3-Face Growth Analysis

Table B.21: 3-Face Type Growth Pattern (EC3FGP) Dimension 3–4

Dimension		3-Face Type	Transition Sequence Index							
n	EC			0	1	2	3	4	5	6
3		B_1	0	0	0	0	1			
		B_2	0	0	0	1	0			
		B_3	0	0	0	0	0			
		B_4	0	0	0	0	0			
		B_5	0	0	0	0	0			
		B_6	0	0	1	0	0			
		B_7	0	0	0	0	0			
		B_8	0	0	0	0	0			
		B_9	0	1	0	0	0			
		B_{10}	0	0	0	0	0			
		B_{11}	0	0	0	0	0			
		B_{12}	1	0	0	0	0			
		B_{13}	0	0	0	0	0			
4		B_1	0	0	0	0	1	1	1	2
		B_2	0	0	0	1	0	1	2	1
		B_3	0	0	0	0	0	0	1	2
		B_4	0	0	0	0	0	0	0	1
		B_5	0	0	0	0	0	0	0	0
		B_6	0	0	2	2	3	3	2	2
		B_7	0	0	0	0	0	1	1	0
		B_8	0	0	0	0	0	0	0	0
		B_9	0	3	2	2	2	1	1	0
		B_{10}	0	0	0	0	1	0	0	0
		B_{11}	0	0	0	0	0	0	0	0
		B_{12}	4	2	2	2	0	1	0	0
		B_{13}	4	3	2	1	1	0	0	0

Table B.22: 3-Face Type Growth Pattern (EC3FGP) Dimension 5 EC 1–2

Dimension		3-Face Type	Transition Sequence Index													
n	EC			0	1	2	3	4	5	6	7	8	9	10	11	12
5	1	B_1	0	0	0	0	0	0	0	0	1	1	1	2	2	2
		B_2	0	0	0	1	2	3	4	5	4	5	6	5	6	7
		B_3	0	0	0	0	0	0	0	0	0	0	2	3	5	9
		B_4	0	0	0	0	0	0	0	0	0	0	1	2	2	3
		B_5	0	0	0	0	0	0	0	0	0	0	0	0	0	0
		B_6	0	0	3	4	5	6	7	8	10	11	10	11	10	7
		B_7	0	0	0	0	0	0	2	3	4	8	7	7	10	9
		B_8	0	0	0	0	0	0	0	0	0	0	0	0	0	0
		B_9	0	6	6	7	8	9	8	8	8	5	5	4	2	2
		B_{10}	0	0	0	0	0	0	1	0	1	0	1	2	1	1
		B_{11}	0	0	0	0	0	1	0	0	1	0	0	1	0	0
		B_{12}	10	8	9	10	11	10	9	11	7	8	6	2	2	0
		B_{13}	30	26	22	18	14	11	9	5	4	2	1	1	0	0
	2	B_1	0	0	0	0	0	0	0	0	0	1	1	2	2	2
		B_2	0	0	0	1	2	3	4	5	6	5	6	5	6	7
		B_3	0	0	0	0	0	0	0	0	1	2	4	6	8	9
		B_4	0	0	0	0	0	0	0	0	0	0	1	1	2	3
		B_5	0	0	0	0	0	0	0	0	0	0	0	0	0	0
		B_6	0	0	3	4	5	6	7	8	8	9	8	8	7	7
		B_7	0	0	0	0	0	0	2	3	3	6	5	7	7	9
		B_8	0	0	0	0	0	0	0	0	0	0	0	0	0	0
		B_9	0	6	6	7	8	9	8	8	9	7	7	6	5	2
		B_{10}	0	0	0	0	0	0	1	0	1	1	2	1	1	1
		B_{11}	0	0	0	0	0	1	0	0	1	0	0	0	0	0
		B_{12}	10	8	9	10	11	10	9	11	7	6	4	3	2	0
		B_{13}	30	26	22	18	14	11	9	5	4	3	2	1	0	0

Table B.23: 3-Face Type Growth Pattern (EC3FGP) Dimension 5 EC 3–4

Dimension		3-Face Type	Transition Sequence Index													
n	EC			0	1	2	3	4	5	6	7	8	9	10	11	12
5	3	B_1	0	0	0	0	0	0	1	1	2	2	2	3	3	3
		B_2	0	0	0	1	2	3	2	3	2	3	4	3	4	5
		B_3	0	0	0	0	0	0	1	1	3	3	4	5	5	9
		B_4	0	0	0	0	0	0	0	0	0	1	1	2	2	2
		B_5	0	0	0	0	0	0	0	0	0	0	0	0	0	0
		B_6	0	0	3	4	5	6	7	8	8	9	9	10	11	8
		B_7	0	0	0	0	0	0	1	3	3	4	6	5	9	11
		B_8	0	0	0	0	0	0	0	0	0	0	0	0	0	0
		B_9	0	6	6	7	8	9	9	8	9	7	6	6	3	2
		B_{10}	0	0	0	0	0	0	2	0	1	1	0	2	1	0
		B_{11}	0	0	0	0	0	1	0	0	0	0	0	1	1	0
		B_{12}	10	8	9	10	11	10	7	10	7	7	7	2	1	0
		B_{13}	30	26	22	18	14	11	10	6	5	3	1	1	0	0
	4	B_1	0	0	0	0	0	0	1	1	2	2	2	2	2	2
		B_2	0	0	0	1	2	3	2	3	2	3	4	5	6	7
		B_3	0	0	0	0	0	0	1	1	3	3	4	6	6	9
		B_4	0	0	0	0	0	0	0	0	0	1	1	2	3	3
		B_5	0	0	0	0	0	0	0	0	0	0	0	0	0	0
		B_6	0	0	3	4	5	6	7	8	8	9	9	8	9	7
		B_7	0	0	0	0	0	0	1	3	3	4	6	5	5	9
		B_8	0	0	0	0	0	0	0	0	0	0	0	0	0	0
		B_9	0	6	6	7	8	9	9	8	9	7	6	6	5	2
		B_{10}	0	0	0	0	0	0	2	0	1	1	0	1	2	1
		B_{11}	0	0	0	0	0	1	0	0	0	0	0	0	2	0
		B_{12}	10	8	9	10	11	10	7	10	7	7	7	5	0	0
		B_{13}	30	26	22	18	14	11	10	6	5	3	1	0	0	0

Table B.24: 3-Face Type Growth Pattern (EC3FGP) Dimension 5 EC 5–6

Dimension		3-Face Type	Transition Sequence Index												
n	EC		0	1	2	3	4	5	6	7	8	9	10	11	12
5	5	B_1	0	0	0	0	0	0	1	1	1	1	1	1	2	2
		B_2	0	0	0	1	2	3	2	3	4	5	6	7	6	7
		B_3	0	0	0	0	0	0	1	1	2	2	2	4	4	7
		B_4	0	0	0	0	0	0	0	0	0	1	1	2	3	4
		B_5	0	0	0	0	0	0	0	0	0	0	0	0	0	0
		B_6	0	0	3	4	5	6	7	8	8	9	10	9	11	9
		B_7	0	0	0	0	0	0	1	3	3	3	7	6	7	8
		B_8	0	0	0	0	0	0	0	0	0	0	0	0	1	1
		B_9	0	6	6	7	8	9	9	8	9	8	5	5	3	1
		B_{10}	0	0	0	0	0	0	2	0	1	2	1	2	1	1
		B_{11}	0	0	0	0	0	1	0	0	0	1	0	0	1	0
		B_{12}	10	8	9	10	11	10	7	10	8	5	6	4	1	0
		B_{13}	30	26	22	18	14	11	10	6	4	3	1	0	0	0
	6	B_1	0	0	0	0	0	0	1	1	1	2	2	2	2	2
		B_2	0	0	0	1	2	3	2	3	4	3	4	5	6	7
		B_3	0	0	0	0	0	0	1	1	4	5	6	8	8	9
		B_4	0	0	0	0	0	0	0	0	0	1	1	2	3	3
		B_5	0	0	0	0	0	0	0	0	0	0	0	0	0	0
		B_6	0	0	3	4	5	6	7	8	6	7	7	6	7	7
		B_7	0	0	0	0	0	0	1	3	2	2	4	3	4	9
		B_8	0	0	0	0	0	0	0	0	0	0	0	0	0	0
		B_9	0	6	6	7	8	9	9	8	10	9	8	8	6	2
		B_{10}	0	0	0	0	0	0	2	0	1	2	1	2	2	1
		B_{11}	0	0	0	0	0	1	0	0	0	0	0	0	1	0
		B_{12}	10	8	9	10	11	10	7	10	7	5	5	3	1	0
		B_{13}	30	26	22	18	14	11	10	6	5	4	2	1	0	0

Table B.25: 3-Face Type Growth Pattern (EC3FGP) Dimension 5 EC 7–8

Dimension		3-Face Type	Transition Sequence Index												
n	EC		0	1	2	3	4	5	6	7	8	9	10	11	12
5	7	B_1	0	0	0	0	0	0	1	1	1	2	2	3	3	3
		B_2	0	0	0	1	2	3	2	3	4	3	4	3	4	5
		B_3	0	0	0	0	0	0	1	1	4	5	6	8	8	9
		B_4	0	0	0	0	0	0	0	0	0	1	1	1	2	2
		B_5	0	0	0	0	0	0	0	0	0	0	0	0	0	0
		B_6	0	0	3	4	5	6	7	8	6	7	7	7	8	8
		B_7	0	0	0	0	0	0	1	3	2	2	4	5	6	11
		B_8	0	0	0	0	0	0	0	0	0	0	0	0	0	0
		B_9	0	6	6	7	8	9	9	8	10	9	8	8	6	2
		B_{10}	0	0	0	0	0	0	2	0	1	2	1	1	1	0
		B_{11}	0	0	0	0	0	1	0	0	0	0	0	0	1	0
		B_{12}	10	8	9	10	11	10	7	10	7	5	5	3	1	0
		B_{13}	30	26	22	18	14	11	10	6	5	4	2	1	0	0
	8	B_1	0	0	0	0	0	1	1	1	1	1	1	2	2	2
		B_2	0	0	0	1	2	1	2	3	4	5	6	5	6	7
		B_3	0	0	0	0	0	0	0	0	1	1	3	3	5	7
		B_4	0	0	0	0	0	0	1	1	1	1	2	2	2	4
		B_5	0	0	0	0	0	0	0	0	0	0	0	0	0	0
		B_6	0	0	3	4	5	7	8	9	9	10	9	11	10	9
		B_7	0	0	0	0	0	1	0	1	1	5	3	6	9	8
		B_8	0	0	0	0	0	0	0	0	0	0	0	0	0	1
		B_9	0	6	6	7	8	8	8	8	9	6	7	5	3	1
		B_{10}	0	0	0	0	0	1	3	2	3	2	4	3	2	1
		B_{11}	0	0	0	0	0	0	0	0	1	0	0	1	0	0
		B_{12}	10	8	9	10	11	9	7	9	5	6	3	1	1	0
		B_{13}	30	26	22	18	14	12	10	6	5	3	2	1	0	0

Table B.26: 3-Face Type Growth Pattern (EC3FGP) Dimension 6

Dimension		3-Face	Transition Sequence Index																										
n	EC	Type		0	1	2	3	4	5	6	7	8	9	10	11	12	13	14	15	16	17	18	19	20	21	22	23	24	25
6		B_1	0	0	0	0	0	1	1	1	1	2	2	2	3	3	3	3	3	3	4	4	4	5	5	5	5	6	6
		B_2	0	0	0	1	2	1	2	3	4	3	4	5	4	5	6	7	8	9	8	9	10	9	10	11	12	11	12
		B_3	0	0	0	0	0	0	0	0	1	3	3	8	9	10	12	12	13	13	15	15	17	18	22	26	29	32	38
		B_4	0	0	0	0	0	0	1	1	1	2	2	2	4	4	5	6	6	6	6	8	11	13	14	15	15	16	20
		B_5	0	0	0	0	0	0	0	0	0	0	0	0	0	0	0	0	0	0	0	1	2	2	3	3	3	4	6
		B_6	0	0	4	6	8	11	13	15	16	17	19	16	18	19	19	21	22	24	25	27	27	29	27	25	24	24	20
		B_7	0	0	0	0	0	1	0	1	1	1	4	3	2	6	5	6	11	13	16	20	18	19	21	22	27	30	26
		B_8	0	0	0	0	0	0	0	0	0	1	1	2	4	4	4	4	4	4	5	4	4	5	4	4	5	5	6
		B_9	0	10	12	15	18	20	22	24	27	28	28	32	32	31	33	33	31	32	32	27	26	24	23	23	21	19	18
		B_{10}	0	0	0	0	0	2	5	4	6	8	5	5	5	3	6	7	8	6	7	8	10	11	12	13	11	9	6
		B_{11}	0	0	0	0	0	0	0	0	1	0	0	0	0	0	0	1	0	1	1	0	0	1	0	1	0	1	0
		B_{12}	20	20	24	28	32	31	30	35	32	29	36	33	31	34	31	30	28	32	26	25	21	16	13	8	7	3	2
		B_{13}	140	130	120	110	100	93	86	76	70	66	56	52	48	41	36	30	26	17	15	12	10	8	6	4	1	0	0

Table B.27: 3-Face Type Growth Pattern (EC3FGP) Dimension 7 EC 1

Dimension		3-Face Type	Transition Sequence Index																										
n	EC			0	1	2	3	4	5	6	7	8	9	10	11	12	13	14	15	16	17	18	19	20	21	22	23	24	···
7	1	B_1	0	0	0	0	1	1	1	2	2	2	2	2	2	2	3	3	3	3	3	3	3	4	4	4	5	5	
		B_2	0	0	0	1	0	1	2	1	2	3	4	5	6	7	6	7	8	9	10	11	12	11	12	13	12	13	
		B_3	0	0	0	0	0	0	1	2	2	3	3	3	6	6	7	7	7	9	10	10	14	15	15	16	16	18	
		B_4	0	0	0	0	0	0	0	1	1	1	2	2	3	3	3	5	6	7	10	10	10	13	15	17	18	19	
		B_5	0	0	0	0	0	0	0	0	0	0	0	0	0	0	0	0	0	0	0	0	0	0	0	0	0	0	
		B_6	0	0	5	8	12	15	17	20	23	25	28	31	31	34	37	40	43	44	46	49	48	51	54	56	60	61	
		B_7	0	0	0	0	0	1	1	0	2	3	3	7	6	9	11	11	12	14	11	14	14	13	15	16	21	22	
		B_8	0	0	0	0	0	0	0	0	0	0	0	0	1	1	2	3	3	5	7	7	9	14	15	18	20	20	
		B_9	0	15	20	26	32	37	43	48	52	57	61	63	68	71	75	77	80	82	85	88	94	95	95	96	95	98	
		B_{10}	0	0	0	0	4	3	6	12	10	12	15	16	21	18	20	23	25	26	30	27	28	25	26	25	26	29	
		B_{11}	0	0	0	0	0	0	0	0	0	0	1	1	0	0	0	0	1	0	1	1	1	1	1	2	1	2	
		B_{12}	35	40	50	60	62	73	76	74	86	90	92	96	93	106	106	107	110	110	106	119	117	118	121	120	119	118	
		B_{13}	525	505	485	465	449	429	413	400	380	364	349	334	323	303	290	277	262	251	241	221	210	200	187	177	167	155	

Dimension		3-Face Type	Transition Sequence Index (cont.)																								
n	EC		···	25	26	27	28	29	30	31	32	33	34	35	36	37	38	39	40	41	42	43	44	45	46	47	48	49
7	1	B_1		5	6	6	6	6	6	6	6	7	7	7	8	8	8	9	9	9	10	10	10	11	11	11	11	11
		B_2		14	13	14	15	16	17	18	19	18	19	20	19	20	21	20	21	22	21	22	23	22	23	24	25	26
		B_3		20	23	23	27	29	30	33	33	35	38	39	40	42	46	49	52	54	56	60	65	70	73	78	82	83
		B_4		19	22	24	25	27	28	31	33	34	37	39	40	40	41	45	48	51	53	54	55	60	64	67	72	76
		B_5		1	3	3	4	4	4	4	4	4	5	5	5	5	5	5	6	8	9	9	11	15	17	21	24	25
		B_6		62	63	66	65	66	68	68	71	73	73	75	78	79	78	79	79	80	82	81	79	78	78	76	75	77
		B_7		28	26	29	31	32	38	38	41	45	46	50	54	59	64	63	66	70	76	81	89	87	91	96	96	102
		B_8		19	17	18	17	18	20	24	24	26	27	29	31	31	35	42	44	44	45	47	47	46	47	44	44	48
		B_9		98	100	99	101	102	100	100	99	99	98	96	96	97	96	95	92	88	84	83	79	77	71	66	62	54
		B_{10}		31	39	39	44	47	46	47	50	53	56	55	55	56	54	49	47	46	47	46	44	44	41	40	39	35
		B_{11}		1	1	2	1	2	2	1	2	2	1	2	6	8	6	7	6	7	7	8	6	7	7	6	7	8
		B_{12}		117	108	110	105	101	100	95	94	86	81	80	71	68	65	60	60	56	49	44	41	33	31	28	22	15
		B_{13}		145	139	127	119	110	101	95	84	78	72	63	57	47	41	37	30	25	21	15	11	10	6	3	1	0

Table B.28: 3-Face Type Growth Pattern (EC3FGP) Dimension 7 EC 2

Dimension		3-Face Type	Transition Sequence Index																										
n	EC			0	1	2	3	4	5	6	7	8	9	10	11	12	13	14	15	16	17	18	19	20	21	22	23	24	···
7	2	B_1	0	0	0	0	1	1	1	2	2	2	2	2	2	2	3	3	3	3	3	3	3	4	4	4	5	5	
		B_2	0	0	0	1	0	1	2	1	2	3	4	5	6	7	6	7	8	9	10	11	12	11	12	13	12	13	
		B_3	0	0	0	0	0	0	1	2	2	3	3	3	6	6	7	7	7	9	10	10	14	15	15	16	16	18	
		B_4	0	0	0	0	0	0	0	1	1	1	2	2	3	3	3	5	6	7	10	10	10	13	15	17	18	19	
		B_5	0	0	0	0	0	0	0	0	0	0	0	0	0	0	0	0	0	0	0	0	0	0	0	0	0	0	
		B_6	0	0	5	8	12	15	17	20	23	25	28	31	31	34	37	40	43	44	46	49	48	51	54	56	60	61	
		B_7	0	0	0	0	0	1	1	0	2	3	3	7	6	9	11	11	12	14	11	14	14	13	15	16	21	22	
		B_8	0	0	0	0	0	0	0	0	0	0	0	0	1	1	2	3	3	5	7	7	9	14	15	18	20	20	
		B_9	0	15	20	26	32	37	43	48	52	57	61	63	68	71	75	77	80	82	85	88	94	95	95	96	95	98	
		B_{10}	0	0	0	0	4	3	6	12	10	12	15	16	21	18	20	23	25	26	30	27	28	25	26	25	26	29	
		B_{11}	0	0	0	0	0	0	0	0	0	0	1	1	0	0	0	0	1	0	1	1	1	1	1	2	1	2	
		B_{12}	35	40	50	60	62	73	76	74	86	90	92	96	93	106	106	107	110	110	106	119	117	118	121	120	119	118	
		B_{13}	525	505	485	465	449	429	413	400	380	364	349	334	323	303	290	277	262	251	241	221	210	200	187	177	167	155	

Dimension		3-Face Type	Transition Sequence Index (cont.)																									
n	EC		···	25	26	27	28	29	30	31	32	33	34	35	36	37	38	39	40	41	42	43	44	45	46	47	48	49
7	2	B_1		5	6	6	6	6	6	6	6	7	7	7	8	8	8	9	9	9	10	10	11	11	11	11	11	11
		B_2		14	13	14	15	16	17	18	19	18	19	20	19	20	21	20	21	22	21	22	21	22	23	24	25	26
		B_3		20	23	23	27	29	30	33	33	35	38	39	40	42	46	49	52	54	56	60	66	68	73	76	80	87
		B_4		19	22	24	25	27	28	31	33	34	37	39	40	40	41	45	48	51	53	54	56	58	62	67	70	74
		B_5		1	3	3	4	4	4	4	4	4	5	5	5	5	5	5	6	8	9	9	11	12	15	19	21	25
		B_6		62	63	66	65	66	68	68	71	73	73	75	78	79	78	79	79	80	82	81	79	80	78	78	77	73
		B_7		28	26	29	31	32	38	38	41	45	46	50	54	59	64	63	66	70	76	81	84	93	93	95	100	103
		B_8		19	17	18	17	18	20	24	24	26	27	29	31	31	35	42	44	44	45	47	48	50	50	47	48	49
		B_9		98	100	99	101	102	100	100	99	99	98	96	96	97	96	95	92	88	84	83	82	75	73	67	62	57
		B_{10}		31	39	39	44	47	46	47	50	53	56	55	55	56	54	49	47	46	47	46	46	42	41	43	39	32
		B_{11}		1	1	2	1	2	2	1	2	2	1	2	6	8	6	7	6	7	7	8	7	6	7	7	8	6
		B_{12}		117	108	110	105	101	100	95	94	86	81	80	71	68	65	60	60	56	49	44	36	35	28	22	18	17
		B_{13}		145	139	127	119	110	101	95	84	78	72	63	57	47	41	37	30	25	21	15	13	8	6	4	1	0

Table B.29: 3-Face Type Growth Pattern (EC3FGP) Dimension 7 EC 3

Dimension		3-Face Type	Transition Sequence Index																									
n	EC			0	1	2	3	4	5	6	7	8	9	10	11	12	13	14	15	16	17	18	19	20	21	22	23	24	⋯
7	3	B_1	0	0	0	0	1	1	1	2	2	2	2	2	2	2	2	2	2	2	3	3	3	4	4	4	5	5	
		B_2	0	0	0	1	0	1	2	1	2	3	4	5	6	7	8	9	10	11	10	11	12	11	12	13	12	13	
		B_3	0	0	0	0	0	0	1	2	2	3	3	3	6	6	7	7	7	9	10	10	14	15	15	16	17	19	
		B_4	0	0	0	0	0	0	0	1	1	1	2	2	3	3	3	4	5	6	9	9	9	12	14	16	18	19	
		B_5	0	0	0	0	0	0	0	0	0	0	0	0	0	0	0	0	0	0	0	0	0	0	0	0	0	0	
		B_6	0	0	5	8	12	15	17	20	23	25	28	31	31	34	36	39	42	43	46	49	48	51	54	56	59	60	
		B_7	0	0	0	0	0	1	1	0	2	3	3	7	6	9	9	12	13	15	13	17	17	16	18	19	21	23	
		B_8	0	0	0	0	0	0	0	0	0	0	0	0	1	1	1	2	2	4	7	7	9	14	15	18	21	21	
		B_9	0	15	20	26	32	37	43	48	52	57	61	63	68	71	77	78	81	83	85	87	93	94	94	95	95	97	
		B_{10}	0	0	0	0	4	3	6	12	10	12	15	16	21	18	21	23	25	26	30	26	27	24	25	24	26	28	
		B_{11}	0	0	0	0	0	0	0	0	0	0	1	1	0	0	1	0	1	0	0	0	0	0	0	1	0	1	
		B_{12}	35	40	50	60	62	73	76	74	86	90	92	96	93	106	107	109	112	112	106	120	118	119	122	121	117	117	
		B_{13}	525	505	485	465	449	429	413	400	380	364	349	334	323	303	288	275	260	249	241	221	210	200	187	177	169	157	

Dimension		3-Face Type	Transition Sequence Index (cont.)																									
n	EC		⋯	25	26	27	28	29	30	31	32	33	34	35	36	37	38	39	40	41	42	43	44	45	46	47	48	49
7	3	B_1		5	6	6	6	6	6	6	6	7	7	7	8	8	8	9	9	9	10	10	10	11	11	11	11	11
		B_2		14	13	14	15	16	17	18	19	18	19	20	19	20	21	20	21	22	21	22	23	22	23	24	25	26
		B_3		21	24	24	28	30	31	34	34	35	38	38	39	41	45	48	51	53	55	60	65	69	72	76	80	81
		B_4		19	22	24	25	27	28	31	33	33	36	38	38	38	39	42	44	47	49	50	52	56	60	63	67	72
		B_5		1	3	3	4	4	4	4	4	4	5	5	5	5	5	5	6	8	9	9	11	14	16	18	21	23
		B_6		61	62	65	64	65	67	67	70	73	73	76	79	80	79	80	80	81	83	81	79	79	79	78	77	79
		B_7		29	27	30	32	33	39	39	42	49	49	52	59	64	69	69	75	79	85	91	96	97	100	104	107	112
		B_8		20	18	19	18	19	21	25	25	27	28	29	31	31	35	39	41	41	42	45	45	45	46	47	47	50
		B_9		97	99	98	100	101	99	99	98	97	97	96	95	96	95	95	91	87	83	81	78	75	70	66	61	52
		B_{10}		30	38	38	43	46	45	46	49	48	52	52	51	52	50	50	47	46	47	45	44	43	41	38	36	33
		B_{11}		0	0	1	0	1	1	0	1	1	0	3	6	8	6	8	6	7	8	7	6	7	7	8	8	8
		B_{12}		116	107	109	104	100	99	94	93	91	85	83	75	72	69	60	61	57	48	44	40	33	30	25	20	13
		B_{13}		147	141	129	121	112	103	97	86	77	71	61	55	45	39	35	28	23	20	15	11	9	5	2	0	0

Table B.30: 3-Face Type Growth Pattern (EC3FGP) Dimension 7 EC 4

Dimension		3-Face	Transition Sequence Index																									
n	EC	Type		0	1	2	3	4	5	6	7	8	9	10	11	12	13	14	15	16	17	18	19	20	21	22	23	24	···
7	4	B_1	0	0	0	0	0	0	0	0	1	1	1	2	2	2	3	3	3	4	4	4	5	5	5	5	5	5	
		B_2	0	0	0	1	2	3	4	5	4	5	6	5	6	7	6	7	8	7	8	9	8	9	10	11	12	13	
		B_3	0	0	0	0	0	0	0	0	0	0	2	3	5	5	6	6	8	10	10	14	15	15	18	18	19	22	
		B_4	0	0	0	0	0	0	0	0	0	0	1	2	2	2	2	3	4	7	7	7	10	12	14	16	17	18	
		B_5	0	0	0	0	0	0	0	0	0	0	0	0	0	0	0	0	0	0	0	0	0	0	0	0	0	1	
		B_6	0	0	5	8	11	14	17	20	24	27	28	31	32	35	38	41	42	44	47	46	49	52	52	55	57	57	
		B_7	0	0	0	0	0	0	2	3	4	8	7	7	10	12	14	15	17	14	18	19	18	20	20	22	23	27	
		B_8	0	0	0	0	0	0	0	0	0	0	0	0	0	0	1	1	3	5	5	7	12	13	17	18	19	18	
		B_9	0	15	20	26	32	38	42	47	52	54	59	63	66	70	74	77	79	82	84	89	90	90	92	92	95	95	
		B_{10}	0	0	0	0	0	0	3	2	5	6	11	16	19	17	19	21	22	28	24	24	21	22	20	21	23	28	
		B_{11}	0	0	0	0	0	1	0	0	1	0	0	1	0	0	0	1	0	0	0	0	0	1	0	0	2	0	
		B_{12}	35	40	50	60	70	78	82	93	94	100	99	96	97	109	109	112	112	105	119	118	119	120	121	124	121	117	
		B_{13}	525	505	485	465	445	426	410	390	375	359	346	334	321	301	288	273	262	254	234	223	213	201	191	178	167	159	

Dimension		3-Face	Transition Sequence Index (cont.)																									
n	EC	Type	···	25	26	27	28	29	30	31	32	33	34	35	36	37	38	39	40	41	42	43	44	45	46	47	48	49
7	4	B_1		5	6	6	6	7	7	7	8	8	8	9	9	9	9	9	9	9	9	9	9	9	10	10	10	11
		B_2		14	13	14	15	14	15	16	15	16	17	16	17	18	19	20	21	22	23	24	25	26	25	26	27	26
		B_3		22	23	26	28	30	33	33	35	38	39	40	41	42	44	46	49	53	57	59	63	66	68	70	76	81
		B_4		19	19	20	22	23	24	25	26	29	31	33	34	35	37	40	43	46	50	54	55	57	59	62	65	72
		B_5		1	1	2	2	2	2	2	2	3	3	4	5	5	6	8	10	12	12	12	12	12	16	17	21	23
		B_6		60	63	63	64	66	66	69	71	71	73	76	78	80	81	82	82	81	80	81	80	80	82	83	80	79
		B_7		30	33	37	38	40	45	50	54	55	59	61	71	75	77	80	85	89	89	89	97	100	108	113	118	112
		B_8		18	19	18	19	20	22	23	25	26	28	27	27	28	29	27	28	29	36	41	45	47	43	44	43	50
		B_9		96	99	99	100	102	101	100	100	99	97	97	91	91	91	88	83	79	77	75	71	70	64	59	54	52
		B_{10}		28	29	34	37	40	41	41	44	47	46	54	54	53	54	60	58	55	48	46	41	42	43	44	40	33
		B_{11}		1	4	2	2	4	3	3	3	2	3	6	4	4	7	7	6	5	5	7	6	8	8	9	7	8
		B_{12}		122	117	113	111	104	100	102	94	89	88	72	71	75	66	57	54	53	52	45	43	35	29	21	19	13
		B_{13}		144	134	126	116	108	101	89	83	77	68	65	58	45	40	36	32	27	22	18	13	8	5	2	0	0

Table B.31: 3-Face Type Growth Pattern (EC3FGP) Dimension 7 EC 5

Dimension		3-Face Type	Transition Sequence Index																									
n	EC		0	1	2	3	4	5	6	7	8	9	10	11	12	13	14	15	16	17	18	19	20	21	22	23	24	···
7	5	B_1	0	0	0	0	0	0	0	0	1	1	1	2	2	2	3	3	3	4	4	4	5	5	5	5	5	5	
		B_2	0	0	0	1	2	3	4	5	4	5	6	5	6	7	6	7	8	7	8	9	8	9	10	11	12	13	
		B_3	0	0	0	0	0	0	0	0	0	0	2	3	5	5	6	6	8	10	10	14	15	15	18	18	19	22	
		B_4	0	0	0	0	0	0	0	0	0	0	1	2	2	2	2	3	4	7	7	7	10	12	14	16	17	18	
		B_5	0	0	0	0	0	0	0	0	0	0	0	0	0	0	0	0	0	0	0	0	0	0	0	0	0	1	
		B_6	0	0	5	8	11	14	17	20	24	27	28	31	32	35	38	41	42	44	47	46	49	52	52	55	57	57	
		B_7	0	0	0	0	0	0	2	3	4	8	7	7	10	12	14	15	17	14	18	19	18	20	20	22	23	27	
		B_8	0	0	0	0	0	0	0	0	0	0	0	0	0	0	1	1	3	5	5	7	12	13	17	18	19	18	
		B_9	0	15	20	26	32	38	42	47	52	54	59	63	66	70	74	77	79	82	84	89	90	90	92	92	95	95	
		B_{10}	0	0	0	0	0	0	3	2	5	6	11	16	19	17	19	21	22	28	24	24	21	22	20	21	23	28	
		B_{11}	0	0	0	0	0	1	0	0	1	0	0	1	0	0	0	1	0	0	0	0	0	1	0	0	2	0	
		B_{12}	35	40	50	60	70	78	82	93	94	100	99	96	97	109	109	112	112	105	119	118	119	120	121	124	121	117	
		B_{13}	525	505	485	465	445	426	410	390	375	359	346	334	321	301	288	273	262	254	234	223	213	201	191	178	167	159	

Dimension		3-Face Type	Transition Sequence Index (cont.)																									
n	EC		···	25	26	27	28	29	30	31	32	33	34	35	36	37	38	39	40	41	42	43	44	45	46	47	48	49
7	5	B_1		5	6	6	6	7	7	7	8	8	8	8	8	8	8	9	9	9	9	9	9	9	10	10	10	11
		B_2		14	13	14	15	14	15	16	15	16	17	18	19	20	21	20	21	22	23	24	25	26	25	26	27	26
		B_3		22	23	26	28	30	33	33	35	38	39	43	44	44	46	48	51	55	59	61	65	68	70	73	79	83
		B_4		19	19	20	22	23	24	25	26	29	31	33	37	38	40	43	47	50	54	58	59	61	63	66	70	76
		B_5		1	1	2	2	2	2	2	2	3	3	5	6	6	7	9	11	13	13	13	13	13	17	19	23	25
		B_6		60	63	63	64	66	66	69	71	71	73	72	74	77	78	80	80	79	78	79	78	78	80	80	77	77
		B_7		30	33	37	38	40	45	50	54	55	59	61	60	66	68	72	74	78	78	78	86	89	97	103	105	102
		B_8		18	19	18	19	20	22	23	25	26	28	26	26	27	28	29	30	31	38	43	47	49	45	45	44	48
		B_9		96	99	99	100	102	101	100	100	99	97	97	96	94	94	90	86	82	80	78	74	73	67	61	57	54
		B_{10}		28	29	34	37	40	41	41	44	47	46	51	56	55	56	56	55	52	45	43	38	39	40	40	37	35
		B_{11}		1	4	2	2	4	3	3	3	2	3	2	5	4	7	6	6	5	5	7	6	8	9	8	7	8
		B_{12}		122	117	113	111	104	100	102	94	89	88	82	72	77	68	63	59	58	57	50	48	40	32	27	24	15
		B_{13}		144	134	126	116	108	101	89	83	77	68	62	57	44	39	35	31	26	21	17	12	7	5	2	0	0

Table B.32: 3-Face Type Growth Pattern (EC3FGP) Dimension 7 EC 6

Dimension		3-Face Type	Transition Sequence Index																									
n	EC		0	1	2	3	4	5	6	7	8	9	10	11	12	13	14	15	16	17	18	19	20	21	22	23	24	···
7	6	B_1	0	0	0	0	0	0	0	0	0	1	1	2	2	2	3	3	3	4	4	4	5	5	5	5	5	5	
		B_2	0	0	0	1	2	3	4	5	6	5	6	5	6	7	6	7	8	7	8	9	8	9	10	11	12	13	
		B_3	0	0	0	0	0	0	0	0	1	2	4	6	8	8	9	9	11	12	12	14	15	15	18	18	19	23	
		B_4	0	0	0	0	0	0	0	0	0	0	1	1	2	2	2	3	4	6	6	6	8	10	12	14	15	17	
		B_5	0	0	0	0	0	0	0	0	0	0	0	0	0	0	0	0	0	0	0	0	0	0	0	0	0	1	
		B_6	0	0	5	8	11	14	17	20	22	25	26	28	29	32	35	38	39	42	45	46	49	52	52	55	57	56	
		B_7	0	0	0	0	0	0	2	3	3	6	5	7	7	9	11	12	13	13	16	18	19	21	21	23	25	26	
		B_8	0	0	0	0	0	0	0	0	0	0	0	0	0	0	1	1	3	4	4	5	10	11	15	16	17	18	
		B_9	0	15	20	26	32	38	42	47	53	56	61	65	69	73	77	80	83	85	88	92	93	93	95	95	97	98	
		B_{10}	0	0	0	0	0	0	3	2	5	9	14	17	21	19	21	23	25	30	27	28	25	26	24	25	26	29	
		B_{11}	0	0	0	0	0	1	0	0	1	0	0	0	0	0	0	1	0	0	0	1	0	1	0	0	2	0	
		B_{12}	35	40	50	60	70	78	82	93	94	94	93	93	93	105	105	108	107	103	116	115	116	117	118	121	119	115	
		B_{13}	525	505	485	465	445	426	410	390	375	362	349	336	323	303	290	275	264	254	234	222	212	200	190	177	166	159	

Dimension		3-Face Type	Transition Sequence Index (cont.)																									
n	EC		···	25	26	27	28	29	30	31	32	33	34	35	36	37	38	39	40	41	42	43	44	45	46	47	48	49
7	6	B_1		5	6	6	6	7	7	7	8	8	8	8	8	8	8	9	9	9	9	9	9	9	10	10	10	11
		B_2		14	13	14	15	14	15	16	15	16	17	18	19	20	21	20	21	22	23	24	25	26	25	26	27	26
		B_3		23	24	27	29	31	34	35	37	39	41	45	47	47	49	51	56	59	63	66	69	72	74	77	83	87
		B_4		18	18	19	21	22	23	24	25	28	31	33	36	37	39	41	45	49	53	57	57	59	61	64	68	74
		B_5		1	1	2	2	2	2	2	2	3	3	5	5	5	6	8	11	13	13	13	13	13	17	19	23	25
		B_6		59	62	62	63	65	65	67	69	70	71	70	71	74	75	77	75	75	74	74	74	74	76	76	73	73
		B_7		30	33	37	38	40	45	49	53	55	56	58	59	65	67	74	75	77	77	76	87	89	97	103	105	103
		B_8		18	19	18	19	20	22	22	24	26	29	27	30	31	32	33	33	35	42	46	48	50	46	46	45	49
		B_9		98	101	101	102	104	103	103	103	101	100	100	99	97	97	92	89	85	83	82	77	77	71	65	61	57
		B_{10}		28	29	34	37	40	41	43	46	47	47	52	52	51	52	51	49	45	38	38	35	37	38	38	35	32
		B_{11}		1	4	2	2	4	3	3	3	2	3	2	4	3	6	4	3	3	3	5	4	6	7	6	5	6
		B_{12}		121	116	112	110	103	99	100	92	88	84	78	72	77	68	64	62	61	60	52	50	41	33	28	25	17
		B_{13}		144	134	126	116	108	101	89	83	77	70	64	58	45	40	36	32	27	22	18	12	7	5	2	0	0

Table B.33: 3-Face Type Growth Pattern (EC3FGP) Dimension 7 EC 7

Dimension		3-Face	Transition Sequence Index																								
n	EC	Type	0	1	2	3	4	5	6	7	8	9	10	11	12	13	14	15	16	17	18	19	20	21	22	23	24	···
7	7	B_1	0	0	0	0	0	1	1	1	1	1	1	2	2	2	3	3	3	3	3	3	3	4	4	4	4	4	
		B_2	0	0	0	1	2	1	2	3	4	5	6	5	6	7	6	7	8	9	10	11	12	11	12	13	14	15	
		B_3	0	0	0	0	0	0	0	1	1	1	2	2	2	5	5	6	9	9	11	14	16	18	22	23	26	26	
		B_4	0	0	0	0	0	0	0	0	1	1	1	2	3	4	5	5	6	7	7	7	9	9	10	11	13	13	
		B_5	0	0	0	0	0	0	0	0	0	0	0	0	0	0	0	0	0	0	0	0	0	0	0	0	1	1	
		B_6	0	0	5	8	11	15	18	20	23	26	28	32	35	35	39	41	41	44	45	45	46	48	47	49	49	52	
		B_7	0	0	0	0	0	1	2	3	2	3	3	4	5	5	7	10	9	11	14	19	19	25	25	28	30	35	
		B_8	0	0	0	0	0	0	0	0	0	0	0	1	1	2	3	3	4	4	4	5	6	7	7	8	9	9	
		B_9	0	15	20	26	32	37	42	47	52	57	63	66	69	73	75	78	83	85	88	89	91	91	95	96	96	97	
		B_{10}	0	0	0	0	0	3	2	4	8	7	10	13	15	19	21	21	26	27	30	31	35	36	41	41	45	40	
		B_{11}	0	0	0	0	0	0	0	0	0	0	0	0	1	0	0	0	0	1	3	1	2	1	1	4	3	3	
		B_{12}	35	40	50	60	70	73	84	88	91	102	105	105	108	106	107	113	108	112	107	108	103	102	98	95	87	102	
		B_{13}	525	505	485	465	445	429	409	393	377	357	341	328	313	302	289	273	263	248	238	227	218	208	198	188	183	163	

Dimension		3-Face	Transition Sequence Index (cont.)																								
n	EC	Type	···	25	26	27	28	29	30	31	32	33	34	35	36	37	38	39	40	41	42	43	44	45	46	47	48	49
7	7	B_1		4	4	4	4	5	5	5	5	5	5	5	6	6	6	7	7	7	7	7	7	7	8	8	8	8
		B_2		16	17	18	19	18	19	20	21	22	23	24	23	24	25	24	25	26	27	28	29	30	29	30	31	32
		B_3		30	30	30	33	33	35	35	37	39	39	40	40	46	51	54	56	58	62	64	67	71	74	77	80	87
		B_4		13	16	18	20	22	24	26	27	29	30	33	34	35	38	40	43	44	46	51	54	56	60	64	66	70
		B_5		1	1	1	1	1	1	1	1	1	2	3	3	3	5	6	6	6	8	12	12	13	16	18	18	22
		B_6		51	54	57	57	61	62	65	66	67	70	72	76	73	71	72	73	74	73	74	74	73	74	74	74	70
		B_7		35	35	36	36	38	41	43	46	46	54	55	62	67	69	74	75	83	89	91	95	98	100	103	110	112
		B_8		11	14	15	19	21	24	25	27	29	28	29	31	36	35	37	39	42	42	40	44	45	45	45	50	50
		B_9		103	103	104	106	106	105	105	106	108	104	103	100	99	97	94	93	89	85	79	75	74	70	65	60	56
		B_{10}		41	41	43	41	43	43	44	44	45	47	49	48	44	47	44	47	44	44	45	42	43	43	44	37	34
		B_{11}		3	3	5	4	5	4	5	4	6	4	5	7	5	4	5	7	8	7	7	6	7	7	7	8	6
		B_{12}		100	101	99	100	96	94	95	96	92	93	88	83	79	73	69	60	55	49	43	42	34	27	21	18	13
		B_{13}		152	141	130	120	111	103	91	80	71	61	54	47	43	39	34	29	24	21	19	13	9	7	4	0	0

Table B.34: 3-Face Type Growth Pattern (EC3FGP) Dimension 7 EC 8

Dimension		3-Face	Transition Sequence Index																									
n	EC	Type		0	1	2	3	4	5	6	7	8	9	10	11	12	13	14	15	16	17	18	19	20	21	22	23	24 ···
7	8	B_1	0	0	0	0	0	1	1	1	2	2	2	3	3	3	3	3	3	3	4	4	4	5	5	5	5	5
		B_2	0	0	0	1	2	1	2	3	2	3	4	3	4	5	6	7	8	9	8	9	10	9	10	11	12	13
		B_3	0	0	0	0	0	0	0	1	2	2	3	3	3	6	6	7	9	9	10	13	15	17	20	21	24	24
		B_4	0	0	0	0	0	0	0	0	1	1	1	2	3	4	5	5	6	7	7	7	9	10	11	12	14	14
		B_5	0	0	0	0	0	0	0	0	0	0	0	0	0	0	0	0	0	0	0	0	0	0	0	0	1	1
		B_6	0	0	5	8	11	15	18	20	23	26	28	32	35	35	38	40	41	44	47	47	48	50	50	52	52	55
		B_7	0	0	0	0	0	1	2	3	2	4	5	6	7	7	8	10	11	13	15	20	20	22	24	27	29	34
		B_8	0	0	0	0	0	0	0	0	0	0	0	1	1	2	2	2	3	3	4	5	6	7	8	9	10	10
		B_9	0	15	20	26	32	37	42	47	52	56	61	64	67	71	74	78	81	83	87	88	90	92	94	95	95	96
		B_{10}	0	0	0	0	0	3	2	4	10	8	10	13	15	19	21	22	27	28	30	31	35	38	40	40	44	39
		B_{11}	0	0	0	0	0	0	0	0	0	0	0	0	1	0	0	1	0	1	4	2	2	3	2	5	4	4
		B_{12}	35	40	50	60	70	73	84	88	86	98	102	102	105	103	108	111	107	111	105	106	103	98	98	95	87	102
		B_{13}	525	505	485	465	445	429	409	393	380	360	344	331	316	305	289	274	264	249	239	228	218	209	198	188	183	163

Dimension		3-Face	Transition Sequence Index (cont.)																								
n	EC	Type	··· 25	26	27	28	29	30	31	32	33	34	35	36	37	38	39	40	41	42	43	44	45	46	47	48	49
7	8	B_1	5	5	5	5	5	5	5	5	6	6	6	7	7	7	8	8	8	8	8	8	8	9	9	9	9
		B_2	14	15	16	17	18	19	20	21	20	21	22	21	22	23	22	23	24	25	26	27	28	27	28	29	30
		B_3	28	28	28	31	31	33	33	35	36	36	37	37	41	46	51	53	58	62	63	66	69	72	75	78	86
		B_4	14	17	19	21	23	24	26	27	30	32	35	36	37	38	42	45	46	50	53	56	58	62	66	68	72
		B_5	1	1	1	1	1	1	1	1	1	2	3	3	3	5	7	7	9	11	12	12	13	16	18	18	21
		B_6	54	57	60	60	63	64	67	68	71	74	76	80	79	77	76	77	75	74	76	76	76	77	77	77	72
		B_7	35	35	36	36	37	43	45	48	47	52	53	60	63	71	70	73	80	80	87	89	95	97	99	106	106
		B_8	12	15	16	20	21	24	25	27	30	29	30	32	34	33	35	37	38	38	41	45	46	46	46	51	53
		B_9	101	101	102	104	105	103	103	104	105	102	101	98	99	95	94	91	88	86	79	77	73	69	65	60	58
		B_{10}	39	39	41	39	41	40	41	41	44	47	49	48	49	50	49	50	46	48	43	42	42	42	44	37	34
		B_{11}	4	4	6	5	7	5	6	5	6	5	6	7	10	7	7	9	7	8	9	9	9	9	9	10	8
		B_{12}	101	102	100	101	99	98	99	100	93	93	88	85	74	70	64	57	56	48	45	40	34	27	20	17	11
		B_{13}	152	141	130	120	109	101	89	78	71	61	54	46	42	38	35	30	25	22	18	13	9	7	4	0	0

Table B.35: 3-Face Type Growth Pattern (EC3FGP) Dimension 7 EC 9

Dimension		3-Face	Transition Sequence Index																									
n	EC	Type		0	1	2	3	4	5	6	7	8	9	10	11	12	13	14	15	16	17	18	19	20	21	22	23	24 ···
7	9	B_1	0	0	0	0	0	1	1	1	2	2	2	2	2	2	2	3	3	3	4	4	4	5	5	5	6	6
		B_2	0	0	0	1	2	1	2	3	2	3	4	5	6	7	8	7	8	9	8	9	10	9	10	11	10	11
		B_3	0	0	0	0	0	0	0	1	2	2	3	3	3	6	6	7	9	9	10	12	14	17	20	22	24	24
		B_4	0	0	0	0	0	0	0	0	1	1	1	2	2	3	4	4	6	7	7	7	8	10	11	12	14	14
		B_5	0	0	0	0	0	0	0	0	0	0	0	0	0	0	0	0	0	0	0	0	0	0	0	1	2	2
		B_6	0	0	5	8	11	15	18	20	23	26	28	31	34	34	37	40	41	44	47	48	49	50	50	51	53	56
		B_7	0	0	0	0	0	1	2	3	2	4	5	5	9	9	10	13	11	13	15	19	22	21	24	28	31	36
		B_8	0	0	0	0	0	0	0	0	0	0	0	0	0	1	1	2	3	3	4	4	5	7	8	7	8	8
		B_9	0	15	20	26	32	37	42	47	52	56	61	65	67	71	74	77	81	83	87	89	90	93	94	94	93	94
		B_{10}	0	0	0	0	0	3	2	4	10	8	10	13	14	18	20	21	27	28	30	32	35	39	40	42	46	41
		B_{11}	0	0	0	0	0	0	0	0	0	0	0	1	1	0	0	0	0	1	3	3	2	3	2	3	2	2
		B_{12}	35	40	50	60	70	73	84	88	86	98	102	104	108	106	111	112	107	111	107	107	105	97	98	95	87	102
		B_{13}	525	505	485	465	445	429	409	393	380	360	344	329	314	303	287	274	264	249	238	226	216	209	198	189	184	164

Dimension		3-Face	Transition Sequence Index (cont.)																									
n	EC	Type	···	25	26	27	28	29	30	31	32	33	34	35	36	37	38	39	40	41	42	43	44	45	46	47	48	49
7	9	B_1		6	7	7	7	7	7	7	7	8	8	8	9	9	9	10	10	10	10	10	10	10	11	11	11	11
		B_2		12	11	12	13	14	15	16	17	16	17	18	17	18	19	18	19	20	21	22	23	24	23	24	25	26
		B_3		28	29	29	32	32	33	33	35	36	36	37	37	41	44	49	52	57	61	62	65	68	71	74	78	86
		B_4		14	17	19	21	23	24	25	26	29	31	34	35	36	37	41	44	46	50	53	56	58	62	66	69	73
		B_5		2	2	2	2	2	2	2	2	2	3	4	4	4	5	7	8	10	12	13	13	14	17	19	21	24
		B_6		55	58	61	61	64	66	69	70	73	76	78	82	81	81	80	80	78	77	79	79	79	80	80	79	74
		B_7		37	36	38	38	40	45	49	52	51	56	57	64	67	76	74	78	83	83	90	92	98	100	103	107	107
		B_8		10	15	16	20	21	22	23	25	28	27	28	30	32	33	35	36	37	37	40	44	45	45	45	46	48
		B_9		99	100	100	102	102	101	101	102	103	100	99	96	97	92	92	88	85	83	76	74	70	66	61	57	55
		B_{10}		41	38	39	37	38	41	42	42	45	48	50	49	50	49	49	49	45	47	42	41	41	41	42	39	36
		B_{11}		2	2	3	2	3	3	3	2	3	2	3	4	6	4	5	5	4	5	6	6	6	6	6	7	5
		B_{12}		101	102	103	104	105	100	101	102	95	95	90	87	78	75	66	62	61	53	50	45	39	32	26	21	15
		B_{13}		153	143	131	121	109	101	89	78	71	61	54	46	41	36	34	29	24	21	17	12	8	6	3	0	0

Table B.36: 3-Face Type Growth Pattern (EC3FGP) Dimension 7 EC 10

Dimension		3-Face	Transition Sequence Index																									
n	EC	Type		0	1	2	3	4	5	6	7	8	9	10	11	12	13	14	15	16	17	18	19	20	21	22	23	24	$\cdots$
7	10	B_1	0	0	0	0	0	0	0	1	1	1	1	1	1	1	2	2	2	3	3	3	3	3	3	3	4	4	
		B_2	0	0	0	1	2	3	4	3	4	5	6	7	8	9	8	9	10	9	10	11	12	13	14	15	14	15	
		B_3	0	0	0	0	0	0	0	0	0	0	0	0	0	0	0	3	7	9	13	14	16	16	19	23	25	28	
		B_4	0	0	0	0	0	0	0	0	1	2	3	3	3	4	4	4	6	7	8	8	9	11	12	14	16	18	
		B_5	0	0	0	0	0	0	0	0	0	0	0	0	0	0	0	0	0	0	0	0	0	1	2	2	3	3	
		B_6	0	0	5	8	11	14	17	21	24	27	30	33	36	39	43	43	42	44	43	45	46	49	49	48	50	50	
		B_7	0	0	0	0	0	0	0	1	1	1	0	1	4	4	8	13	11	14	13	17	19	23	27	27	29	31	
		B_8	0	0	0	0	0	0	0	0	0	0	0	0	0	0	1	2	4	5	5	5	6	5	4	6	6	8	
		B_9	0	15	20	26	32	38	44	49	53	57	62	67	70	74	76	77	81	82	87	89	91	89	89	91	91	91	
		B_{10}	0	0	0	0	0	0	0	3	6	9	13	12	14	17	19	20	24	26	32	31	35	39	44	46	49	51	
		B_{11}	0	0	0	0	0	0	0	0	0	0	0	1	0	1	2	0	0	0	0	2	2	3	1	1	1	1	
		B_{12}	35	40	50	60	70	80	90	93	97	101	104	113	118	120	117	118	112	110	105	108	103	98	94	90	86	81	
		B_{13}	525	505	485	465	445	425	405	389	373	357	341	322	306	291	280	269	261	251	241	227	218	210	202	194	186	179	

Dimension		3-Face	Transition Sequence Index (cont.)																									
n	EC	Type	$\cdots$	25	26	27	28	29	30	31	32	33	34	35	36	37	38	39	40	41	42	43	44	45	46	47	48	49
7	10	B_1		4	4	4	4	4	4	4	5	5	5	5	5	5	5	6	6	6	7	7	7	7	7	7	8	8
		B_2		16	17	18	19	20	21	22	21	22	23	24	25	26	27	26	27	28	27	28	29	30	31	32	31	32
		B_3		28	30	30	32	34	34	35	35	37	41	42	42	45	47	50	53	57	59	61	62	69	73	76	81	87
		B_4		18	18	19	20	23	25	27	28	29	30	32	34	36	39	41	44	46	48	52	55	57	59	61	63	70
		B_5		3	3	3	3	3	3	3	3	3	5	5	5	6	6	7	7	7	7	9	10	13	13	14	18	22
		B_6		53	54	57	58	59	62	64	68	69	68	70	73	73	74	75	75	74	76	77	79	75	74	74	73	70
		B_7		35	37	40	43	41	43	44	50	54	60	64	68	72	73	79	82	83	88	90	94	96	102	108	117	112
		B_8		8	9	10	12	17	18	21	23	23	21	24	27	29	32	35	39	40	45	46	47	45	49	50	49	50
		B_9		93	97	98	99	101	101	102	100	100	98	96	94	92	91	87	84	85	82	78	74	74	70	66	59	56
		B_{10}		47	48	50	50	47	48	47	47	52	55	51	49	48	48	46	44	48	44	45	44	47	42	42	37	34
		B_{11}		1	3	3	2	2	3	4	4	5	3	4	6	5	7	6	5	6	6	5	7	6	7	9	6	6
		B_{12}		95	92	92	93	94	95	94	92	84	80	82	79	76	70	64	62	54	50	45	41	32	28	18	17	13
		B_{13}		159	148	136	125	115	103	93	84	77	71	61	53	47	41	38	32	26	21	17	11	9	5	3	1	0

Table B.37: 3-Face Type Growth Pattern (EC3FGP) Dimension 7 EC 11

Dimension		3-Face	Transition Sequence Index																									
n	EC	Type		0	1	2	3	4	5	6	7	8	9	10	11	12	13	14	15	16	17	18	19	20	21	22	23	24 ···
7	11	B_1	0	0	0	0	0	0	0	1	1	1	1	1	1	1	2	2	2	3	3	3	4	4	4	4	4	4
		B_2	0	0	0	1	2	3	4	3	4	5	6	7	8	9	8	9	10	9	10	11	10	11	12	13	14	15
		B_3	0	0	0	0	0	0	0	0	0	0	0	0	0	0	0	3	7	9	13	14	18	18	22	26	28	31
		B_4	0	0	0	0	0	0	0	0	1	2	3	3	3	4	4	4	6	7	8	8	9	12	13	15	17	18
		B_5	0	0	0	0	0	0	0	0	0	0	0	0	0	0	0	0	0	0	0	0	2	3	4	4	4	4
		B_6	0	0	5	8	11	14	17	21	24	27	30	33	36	39	43	43	42	44	43	45	45	48	47	46	47	47
		B_7	0	0	0	0	0	0	0	1	1	1	0	1	4	4	8	13	11	14	13	17	18	20	22	22	23	28
		B_8	0	0	0	0	0	0	0	0	0	0	0	0	0	0	1	2	4	5	5	5	3	2	1	3	4	6
		B_9	0	15	20	26	32	38	44	49	53	57	62	67	70	74	76	77	81	82	87	89	92	90	92	94	95	94
		B_{10}	0	0	0	0	0	0	0	3	6	9	13	12	14	17	19	20	24	26	32	31	38	42	47	49	52	53
		B_{11}	0	0	0	0	0	0	0	0	0	0	0	1	0	1	2	0	0	0	0	2	1	2	1	1	2	1
		B_{12}	35	40	50	60	70	80	90	93	97	101	104	113	118	120	117	118	112	110	105	108	99	96	91	87	83	79
		B_{13}	525	505	485	465	445	425	405	389	373	357	341	322	306	291	280	269	261	251	241	227	221	212	204	196	187	180

Dimension		3-Face	Transition Sequence Index (cont.)																									
n	EC	Type	···	25	26	27	28	29	30	31	32	33	34	35	36	37	38	39	40	41	42	43	44	45	46	47	48	49
7	11	B_1		4	4	4	4	4	4	4	5	5	5	6	6	6	6	6	6	6	7	7	7	8	8	8	9	9
		B_2		16	17	18	19	20	21	22	21	22	23	22	23	24	25	26	27	28	27	28	29	28	29	30	29	30
		B_3		31	33	33	35	37	37	38	38	40	44	47	47	51	53	55	58	62	64	66	67	68	72	77	82	86
		B_4		18	18	19	20	23	25	27	28	29	30	34	37	39	42	44	47	49	51	55	58	59	61	63	68	72
		B_5		4	4	4	4	4	4	4	4	4	6	8	8	9	9	9	9	9	9	11	12	12	12	15	19	21
		B_6		50	51	54	55	56	59	61	65	66	65	66	69	68	69	70	70	69	71	72	74	77	76	74	73	72
		B_7		32	34	37	40	38	40	41	47	51	57	56	59	61	62	69	71	72	77	79	83	91	94	102	101	106
		B_8		6	7	8	10	15	16	19	21	21	19	20	23	25	28	33	37	38	43	44	45	49	53	52	51	53
		B_9		96	100	101	102	104	104	105	103	103	101	100	97	97	96	91	89	90	87	83	79	75	74	68	65	58
		B_{10}		49	50	52	52	49	50	49	49	54	57	58	55	54	54	49	48	52	48	49	48	43	41	39	38	34
		B_{11}		1	3	3	2	2	3	4	4	5	3	3	4	4	6	5	4	5	5	4	6	8	11	8	9	8
		B_{12}		93	90	90	91	92	93	92	90	82	78	73	75	71	65	63	60	52	48	43	39	34	23	21	14	11
		B_{13}		160	149	137	126	116	104	94	85	78	72	67	57	51	45	40	34	28	23	19	13	8	6	3	2	0

Table B.38: 3-Face Type Growth Pattern (EC3FGP) Dimension 7 EC 12

Dimension		3-Face Type		Transition Sequence Index																									
n	EC			0	1	2	3	4	5	6	7	8	9	10	11	12	13	14	15	16	17	18	19	20	21	22	23	24	···
7	12	B_1	0	0	0	0	0	0	0	1	1	1	1	1	1	1	2	2	2	3	3	3	4	4	4	4	4	4	
		B_2	0	0	0	1	2	3	4	3	4	5	6	7	8	9	8	9	10	9	10	11	10	11	12	13	14	15	
		B_3	0	0	0	0	0	0	0	0	0	0	0	0	0	0	0	3	7	9	13	14	18	18	22	26	28	31	
		B_4	0	0	0	0	0	0	0	0	1	2	3	3	3	4	4	4	6	7	8	8	9	12	13	15	17	18	
		B_5	0	0	0	0	0	0	0	0	0	0	0	0	0	0	0	0	0	0	0	0	2	3	4	4	4	4	
		B_6	0	0	5	8	11	14	17	21	24	27	30	33	36	39	43	43	42	44	43	45	45	48	47	46	47	47	
		B_7	0	0	0	0	0	0	0	1	1	1	0	1	4	4	8	13	11	14	13	17	18	20	22	22	23	28	
		B_8	0	0	0	0	0	0	0	0	0	0	0	0	0	0	1	2	4	5	5	5	3	2	1	3	4	6	
		B_9	0	15	20	26	32	38	44	49	53	57	62	67	70	74	76	77	81	82	87	89	92	90	92	94	95	94	
		B_{10}	0	0	0	0	0	0	0	3	6	9	13	12	14	17	19	20	24	26	32	31	38	42	47	49	52	53	
		B_{11}	0	0	0	0	0	0	0	0	0	0	0	1	0	1	2	0	0	0	0	2	1	2	1	1	2	1	
		B_{12}	35	40	50	60	70	80	90	93	97	101	104	113	118	120	117	118	112	110	105	108	99	96	91	87	83	79	
		B_{13}	525	505	485	465	445	425	405	389	373	357	341	322	306	291	280	269	261	251	241	227	221	212	204	196	187	180	

Dimension		3-Face Type	Transition Sequence Index (cont.)																									
n	EC		···	25	26	27	28	29	30	31	32	33	34	35	36	37	38	39	40	41	42	43	44	45	46	47	48	49
7	12	B_1		4	5	5	5	6	6	6	7	7	7	8	8	8	9	9	9	9	9	9	9	10	10	10	11	11
		B_2		16	15	16	17	16	17	18	17	18	19	18	19	20	19	20	21	22	23	24	25	24	25	26	25	26
		B_3		31	33	33	35	37	39	40	41	41	45	47	47	51	53	56	60	62	64	69	70	72	75	79	82	86
		B_4		18	18	20	23	26	26	27	28	30	32	36	37	39	43	46	49	53	56	57	59	60	63	67	71	73
		B_5		4	4	4	4	4	4	4	5	5	7	8	8	9	11	12	14	15	15	16	16	18	20	23	24	24
		B_6		50	52	55	56	58	59	61	64	67	66	68	71	70	72	72	71	72	73	71	73	75	75	74	75	74
		B_7		32	35	39	38	36	42	44	50	54	56	54	61	62	63	66	69	70	71	79	84	92	97	99	100	107
		B_8		6	9	12	17	19	19	20	21	24	22	23	24	26	27	29	30	33	36	38	40	40	40	40	43	48
		B_9		96	99	97	98	100	100	102	100	98	98	98	95	96	93	90	87	84	83	79	76	72	67	63	60	55
		B_{10}		49	47	45	41	46	46	47	47	45	50	55	53	53	54	52	50	47	47	45	43	41	42	41	40	36
		B_{11}		1	2	1	1	2	2	4	4	4	3	4	3	4	4	4	3	3	6	3	5	7	6	5	7	5
		B_{12}		93	91	94	96	88	90	88	84	85	79	70	76	69	63	61	59	59	51	48	46	38	32	28	19	15
		B_{13}		160	150	139	129	122	110	99	92	82	76	71	58	53	49	43	38	31	26	22	14	11	8	5	3	0

Appendix C

m-Face Data

C.1 2-Face Types

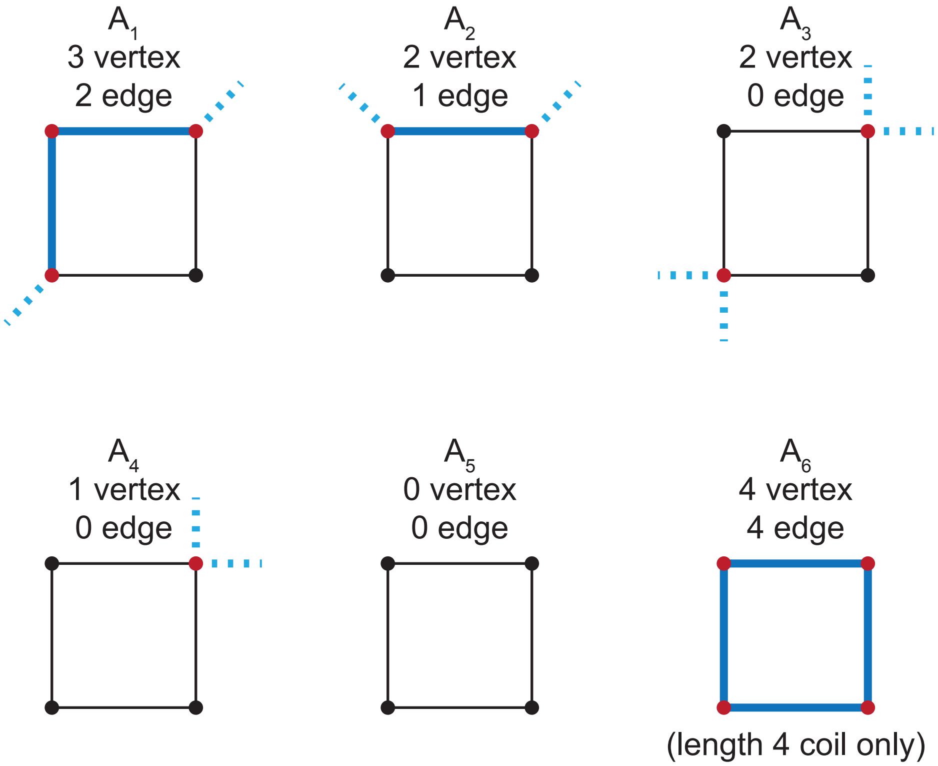

Figure C.1: 2-Dimensional Hypercube Snake Path Types (square / face / 2-face) [23]

C.2 3-Face Types

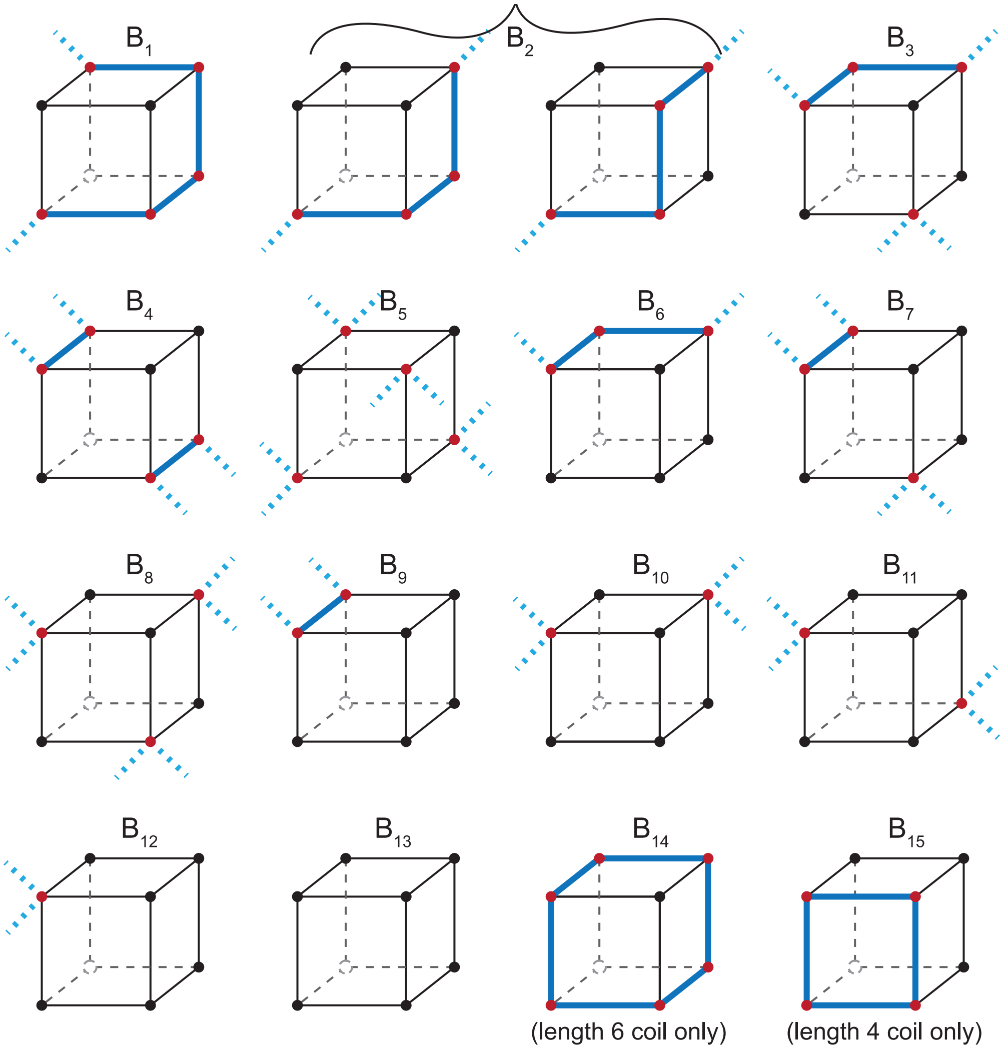

B_n	Vertex	Edge	Elbow
1	5	4	3
2	4	3	2
3	4	2	1
4	4	2	0
5	4	0	0
6	3	2	1
7	3	1	0
8	3	0	0
9	2	1	0
10	2	0	0
11	2	0	0
12	1	0	0
13	0	0	0
14	6	6	6
15	4	4	4

Figure C.2: 3-Dimensional Hypercube Snake Path Types (cell / cube / 3-face)

Appendix D

Hypercube Level Structure

D.1 Pascal's Triangle

Table D.1: Pascal's Triangle

Row (n)	Sum (2^n)																															
0	1																1															
1	2															1		1														
2	4														1		2		1													
3	8													1		3		3		1												
4	16												1		4		6		4		1											
5	32											1		5		10		10		5		1										
6	64										1		6		15		20		15		6		1									
7	128									1		7		21		35		35		21		7		1								
8	256								1		8		28		56		70		56		28		8		1							
9	512							1		9		36		84		126		126		84		36		9		1						
10	1 024						1		10		45		120		210		252		210		120		45		10		1					
11	2 048					1		11		55		165		330		462		462		330		165		55		11		1				
12	4 096				1		12		66		220		495		792		924		792		495		220		66		12		1			
13	8 192			1		13		78		286		715		1287		1716		1716		1287		715		286		78		13		1		
14	16 384		1		14		91		364		1001		2002		3003		3432		3003		2002		1001		364		91		14		1	
15	32 768	1		15		105		455		1365		3003		5005		6435		6435		5005		3003		1365		455		105		15		1

D.2 Dimension 1–7 Hypercube Level Structure Node Distribution

Table D.2: Dimension 1–7 Hypercube Level Structure Node Distribution

Dimension	Level	Hypercube Nodes
1	0	0
	1	1
2	0	0
	1	1, 2
	2	3
3	0	0
	1	1, 2, 4
	2	3, 5, 6
	3	7
4	0	0
	1	1, 2, 4, 8
	2	3, 5, 9, 6, 10, 12
	3	7, 11, 13, 14
	4	15
5	0	0
	1	1, 2, 4, 8, 16
	2	3, 5, 9, 17, 6, 10, 18, 12, 20, 24
	3	7, 11, 19, 13, 21, 25, 14, 22, 26, 28
	4	15, 23, 27, 29, 30
	5	31
6	0	0
	1	1, 2, 4, 8, 16, 32
	2	3, 5, 9, 17, 33, 6, 10, 18, 34, 12, 20, 36, 24, 40, 48
	3	7, 11, 19, 35, 13, 21, 37, 25, 41, 49, 14, 22, 38, 26, 42, 50, 28, 44, 52, 56
	4	15, 23, 39, 27, 43, 51, 29, 45, 53, 57, 30, 46, 54, 58, 60
	5	31, 47, 55, 59, 61, 62
	6	63
7	0	0
	1	1, 2, 4, 8, 16, 32, 64
	2	3, 5, 9, 17, 33, 65, 6, 10, 18, 34, 66, 12, 20, 36, 68, 24, 40, 72, 48, 80, 96
	3	7, 11, 19, 35, 67, 13, 21, 37, 69, 25, 41, 73, 49, 81, 97, 14, 22, 38, 70, 26, 42, 74, 50, 82, 98, 28, 44, 76, 52, 84, 100, 56, 88, 104, 112
	4	15, 23, 39, 71, 27, 43, 75, 51, 83, 99, 29, 45, 77, 53, 85, 101, 57, 89, 105, 113, 30, 46, 78, 54, 86, 102, 58, 90, 106, 114, 60, 92, 108, 116, 120
	5	31, 47, 79, 55, 87, 103, 59, 91, 107, 115, 61, 93, 109, 117, 121, 62, 94, 110, 118, 122, 124
	6	63, 95, 111, 119, 123, 125, 126
	7	127